12-16-2016

# Design and Synthesis of Next Generation Propargyl-Linked Antifolates

Eric Scocchera
eric.scocchera@uconn.edu

Design and Synthesis of Next Generation Propargyl-Linked Antifolates

Eric W. Scocchera

University of Connecticut, 2017

## Abstract

Antibiotic resistance is an ever-present problem that reduces the arsenal of antibiotics human's possess to fight pathogenic infections. New generations of antibiotics are therefore always required. Recent history has seen few novel classes of antibiotics, instead structural modifications of previous classes are often the source of new antibiotics. Antifolates are a colloquial name given to various compound classes that are capable of inhibiting the bacterial production of folate or enzymes that require folate for proper cellular function. Dihydrofolate reductase (DHFR) is a crucial enzyme in this pathway, and is inhibited in bacteria only by trimethoprim (TMP). TMP is used clinically as a broad-spectrum antibiotic, with activity against Gram-negative and Gram-positive pathogens. TMP resistance, both innate and acquired, has been well researched and has attracted many pharmaceutical companies to design the next generation antibacterial DHFR drug. To date, TMP is the only clinically approved antibacterial DHFR inhibitor.

This thesis is a discussion about the culmination of years of research to rationally design new DHFR inhibitors, based on a modified TMP-scaffold, for use against TMP-resistant bacteria. These charged propargyl-linked antifolates (PLAs) have low nanomolar DHFR affinity for both wild-type *Staphylococcus aureus* DHFR and known

resistant DHFR mutants. They have excellent antibacterial activity against methicillin-resistant *S. aureus* (MRSA) and TMP-resistant MRSA clinical isolates with known resistance mechanisms. Charged PLAs also inhibit *Mycobacterium tuberculosis* (Mtb) growth at nanomolar concentrations, as well as multi-drug resistant Mtb and extensively-drug resistant Mtb. A new PLA scaffold was identified with hopes of improving antibacterial activity of PLAs against Gram-negative bacteria such as *Escherichia coli* and *Klebsiella pneumoniae*. New synthetic methods are reported to make PLA generation simpler and more efficient. PLAs represent promising novel antifolates that could be used as antibacterial therapies in the future.

# Design and Synthesis of Next Generation Propargyl-Linked Antifolates

Eric W. Scocchera

B.S., Allegheny College

A Dissertation

Submitted in Partial Fulfillment of the

Requirements for the Degree of

Doctor of Philosophy

at the

University of Connecticut

2017

APPROVAL PAGE

Doctor of Philosophy Dissertation

Design and Synthesis of Next Generation Propargyl-Linked Antifolates

Presented by

Eric W. Scocchera, B.S.

Major Advisor_____

Dennis L. Wright, Ph.D.

Associate Advisor _____

Amy R. Howell, Ph.D.

Associate Advisor _____

Kyle Hadden, Ph.D.

University of Connecticut

2017

**Acknowledgements**

I would like to first thank Dr. Dennis Wright for the opportunity he gave me to work in his lab and learn the ways of structure based drug design. Dennis' knowledge, guidance, especially his enthusiasm when new compounds are synthesized or new biological data is acquired, is infectious. I sincerely thank him for the opportunity and for putting up with me for a bit longer than he probably would have liked.

I would like to simultaneously thank Dr. Amy Anderson for being her. Those who knew her know what I mean. Amy's attitude was infectious. Her excitement any time there was a conversation about science was palpable, and I always remember leaving her presence feeling energized to do more. Although she was invaluable as a mentor, she was an even better person. I hope to acquire as many characteristics that Amy possessed as I possibly can, fully aware that I will most certainly fall short. I'll take comfort in knowing that any step in her direction is a right one.

To my lab mates: Zack, your friendship and mentorship has been invaluable to me, and helped me get through the difficult challenge that is graduate school. I admire your work ethic and have learned a lot from watching you succeed as you certainly have. When I think of grad school, I'll think of everything from good times at "the dirty bird" to just talking chemistry over some beers. Mike, your attitude in the lab made it a great place to be every day. I'll certainly remember all the good times we had, especially in Somers. Naren, it has been a lot of fun working across from you for years. The days in the lab can be long, but our conversations about every- and anything certainly made it better… and the Seinfeld references. Also, thank you for being a great roommate, and thank you for even offering your spare room to me in the

first place. I want to thank you, Santosh, for helping me be a better chemist. I always enjoyed our white board conversations and our chemistry talks in general. I always enjoyed our life conversations with you and Naren. Thanks for showing me how to make a proper curry too. To Behnoush, the world-traveler who ended up in Storrs, CT. I'm glad you did because had you not, I would have one less great friend. Among so many other things, you're a great cook, great photographer, great conversationalist, and great friend. Oh, and the dinosaur juice boxes don't forget. To so many other graduate students: Kishore, Harold, Stephanie, Mike, Alex, and so many more, thank you for being great people who made it a great place to work and learn.

Fred, without your friendship I may have gone crazy, you know what I mean. I'll never properly tell you and Brittany how much you two making me a part of your friends and family has meant to me. Sean, we became good friends later on in my time here, but I'm damn glad we did. I've laughed and learned a lot from our conversations and time spent in the gym. To Zach, Josh, Lylah, Matt, Laura, Kiran, Megha, Bobby: Thank you all for the good times we had that were always a much-needed break from the daily grind.

Finally, I'd like to thank my family, who have supported me in so many ways throughout my life and graduate school that I've lost count. From simply talking on the phone to you visiting me in Connecticut to the long trips back home for Christmas, you have helped get me through to this point. Thank you seems underwhelming for the effect but ---**THANK YOU---**, a million times over.

## Table of Contents

## List of Figures

## List of Tables

## List of Schemes

# 1 Antifolates: Mechanism of action, resistance, and recent work

## 1.1 Folate Biosynthesis

Rapidly growing cells are in need of a constantly-replenishing supply of a multitude of metabolites to ensure survival and replication. In fact, disrupting metabolite biosynthesis has been a proven method of antiproliferative therapy since the late 1930s. That decade the sulfonamide drug class was discovered and with it a solution to bacterial infections that had plagued humanity throughout time. Unknown at the time of their discovery, the sulfonamides act by interrupting bacterial folate biosynthesis, a multi-step enzymatic pathway that utilizes 7,8-dihydrofolate (DHF) to generate essential metabolites such as thymidine, methionine, histidine, and purines. Since the discovery of sulfonamides, other drug classes, colloquially referred to as "antifolates", that target other essential enzymes along the folate biosynthesis pathway have been used as anticancer, antiprotozoal, and antibacterial agents.

The sulfonamides had an early advantage as antibacterials by targeting an enzyme not found in humans, limiting the potential for side effects. While humans are able to acquire DHF from the diet via active transport of its precursor, folic acid (vitamin $B_9$), bacteria lack folate transporters and must synthesize DHF in the cell. This has limited antifolate use as antibacterials because classical antifolates containing the glutamate tail found in natural folate substrates are too highly charged to passively diffuse across lipid bilayers. Classical antifolates have instead found their use in anticancer treatments, where they are taken into human cells via folate transporters.

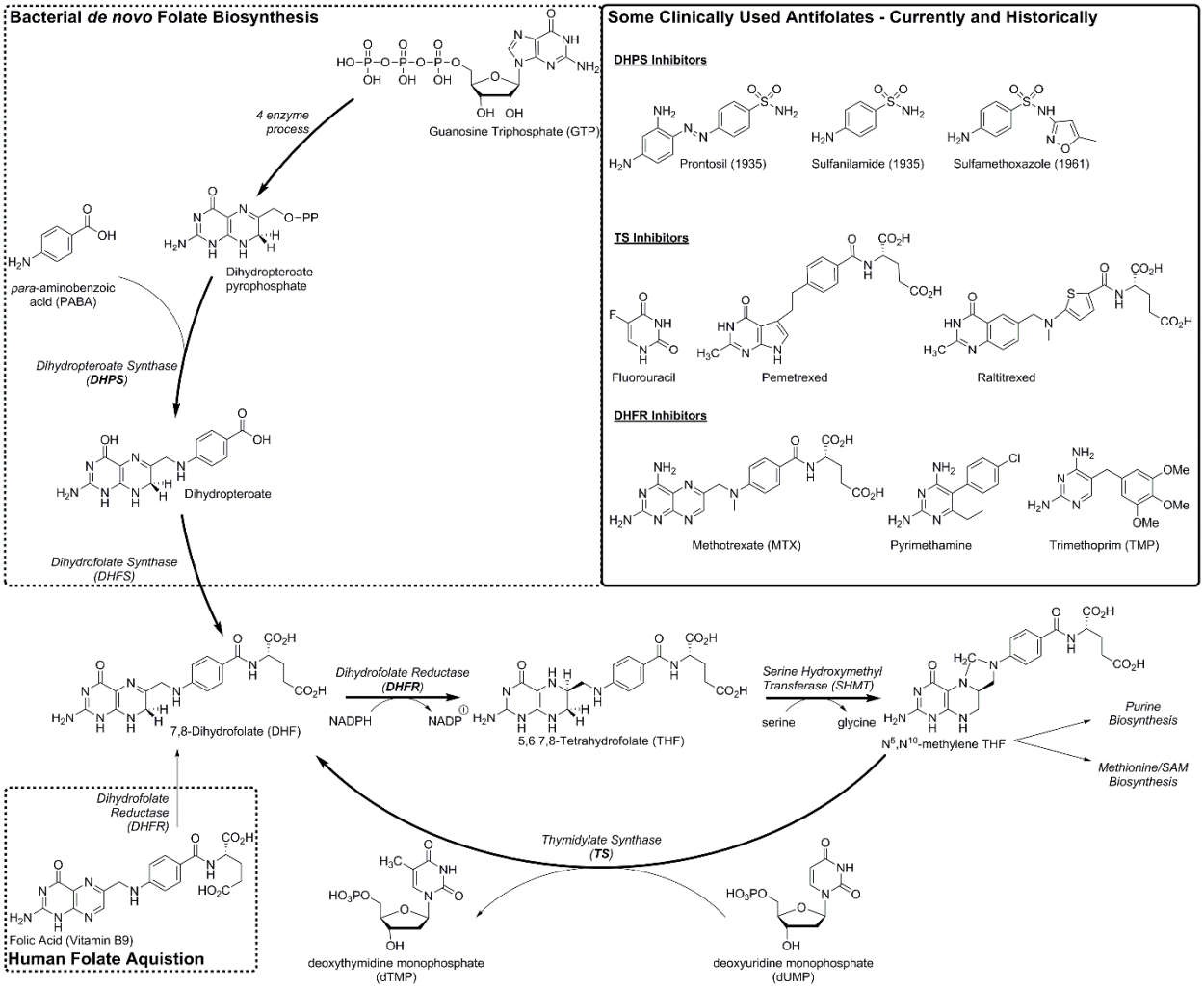


**Figure 1.1** Folate Biosynthetic Pathway and Clinically-Used Antifolates

Bacterial *de novo* folate biosynthesis is a six-step enzymatic process that converts guanosine triphosphate (GTP) to DHF (**Figure 1.1**). Two enzymatic steps convert GTP to 6-hydroxymethyl-7,8-dihydropterin, which is then converted to dihydropteroate pyrophosphate via hydroxymethyl-7,8-dihydropterin pyrophosphokinase (HPPK). Here, two distinct pathways converge to generate dihydropteroate. Dihydropteroate synthase (DHPS) catalyzes the reaction between dihydropteroate pyrophosphate and

*para*-aminobenzoic acid (PABA), a metabolite of the shikimate pathway intermediate chorismate. Dihydrofolate synthase adds a glutamate tail to dihydropteroate to generate DHF and complete *de novo* folate biosynthesis. From DHF, the bacterial and human folate pathways are nearly identical. Dihydrofolate reductase (DHFR) utilizes nicotinamide adenine dinucleotide phosphate (NADPH) as a reducing agent to catalyze the conversion of DHF to 5,6,7,8-tetrahydrofolate (THF). Serine hydroxymethyl transferase (SHMT) transfers a methyl group to a pterin-nitrogen and the aromatic amine of THF to generate $N^5$,$N^{10}$-methylene THF ($CH_2$THF). Here the folate biosynthetic pathway diverges, as various enzymes catalyze a one carbon transfer to synthesize metabolites essential for normal cell function and replication:

- Thymidylate synthase (TS) utilizes $N^5$,$N^{10}$-methylene THF to transfer a methyl group to deoxyuridine monophosphate (dUMP), generating deoxythymidine monophosphate (dTMP) and recycling DHF. Without dTMP, cells are unable to synthesize RNA and suffer a “thymine-less death.”
- Methylene tetrahydrofolate reductase (MTHFR) reduces $N^5$,$N^{10}$-methylene THF to $N^5$-methyl-THF, which is used to generate methionine via remethylation of homocysteine by methionine synthase (MTR). Methionine is required to generate S-adenosyl-methionine (SAM), one of the most ubiquitous enzyme cofactors, responsible for post translational methylation and essential to proper cell function.
- Methylenetetrahydrofolate dehydrogenase and methenyltetrahydrofolate cyclohydrolase sequentially act to convert $N^5$,$N^{10}$-methylene THF to $N^{10}$-formyl THF, which is essential for purine biosynthesis and DNA biosynthesis.

The folate biosynthetic pathway is fundamental to cell survival and highly conserved among all organisms, which has made it an attractive target for drug discovery efforts. Herein we will review the history of antifolate drug targets and the current state of their clinical relevance.

## 1.2 DHPS Inhibition – The Sulfonamides

In the interwar period of the 1920s and 1930s, researchers at Bayer AG synthesized a large number of organic dyes to treat bacterial infections. They believed that if the dyes were capable of binding to bacteria they may be also capable of halting growth. Gerhard Domagk discovered Prontosil and showed it was effective at reducing streptococcal infections in animal models.[1,2] Soon after, researchers discovered that Prontosil was a prodrug that was cleaved to the active component sulfanilamide,[3] a known compound synthesized years earlier. This marked the beginning of the sulfonamide (sulfa) drug class of antibiotics, a class that would see a myriad of structural modifications to improve upon the drug-like properties of sulfanilamide.

DHPS, encoded by *folP*, catalyzes the reaction of DHPP and PABA to generate dihydropteroate, the immediate precursor to DHF. Sulfonamides act as PABA mimics by binding in the PABA region of DHPS. Structurally, sulfa drugs are almost identical to pABA, with the aromatic sulfonamide moiety acting as a bioisostere for the benzoic acid present in PABA. The aryl amine moiety of sulfa drugs undergoes the same condensation reaction with DHPP, forming a dihydropteroate-like product that cannot undergo subsequent DHF synthesis.[4,5] A critical reduction in bacterial folate levels

follows, leading to thymine depletion and what has been termed a “thymine-less death” of the cell.[6]

Structurally, sulfonamides are all based on the sulfanilamide scaffold with varying substituents on the aryl sulfonamide nitrogen. These substituents confer greater tolerability, increased potency against acquired or innately resistant enzymes, and better pharmacokinetic properties. They also allow for *folP* mutations to encode resistant enzymes with amino acid changes exclusively found where these substituents bind without affecting PABA binding. As we will discuss, this is a common resistance mechanism to sulfonamides.

Historically, sulfanilamide was used to treat streptococcal infections such as pneumonia and scarlet fever, and sulfadoxine was used as a combination therapy to treat malaria. Today, sulfonamides are rarely used as mono-therapies. Sulfadiazine is used as a combination therapy with pyrimethamine to treat malaria. Sulfamethoxazole is the most widely used sulfa drug as part of a combination therapy with trimethoprim (TMP) to treat urinary tract infections caused by *Escherichia coli*, skin and soft tissue infections caused by *Staphylococcus aureus*, and as prophylaxis in HIV/AIDs patients.

## 1.3 Thymidylate Synthase Inhibition

### *1.3.1 Fluorouracil and its Prodrugs*

In 1954 researchers at Jefferson Medical College observed that hepatoma growth in rats was accelerated with the addition of exogenous uracil.[7] They also found that hepatomas utilized uracil more rapidly than normal cells, indicating that uracil metabolism was a crucial difference between cancer cells and healthy cells. At the time, many observations had been made about the profound effect of substituting fluorine for hydrogen in biologically relevant molecules, leading to the synthesis of 5-fluorouracil (5-FU). Researchers at Hoffmann-LaRoche found that 5-FU inhibited tumor growth in rats, paving the way for antimetabolite cancer therapies.[8]

Since, 5-FU's anticancer activity has been explained via two mechanisms: 1) its incorporation into RNA which disrupts normal RNA function and processing and 2) inhibition of thymidylate synthase (TS) which leads to thymidine depletion in cells. 5-FUs ability to disrupt normal DNA replication ultimately leads to cell death. 5-FU and 5-FU pro-drugs, such as flucytosine, capecitabine, and tegafur, have been used as anticancer and antifungal therapies. Herein, our focus will remain on 5-FUs ability to inhibit TS as it relates to the folate biosynthetic pathway.[9]

5-FU enters cells via the same transport mechanism as uracil[10] where it is converted to several active metabolites. Thymidine phosphorylase (TP) catalyzes the conversion of 5-FU to fluorodeoxyuridine (FUDR) which is subsequently acted up by thymidine kinase (TK) which adds a phosphate and generates fluorodeoxyuridine monophosphate (FdUMP). Normal TS function transfers a methyl group from $N^5$,$N^{10}$-methylene THF ($CH_2THF$) to C-5 of deoxyuridine monophosphate (dUMP), generating

deoxythymidine monophosphate (dTMP) to be used for DNA synthesis. However, FdUMP binds to the nucleotide binding site in TS and forms a ternary complex with $CH_2THF$, thereby blocking dUMP binding and normal function of TS.

Capecitabine is a rationally designed, orally available TS inhibitor that is converted to 5-FU once it has entered cancer cells and is acted upon by thymidine phosphorylase (TP). A greater tolerance and selectivity can be achieved as many cancers see an increase in TP activity relative to healthy cells. It is currently employed in the treatement of colorectal cancers. Flucytosine, an antifungal drug that is converted to 5-FU once taken up into fungal cells, is co-administered with amphotericin B as a first-line therapy against cryptococcal meningitis.

### *1.3.2 Classical Antifolate TS Inhibitors*

More recently, competitive antagonists of $CH_2THF$ have begun to see clinical utility as alternatives to 5-FU. Raltitrexed (Tomudex, TDX), first synthesized by ICI Pharmaceuticals in 1991,[11] was approved for use against colorectal cancers, especially in cases where 5-FU is not well tolerated.[12] Raltitrexed is considered a classical antifolate, characterized by the glutamate tail found in THF.

Pemetrexed (PMX), a classical antifolate first synthesized by Eli Lilly and Company in 1992,[13] has been approved for use against pleural mesothelioma and non-small cell lung cancers. PMX is unique among antifolates in that it inhibits multiple enzymes along the folate pathway, TS and DHFR.

While nucleic acid mimics such as 5-FU and classical antifolate $CH_2THF$ mimics have seen success as cancer therapies, they have not had activity as antibacterials.

This is likely due to the highly conserved nature of TS leading to a propensity for toxicity via human TS inhibition. Recently researchers have identified allosteric sites capable of TS inhibition, sites that may be less conserved between humans and bacterial species.[14] Still, thymine depletion remains an attractive and untapped method for antibacterial therapies to exploit.

## 1.4 Flavin-Dependent Thymidylate Synthase

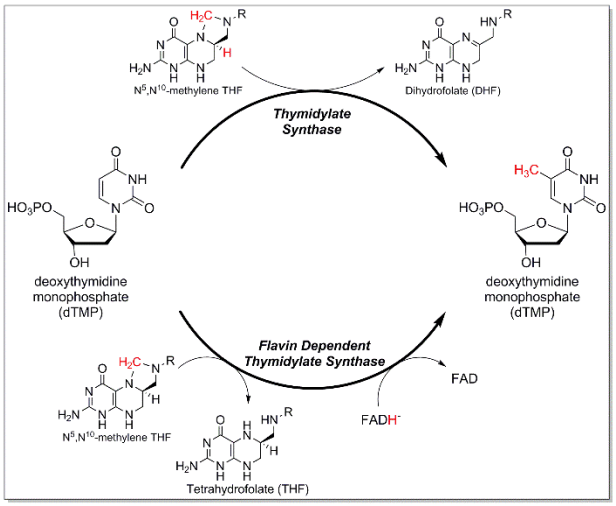


**Figure 1.2** Comparison of *ThyA* TS and *ThyX* FDTS

Until recently, it was believed that the only mechanism by which a cell could acquire thymine was *de novo* biosynthesis via the action of both DHFR and TS (encoded by the *thyA* gene) or via thymidine kinase (*tdk*) salvage from the extracellular environment. However, genomic studies have revealed that some microorganisms lack both *thyA* and *tdk*, meaning another process to acquire thymine must exist.[15] In 1989, researchers discovered the *thyX* gene and identified the protein it encodes, flavin-dependent thymidylate synthase (FDTS), and showed it was capable of

rescuing *thyA* deletion in bacteria.[15,16] Organisms possessing *thyX* may be capable of rescuing DHFR or TS inhibition. FDTS has been shown to catalyze the same reaction as traditional TS, the methylation of dUMP to dTMP, albeit via a different mechanism and using different cofactors.[17] TS encoded by *thyA* uses $CH_2THF$ as both a one carbon donor and a reducing agent to methylate dUMP, generating dTMP and DHF (**Figure 1.2**). Recently it has been found that FDTS utilizes reduced FAD as a methylene shuttle from $CH_2THF$ to dUMP, liberating THF. Methylene reduction is accomplished via $FADH^-$, instead of THF oxidation to DHF.[17,18] This can be seen in crystal structures of various folates bound to FDTS, with FAD stacked between dUMP and the folate binding site, perfectly situated to shuttle the methylene from $CH_2THF$ to dUMP (**Figure 1.3**).[19] Given the folate products of each enzyme, it is not surprising that all organisms that only carry *thyA* also DHFR to catalyze the reduction of DHF to THF, while some organisms carrying *thyX* have been identified without DHFR. FDTS shares no sequence or structural homology with traditional TS (*thyA*) or DHFR and is found in many pathogenic organism such as *Bacillus anthracis*, *Mycobacterium tuberculosis*, *Helicobacter pylori*, and *Clostridium difficile*, but not in humans. FDTS represents an exciting new drug target and a potential route to use thymine depletion mechanisms as antibacterial therapy.

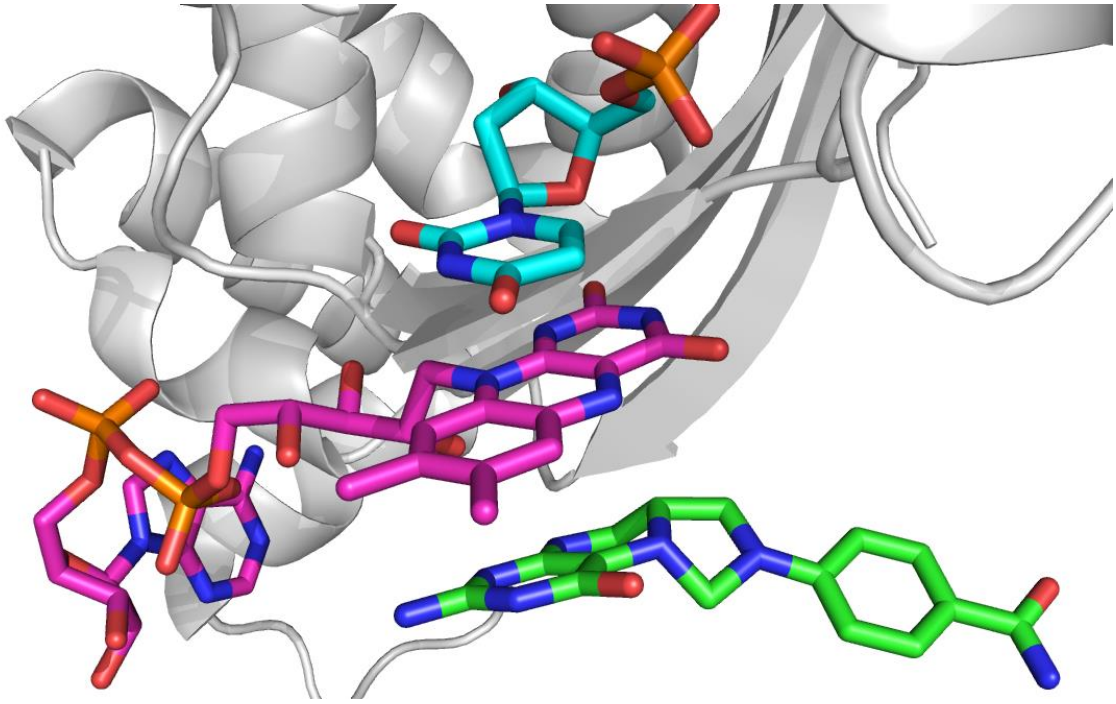

**Figure 1.3** Crystal Structure of ThyX Bound to Folate (PDB: 4GT9)[19]

Recent efforts to find FDTS small molecule inhibitors have yielded compounds with enzyme inhibition activity in the 50-100 nM range; however this research is in its infancy although it should provide interesting drug candidates in the future. Chemical structures of recently synthesized FDTS inhibitors are shown in **Figure 1.4**.[20-24]

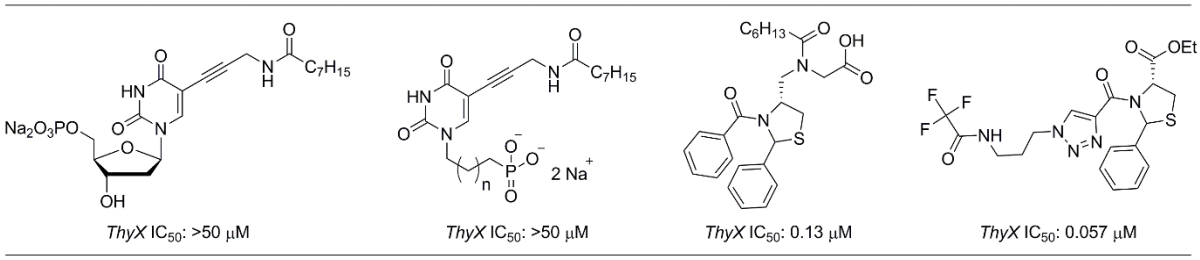


**Figure 1.4** Recently Reported *ThyX* (FDTS) Inhibitors

## 1.5 Dihydrofolate Reductase Inhibition

### *1.5.1 Methotrexate*

DHFR catalyzes the reduction of DHF to THF using NADPH as the reducing co-factor in prokaryotes and eukaryotes alike. Antiproliferative therapies targeting DHFR were first accomplished with the introduction of the classical antifolate aminopterin in 1947 to treat various cancers.[25] Aminopterin was rationally designed as a competitive antagonist of DHF by replacing the pterin ring in DHF with a diaminopteridine ring (**Figure 1.5**). It was soon replaced with its *N*-methylated analog methotrexate (MTX),[26] which is still used today as anticancer therapy and an immunosuppressant to treat rheumatoid arthritis.[27-29] MTX has not found use as antimicrobial therapy despite nanomolar in vitro enzyme activity in various species. Classical antifolates, such as MTX, TDX, and PMX, are highly charged due to their glutamate tail and therefore cannot diffuse across lipid bilayers. This has constrained their use to anticancer therapies, where they enter human cells via folate transporters found only in higher eukaryotes.

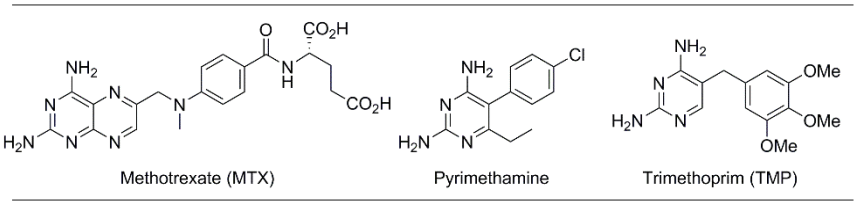


**Figure 1.5** Clinically Used DHFR Inhibitors

### *1.5.2 Pyrimethamine/Trimethoprim*

The first non-classical DHFR inhibitors were discovered soon after MTX at Wellcome laboratories by George Hitchings. Instrumental in determining folate biosynthesis and function, Hitchings rationally designed the antimalarial DHFR inhibitor pyrimethamine.[30] Pyrimethamine was synthesized after Hitchings realized that Proguanil, an antimalarial treatment at the time,[31] was similar in structure to 2,4-diaminopyrimidines. Hitchings had previously identified 2,4-diaminopyrimidines interrupted folate utilization in *Lactobacillus casei*.[32]

Pyrimethamine is a competitive inhibitor of DHFR due to the similar binding motif of 2,4-diaminopyrimidines and the pterin ring of the natural substrate. Pyrimethamine is now co-administered with sulfadioxazine, a member of the sulfa drug class, to treat/prevent malarial infections. Co-administration of DHFR and DHPS inhibitors is the preferred strategy for anti-infective therapy.

Hitchings continued his work on 2,4-diaminopyrimidines, culminating in the discovery of trimethoprim (TMP),[33] the first antibacterial DHFR inhibitor (Hitchings would later receive the Nobel Prize in medicine along with his partner, Gertrude Elion). TMP is similar in structure with pyrimethamine, with a methylene joining the 2,4-diaminopyrimidine ring and the trimethoxybenzene ring. Today, TMP is used in combination therapy with sulfamethoxazole (TMP-SMX, Bactrim) for the treatment of Gram-positive and Gram-negative infections. Their wide-spectrum of activity, tolerability, resistance rates, and low cost have made TMP and the sulfonamides widely used antibiotics. To date, TMP and the sulfonamides represent the only antibacterial antifolates used in a clinical setting.

## 1.6 Bacterial Resistance to Antifolates

Bacteria have evolved a myriad of ways to overcome environmental pressures including human ingenuity in the form of modern antibiotics. Despite the large arsenal of antibacterial therapies available to clinicians, resistant organisms in clinical settings are often difficult to treat. Whether it be drug-modifying enzymes, membrane permeability alterations, extracellular metabolite scavenging, target enzyme mutations/upregulation, or horizontal gene transfer, bacterial resistance is an ever-increasing problem that requires an ever-expanding antibacterial arsenal.

Resistance to Bactrim began to appear in the 1970s[34] shortly after its introduction and widespread use clinically. By the end of the 1980s, reports of *E.coli* resistance rates of 15% and *Proteus spp.* of 24.9% represented a 7- and 4-fold increase in the decade.[35,36] In the 1990s, large differences in resistance rates between the developed world and the developing world began to appear. The international WHONET surveillance program reported that 62% of *E.coli* and 53% of *K. pneumoniae* were resistant to TMP-SMX in Latin America, whereas the corresponding rates in the United States were only 13% and 23%.[37] Simultaneously, an international collection of methicillin-resistant *S. aureus* (MRSA) resistance rates to TMP and SMX were 28% and 35% respectively, while *S. epidermis* resistance rates were 69% for both.[38] Today, resistance rates to *E. coli* and *K. pneumoniae* infection is estimated between 20-30%, while resistance rates to hospital acquired-MRSA infections have been reported to be as high as 50%.[39] Community-acquired MRSA infections are almost completely susceptible to Bactrim, making it a first-line therapy for skin and soft tissue infections cause by MRSA.[40,41]

### *1.6.1 TMP Resistance*

In Gram-positive pathogens, such as *staphylococci*, TMP resistance has been conferred via chromosomal mutations to *dfrB*, the gene that encodes DHFR. Chromosomal mutations have been shown to account for a 256-fold reduction in minimum inhibitor concentration (MIC) and accounted for 88% of resistant strains tested.[42] Of the chromosomal mutations, a single mutation in Phe98 to Tyr98 (F98Y) was identified to reduce the enzyme activity of TMP >400 times ($IC_{50}$ values were 0.01 vs 4.1 μM against against wild-type (wt) DHFR and F98Y DHFR respectively).[42] A second mutation was typically seen, either in H30N or H149R, which restored enzyme fitness to wild-type levels (**Figure 1.6**). The dual mutants, either F98Y/H30N or F98Y/H149R, saw 800- to 2400-fold reductions in TMP activity compared to wild-type activity.[42] Crystal structure analysis of wild-type DHFR revealed two hydrogen bond interactions between the carbonyl oxygen of Phe92, the carbonyl of Leu5, and the deprotonated 4-amino group of TMP. In the F98Y DHFR mutant, Phe92 is oriented unfavorably for hydrogen bonding with TMP, and simultaneously forms a hydrogen bond with Leu5, removing the other hydrogen bond seen in wild-type DHFR.[42]

```
WTSa        1 MTLSILVAHDLQRVIGFENQLPWHLPNDLKHVKKLSTGHTLVMGRKTFESIGKPLPNRRN    60
dfrA        1 MTLSIIVAHDKQRVIGYQNQLPWHLPNDLKHIKQLTTGNTLVMARKTFESIGKPLPNRRN    60
dfrG        1 MKVSLIAAMDKNRVIGKENDIPWRIPKDWEYVKNTTKGHPIILGRKNLESIGRALPDRRN    60
WTEc        1 M-ISLIAALAVDRVIGMENAMPWNLPADLAWFKRNTLNKPVIMGRHTWESIGRPLPGRKN    59
dfrA1       1 MKLSLMVAISKNGVIGNGPDIPWSAKGEQLLFKAITYNQWLLVGRKTFESMGA-LPNRKY    59
dfrA17     26 LKISLISAVSENGVIGSGPDIPWSVKGEQLLFKALTYNQWLLVGRKTFDSMGV-LPNRKY    84

WTSa           VVLTSD-TSFNVEGVDVIHSIEDI-YQLP---GHVFIFGGQTLFEEMIDKVDDMYITVIE    115
dfrA           VVLTNQ-ASFHHEGVDVINSLDEI-KELS---GHVFIFGGQTLYEAMIDQVDDMYITVID    115
dfrG           IILTRD-KGFTFNGCEIVHSIEDV-FELCKNEEEIFIFGGEQIYNLFFPYVEKMYITKIH    118
WTEc           IILSSQ-PGTD-DRVTWVKSVDEA-IAACGDVPEIMVIGGGRVYEQFLPKAQKLYLTHID    116
dfrA1          AVVTRSSFTSDNENVLIFPSIKDALTNLKKITDHVIVSGGGEIYKSLIDQVDTLHISTID    119
dfrA17         AVVSKNGISSSNENVLVFPSIENALKELSKVTDHVYVSGGGQIYNSLIEKADIIHLSTVH    144

WTSa           GKFRGDTFFPPYTFEDWEVASSVEGKLDEKNTIPHTFLHLIRKK---- 159
dfrA           GKFQGDTFFPPYTFEDWEVESSVEGQLDEKNTIPHTFLHLVRRGK--- 160
dfrG           HEFEGDTFFPEVNYEEWNEVFAQKGIKNDKNPYNYYF-HVYERKNLLS 165
WTEc           AEVEGDTHFPDYEPDDWESVFSEFHDADAQNSHSYCFEILERR----- 159
dfrA1          IEPEGDVYFPEI-PSNFRPVFTQDFASN----INYSYQIW-QKG---- 157
dfrA17         VEVEGDIKFPIM-PENFNLVFEQFFMSN----INYTYQIW-KKG---- 182
```

**Figure 1.6** Amino Acid Sequence Alignment of DHFRs. SaDHFR F98 is highlighted. Also the V31I and G43A S1DHFR mutations are highlighted.

*S. aureus* TMP resistance conferred via horizontal gene transfer of plasmids was first identified as a resistance mechanism in 1984.[43,44] Shortly afterwards a *dfrA* gene was discovered encoding a TMP-resistant commonly referred to as S1 DHFR.[45] Believed to originate from *S. epidermis*, S1 DHFR is 80% homologous to wt DHFR.[46] S1 DHFR is characterized by three point mutations, F98Y, V31I, and G43A, that lead to a >1000-fold reduction in TMP activity relative to chromosomal *S. aureus* DHFR.[47] It is interesting to find the F98Y mutation, discussed earlier as a chromosomal mutation, is found in S1 DHFR. Disruption of TMP diaminopyrimidine binding is a fruitful method of resistance. Crystal structure analysis of S1 DHFR bound to TMP revealed a similar hydrogen bonding competition between Tyr98, Leu5, and the diaminopyrimidine ring of TMP discussed earlier (**Figure 1.7**).[48] TMP and NADPH

binding is also synergistic in wt DHFR, whereas in S1 DHFR Ala43 projects into the NADPH binding site resulting in a loss of NADPH enzyme affinity and binding synergism with TMP.[48] When the Ala43 and Tyr98 residues were incorporated into wt *S. epidermis*, S1 DHFR-comparable resistance levels were observed, indicating that binding thermodynamics are the likely culprit of resistance.[47]

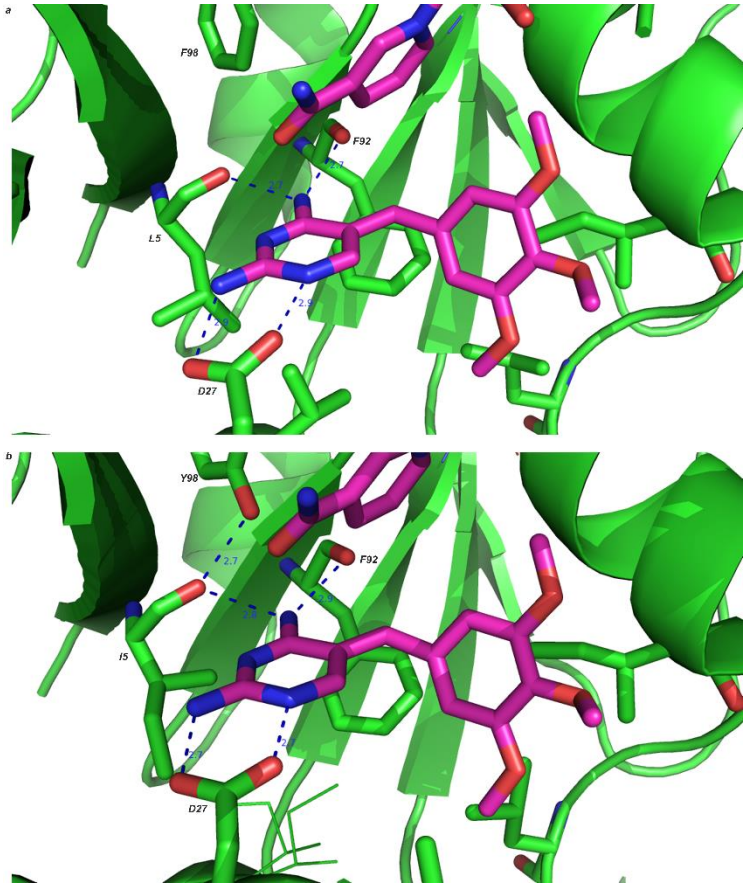


**Figure 1.7** a) TMP Bound to wt SaDHFR (PDB: 3FRE)[49] and b) S1DHFR (PDB: 2W9S)[48]

Recently, plasmids have been discovered carrying new resistance genes encoding for TMP-resistant DHFRs. S3 DHFR, encoded by the *dfrG* gene, was discovered in Thailand in 2005 and showed a 20,000-fold reduction in TMP activity relative to Sa DHFR.[50] All of the 43 strains analyzed from Thailand were TMP-resistant and

contained *dfrG*, whereas only one of 244 strains from Japan was resistant and contained *dfrG*. Although its evolutionary origin is unknown, S3 DHFR was 79% homologous with TMP-resistant *S. haemolyticus* DHFR and only 41% homologous with TMP-sensitive *S. aureus* DHFR. In 2010, genome sequencing identified *dfrG* in a highly-resistant MRSA outbreak in a London hospital.[51] In 2014, a study of 598 MRSA strains from sub-saharan Africa showed that 54% were TMP-resistant.[52] Of those 324 TMP-resistant strains, 94% were carrying *dfrG*. Also, out of 47 MRSA strains isolated in European clinics from travelers to Africa, 57% (27 strains) were TMP-resistant, and all were carrying *dfrG*. Surprisingly, < 1% of TMP-resistant MRSA strains carried the F98Y mutation in *dfrB*. This would suggest that plasmid-acquisition of resistant DHFRs constitutes a larger percentage of clinically relevant TMP-resistant MRSA isolates than previously thought. The molecular mechanism of *dfrG* resistance is still unknown as no S3 DHFR structure has been solved to date.

In 2009, a new plasmid-acquired DHFR was identified from a porcine MRSA isolate, and the gene was named *dfrK*.[53] The presence of *dfrK* led to a dramatic loss in TMP MIC (>256 μg/mL). Sequence homology between *dfrK* and *dfrG* shows 89% similarity; however, *dfrK* shares only 39% and 42% similarity with *dfrA* and *dfrB*, respectively. In 2012, two patients were identified in Spain infected with a MRSA strain that was shown to be carrying *dfrK*, indicating the transfer of resistance factors from animals to humans.[54]

In Gram-negative pathogens, TMP resistance is almost exclusively due to plasmid acquisition of genes encoding for a resistant DHFR enzyme. In 1972, the first report of transmissible resistance factors led to an increase in *E. coli* and *Klebsiella*

*aerogenes* MIC values to >1 mg/mL.[34] This discovery of acquired genes that encode for a resistant protein target represented a novel resistance mechanism.[55] At the time, the study of resistance factors was primarily focused on gene acquisition of drug-modifying enzymes, namely the beta-lactamases.[56] Soon after, a plasmid was found in TMP-resistant *E. coli* that carried a gene encoding for a TMP-sensitive DHFR.[57] It was shown to confer resistance via a novel mechanism: increasing TMP concentrations induced overexpression of the plasmid-acquire gene, thus conferring resistance.[58] To date, over 30 *dfr* genes have been identified. Nomenclature was historically confusing, and scientists have since adopted the convention of White and Rawlinson.[59] There are two distinct DHFR proteins encoded for by *dfr* genes, type A and B. Plasmid acquired *dfrA* genes are the most commonly identified TMP-resistant genes and code for DHFR proteins similar in size and homology. They are numbered *drfAX*, where X is an Arabic numeral. A literature search shows *dfrA30* is the latest to be identified.[60] The B family consists of three genes, *dfrB1*, *dfrB2*, *dfrB3*, that code for smaller DHFR proteins.[59] Genes of both types are often found on plasmids carrying genes that confer resistance to other antibiotics.

More recently, researchers have tried to identify the prevalence of *dfr* genes that confer resistance. A 2006 study found that 47% of 350 E. coli strains tested were TMP-resistant. Of those, 66% were carrying an extrachromosomal *dfr* gene. Among the genes identified, *dfrA1* and *dfrA17* were found in 45% and 30% of resistant strains respectively, although there were marked regional differences.[61] A similar study found that, out of 320 TMP-resistant E. coli strains, 34% carried *dfrA1,* 26% carried *dfrA17*, and 16% carried *dfrA5*.[62] The same study also tested TMP-resistant *K.*

*pneumoniae* strains and found *dfrA1* (15%), *dfrA5* (13%), *dfrA8* (13%), and *dfrA12* (13%) to be most prevalent. A recent study of Peruvian children found that out of 107 TMP-resistant clinical isolates 13% were carrying *dfrA15* and 10% were carrying *dfrA1*.[63] Strains carrying dfrA17 only made up 2% of resistant strains. Also, 66% of isolates did not have a *dfr* gene that the researchers tested for. Perhaps the low sample size or cohort age affected the results, or perhaps the common TMP-resistant mechanism in Peru varies drastically from other areas. Clearly there is high variability of resistance mechanisms due to geography, cohort, and disease state.

### *1.6.2 Sulfonamide Resistance*

Sulfonamides have been used to treat infections since the 1930s and have seen their clinical relevance change over time as resistant organisms have been identified. As with TMP-resistance, sulfa-resistance is driven primarily by point mutations in the chromosomal gene, *folP*, or acquisition of sulfa-resistant DHPS from mobile gene elements. Understanding how DHPS catalyzes PABA addition to DHPP can yield insight into the molecular mechanisms underpinning DHPS resistance. Until 2012, PABA was believed to nucleophilically displace the pyrophosphate of DHPP via an $S_N2$ mechanism.[64] However, it was shown to proceed via pyrophosphate displacement and carbocation generation in an $S_N1$ fashion.[65] The carbocation is delocalized through the pterin ring and in *Yersinia pestis* is stabilized by Asp184 and Asp101, which are highly conserved across species. The incoming aryl amine of PABA adds to the carbocation in an $S_N1$ fashion to generate DHP. Sulfonamides act by both competing with PABA and acting as a substrate for DHPS, generating

nonfunctional metabolites as a suicide inhibitor. Mutations are more likely to occur outside of the substrate-binding site as binding-site mutations are expected to reduce enzyme affinity for the natural substrate.[66] Many sulfa drugs have moieties attached to aryl sulfonamide functionality that project out of the substrate envelope in close proximity to Phe33 and Pro69. This is the likely reason for known YpDHPS mutations in Phe33, Thr67, and Pro69.

A single point mutation in *E. coli* DHPS, Phe28Leu, led to a 150-fold loss in sulfathiazole DHPS binding, with a 10-fold reduction in enzyme efficiency for PABA binding.[67] Similarly, a later study found a Phe28Leu mutation conferred resistance in *E. coli* DHPS.[68] A Pro64Ser mutation was reported to cause a 100-fold loss in enzyme potency of sulfathiazole.[69,70]

In *S. aureus*, the chromosomal mutation explanation of resistance is complicated. Nine sulfa-resistant clinical isolates were found to exhibit *folP* mutations that identified at least 14 distinct residues implicated in DHPS resistance.[71] No discernable pattern was deduced from the placement of the residues, as they appeared to be scattered across the DHPS surface. In *S. pneumonieae*, sulfa-resistance has been identified via nucleotide repeats that lead to amino acid repeats in critical areas of DHPS tertiary structure. One study identified a 6-nucleotide repeat that led to the duplication of Ile66 and Glu67.[72] Deletion of the 6-nucleotide sequence led to a reduction in $K_m$ of PABA, 2.0 to 0.8 μM, and a reduction in $K_i$ of sulfathiazole, 18 to 0.4 μM. Other studies did not confirm the same duplication, but did confirm the existence of other duplicates as the cause of sulfa-resistance.[73,74] In *Staphylococcus pyogenes*, resistance has existed since sulfanilamide was used in military camps during WWII.[75] Sulfa-resistant

*S. pyogenes folP* was shown to exhibit 111 nucleotide point mutations, resulting in a 30 amino acid difference in DHPS compared to DHPS from susceptible *S. pyogenes*.[76] Resistant DHPS saw a 137-fold loss in $K_i$ of sulfathiazole and a 3.6-fold loss in K*m* of PABA, indicating a small fitness cost of the mutations. The authors concluded that such a large sequence variability in resistant-DHPS versus susceptible-DHPS must be due to a recombination genetic event effecting chromosomal *folP*.

Sulfonamide resistance can also be transferred by mobile gene elements carrying *sul1*, *sul2*, or *sul3* that encode for resistant DHPS.[77-81] In 2006, out of 350 Bactrim-resistant *E .coli* isolates tested, 208 strains were SMX-resistant. Of those strains, *sul1* was identified in 16%, *sul2* in 44%, *sul3* in 3%, and *sul1* and *sul2* in 36.5%. Seven strains out of 208 were SMX-resistant but did not carry one of these plasmid-acquired genes.[61] A 2016 study of various Gram-negative species, all Bactrim-resistant, revealed that 98% of 123 isolates contained at least one plasmid-acquired *sul* gene.[82] In 44 *K. pneumoniae* isolates, 21 carried *sul1* only, 9 carried *sul2*, 11 carried both *sul1* and *sul2*, and 2 carried both *sul1* and *sul3* genes. In 43 *E. coli* isolates, 24 carried *sul2* and 19 carried both *sul1* and *sul2* genes. New therapies targeting DHPS must contend with these well-known and well distributed resistance mechanisms.

While certainly not exhaustive, the resistance mechanisms discussed represent a summary of the problems facing any new antifolate antibacterial therapy. Acquired resistance to the often first-line treatment option TMP represents a possible dangerous reduction in the available antibiotic arsenal that should motivate future drug discovery efforts to design new antifolates to overcome these foreseeable resistance mechanisms.

## 1.7 Recent Antibacterial Antifolates

New antibacterial antifolates should aim to increase the in vitro and in vivo activity of DHPS, DHFR, TS, or FDTS inhibitors. For broad spectrum uses, they should improve upon the activity of currently used therapies and improve activity against clinically-relevant resistance mechanisms. For narrow spectrum use they should target organisms that are innately resistant to current therapies. They should also display activity against emerging bacterial species resistant to commonly used antibiotics such as methicillin, vancomycin, macrolides, and others.

### *1.7.1 DHPP Mimics*

Researchers have attempted to inhibit DHPS by designing competitive antagonists capable of binding to the pterin binding site. While the PABA binding site is highly flexible, the pterin binding site is highly conserved making resistance due to point mutations in the active site less likely. In 1985, Lever et al. reported monocyclic 6-(alkylamino)-5-nitrosoisocytosines inhibited DHPS at low micromolar concentrations, although no antibacterial acitivity was observed (**Figure 1.8**).[83,84] Crystal structure analysis of a single compound revealed conserved pterin-binding interactions.[85] It has been argued that pterin-based inhibitors are limited due to their highly planar structure resulting in poor solubility and lack of scaffold diversity.[86] However, the highly-conserved nature of the pterin-binding site in DHPS requires pterin-like scaffolds. This has led some to extend pterin-based inhibitors further into the anion-binding site, thus introducing $sp^3$-hybridized carbons to reduce planarity and perhaps

design better inhibitors. In 2012, Lee reported novel pyrimido[4,5-c]pyridazine derivatives with *Bacillus anthracis* DHPS inhibition in the low micromolar range that introduced extended carboxylic acids to reach the anionic binding site.[87] Pterin-sulfa conjugates that were designed to act as competitive antagonists of both DHPP and PABA showed low micromolar BaDHPS inhibition.[88] Crystal structure analysis revealed a close similarity to DHPP and PABA binding. Analogs designed to act as transition state mimics, containing a conjugated pterin, sulfa, and phosphate also showed promising activity.[89] Structural analysis showed three interactions missing from the conjugated inhibitor that are present in the natural enzyme substrates. Rational drug design could lead to better enzyme binding and better inhibitors.

### *1.7.2 Iclaprim*

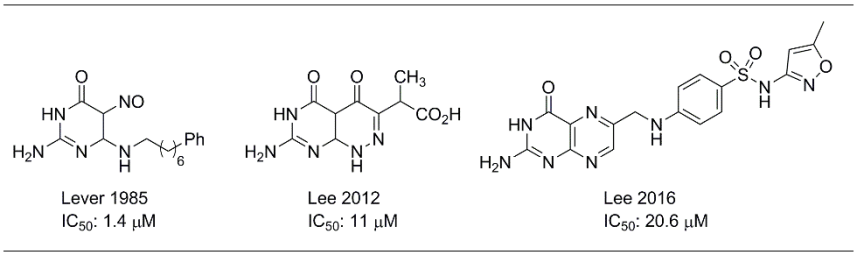


**Figure 1.8** Examples of Pterin-based DHPS Inhibitors

With the success of TMP, many pharmaceutical companies invested in the 2,4-diaminopyrimidine scaffold to find new antifolate antibacterials with little commercial success. Iclaprim, initially patented by Hoffmann-La Roche in 1997,[90] was licensed to and developed by Arida AG. In 2008, after several Phase III trials, the FDA denied Arpida approval to market Iclaprim on the basis that it did not demonstrate superiority to currently used therapies. In 2015, the U.S. FDA granted Motif Bio plc fast-track

status to intravenous Iclaprim for the treatment of acute bacterial skin and skin structure infections. Iclaprim is currently undergoing Phase III clinical trials.

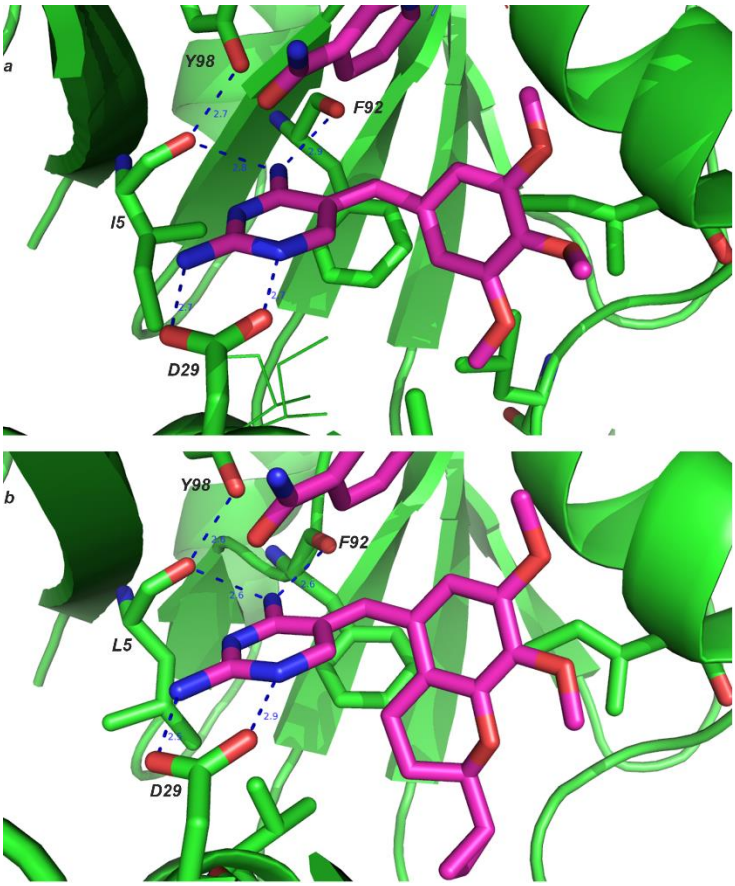


**Figure 1.9** a) TMP Bound to S1DHFR Carrying F98Y Mutation (PDB: 2W9S)[48] b) Iclaprim Bound to F98Y DHFR Mutant (PDB: 3FRA)[49]

Iclaprim's structure is inspired by TMP, with a 4,5-dihydropyran ring fused to C2 and C3 of the trimethoxybenzene of TMP. A cyclopropane extends from C6 of the dihydropyran ring (**Figure 1.9**). It has demonstrated excellent in vitro activity against a broad spectrum of pathogenic bacteria such as MRSA, penicillin-resistant pneumococci, TMP-resistant staphylococci and pneumococci, *H. influenza* and *Moraxella catarrhalis*, *C. pneumoniae*, and Enterobacteriaceae.[91-97] Crystal structure analysis of TMP-resistant MRSA carrying the F98Y DHFR mutation revealed that the

4-amino moiety on the diaminopyrimidine ring of Iclaprim was able to hydrogen bond with Leu5 thus restoring activity (**Figure 1.9**). Iclaprim was also shown to have very low resistance frequency, calculated to be below $10^{-10}$. Resistance induction experiments revealed little change in Iclaprim sensitivity after 15 generations at sub-optimal concentrations, compared to high level resistance observations for TMP after five generations.[91]

### *1.7.3 Propargyl-Linked Antifolates*

Although TMP has broad antibacterial activity, organisms such as *Pseudomonas aeruginosa*, *Acinetobacter*, *Neisseria*, *Brucella*, *Campylobacter*, *Actinomycetes*, mycobacteria, *Clostridium* spp., and others are still innately resistant to TMP due to a resistant DFHR enzyme. This untapped area of antifolates lends itself to rational design of new drugs capable of inhibiting these innately resistant enzymes. In 2007, Anderson and Wright reported the rational design of propargyl-linked antifolates (PLAs) with increased enzyme activity against innately TMP-resistant *Cryptosporidium hominis* and *Toxoplasma gondii* DHFRs.[98] In silico modeling of TMP and methotrexate in both ChDHFR and TgDHFR revealed a large hydrophobic pocket in the PABA ring region of MTX that the trimethoxybenzene ring in TMP was not able to fully extend into.[99] Multiple TMP-derived compounds were synthesized with various carbon-linkers. An alkyne linker was perfectly suited to extend the trimethoxybenzene ring further into the hydrophobic pocket without changing the relative geometry of the diaminopyrimidine ring and the trimethoxybenzene ring. A methyl group was added to the C6 position of the diaminopyrimidine ring to maintain hydrophobic contacts lost

by the extension of the hydrophobic trimethoxybenzene ring. Finally, a chiral methyl group was added to the propargyl position to increase interactions in the hydrophobic pocket. UCP111A-R (**Scheme 1.1**) saw a 368-fold increase in ChDHFR affinity relative to TMP as measured by $IC_{50}$ (0.038 μM and 14 μM respectively) and a 5,714-fold increase in TgDHFR affinity relative to TMP (0.0014 μM and 8 μM respectively). Crystal structure analysis revealed that indeed PLAs make favorable interactions with the hydrophobic pocket previously unreachable by TMP.

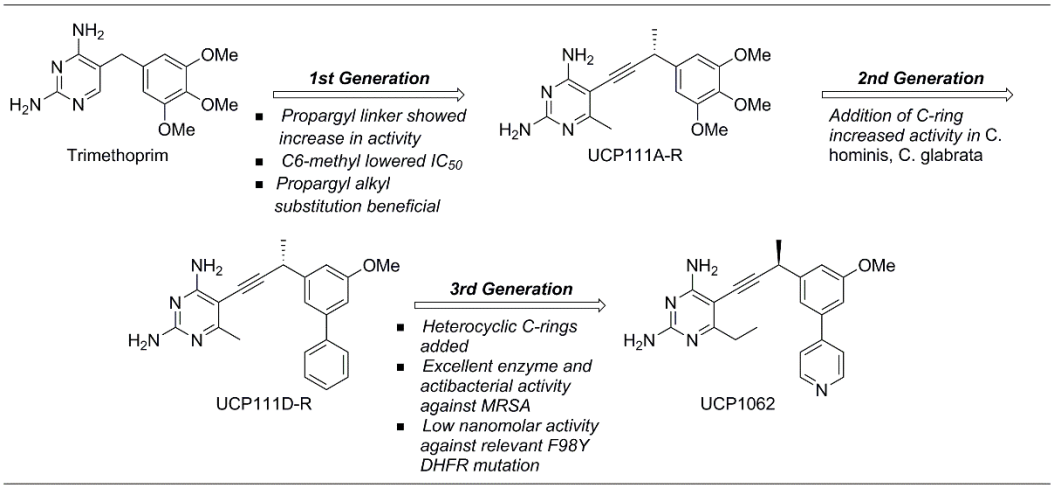


**Scheme 1.1** Evolution of Propargyl-Linked Antifolate (PLA) Scaffold

An iterative process of PLA design, biological evaluation, structure determination, and next generation PLA design has led to a plethora of PLAs with interesting biological activity. Structure analysis of human DHFR revealed a four residue loop (P61, E62, K63, N64, or PEKN) that was absent in ChDHFR. A second generation of biphenyl PLAs was synthesized to exploit this difference by adding a second benzene ring projecting from the trimethoxybenzene ring in the first generation PLAs. UCP111D-R saw a 38-fold increase in ChDHFR affinity relative to the first generation

PLAs without an increase in HuDHFR, leading to a 35-fold increase in selectivity of ChDHFR over HuDHFR.[100] PLAs were tested for antifungal activity in *Candida glabrata* and *Candida albicans*.[101] Second generation PLAs were 13,272 times more active against CgDHFR than TMP as measured by $IC_{50}$ (0.55 nM and 7,300 nM respectively) and 2,470 times more active against CaDHFR than TMP. Second generation PLAs also saw good selectivity over HuDHFR in *C. glabrata*.[102]

TMP-resistance in *S. aureus* is often cause by the F98Y chromosomal mutation discussed earlier. Second generation PLAs saw a 10-fold increase in potency against F98Y SaDHFR relative to TMP as measured by $IC_{50}$ (0.17 μM and 1.70 μM respectively).[103] A third generation of PLAs introduced heterocyclic functionality to move away from the simplified biphenyl PLAs. While retaining low nanomolar activity against SaDHFR, UCP1062 saw a 684-fold increase in *S. pyogenes* DHFR relative to TMP (0.019 μM and 13.0 μM respectively).[104] These compounds also saw an increase in MIC values relative TMP. Against MRSA, the best PLA saw a 7-fold increase in growth inhibition relative to TMP (0.02 μM and 0.14 μM). Against *S. pyogenes*, the UCP1062 saw a 48-fold increase (0.012 μM and 0.58 μM). Against MRSA clinical isolates the UCP1062 showed 33 times more activity than TMP.[104] Nonracemic PLAs showed excellent activity (111 nM) against F98Y DHFR (TMP - 3503 nM) and against MRSA isolates carrying the F98Y DHFR mutation showed increased activity relative to TMP (0.625 μM versus 10 μM respectively).[105]

## 1.8 Summary and Closing Remarks

Antifolates have been staples in the antibiotic arsenal since the discovery of the sulfonamides in the 1930s and the non-classical antifolate TMP in the 1960s. Their wide spectrum of activity, relatively low resistance rates, good tolerability, and low cost have led to their success. Both TMP and multiple sulfonamides have been added to the WHO's list of required therapies for developing countries. However, like all antibiotics, ever-growing bacterial resistance threatens their long-term efficacy and clinical relevance. To that end new drugs are required to take up the antifolate mantle into the future. We have discussed the history of, resistance to, and potential next-generations of antifolates. All the resources available to modern structure based drug design must be employed if we are to be successful and avoid entering the post-antibiotic era.

## 1.9 References


(1) Domagk, G. *Dtsch med Wochenschr* **1935**, *61* (7), 250.

(2) Domagk Gerhard. *Hoppe-Seyler´s Zeitschrift für physiologische Chemie*. 1942, 55.

(3) Trefouel, J.; Trefouel, M. J.; Nitti, F.; Bovet, D. *Press. Medicale* **1937**, *45*, 839.

(4) Roland, S.; Ferone, R.; Harvey, R. J.; Styles, V. L.; Morrison, R. W. *J. Biol. Chem.* **1979**, *254* (20), 10337.

(5) Achari, a; Somers, D. O.; Champness, J. N.; Bryant, P. K.; Rosemond, J.; Stammers, D. K. *Nat. Struct. Biol.* **1997**, *4* (6), 490.

(6) Then, R.; Angehrn, P. *J. Gen. Microbiol.* **1973**, *76* (2), 255.

(7) Rutman, R. J.; Cantarow, A.; Paschkis, K. E. *Cancer Res.* **1954**, *14*, 119.

(8) Heidelberger, C.; Chaudhuri, N. K.; Danneberg, P.; Mooren, D.; Griesbach, L.; Duschinsky, R.; Schnitzer, R. J.; Pleven, E.; Scheiner, J. *Nature* **1957**, *179* (4561), 663.

(9) Longley, D.; Harkin, D.; Johnston, P. *Nat. Rev. Cancer* **2003**, *3* (5), 330.

(10) Wohlhueter, R. M.; McIvor, R. S.; Plagemann, P. G. *J. Cell. Physiol.* **1980**, *104* (3), 309.

(11) Jackman, A. L.; Taylor, G. A.; Gibson, W.; Kimbell, R.; Brown, M.; Calvert, A. H.; Judson, I. R.; Hughes, L. R. *Cancer Res.* **1991**, *51* (20), 5579.

(12) Cunningham, D.; Cocconi, G.; Van Cutsem, E.; Francois, E.; Gustavsson, B.; Van Hazel, G.; Kerr, D.; Possinger, K.; Hietschold, S. M. *J. Clin. Oncol.* **1998**, *16* (9), 2943.

(13) Taylor, E. C.; Kuhnt, D.; Shih, C.; Rinzel, S. M.; Grindey, G. B.; Barredo, J.;

Jannatipour, M.; Moran, R. G. *J. Med. Chem.* **1992**, *35* (23), 4450.

(14) Hammoudeh, D. I.; Daté, M.; Yun, M. K.; Zhang, W.; Boyd, V. A.; Viacava Follis, A.; Griffith, E.; Lee, R. E.; Bashford, D.; White, S. W. *ACS Chem. Biol.* **2014**, *9* (6), 1294.

(15) Myllykallio, H.; Lipowski, G.; Leduc, D.; Filee, J.; Forterre, P.; Liebl, U. *Science* **2002**, *297* (5578), 105.

(16) Dynes, J. L.; Firtel, R. A. *Proc. Natl. Acad. Sci. U. S. A.* **1989**, *86* (20), 7966.

(17) Mishanina, T. V.; Yu, L.; Karunaratne, K.; Mondal, D.; Corcoran, J. M.; Choi, M. A.; Kohen, A. *Science (80-. ).* **2016**, *351* (6272), 507.

(18) Choi, M.; Karunaratne, K.; Kohen, A. *Molecules* **2016**, *21* (5), 654.

(19) Koehn, E. M.; Perissinotti, L. L.; Moghram, S.; Prabhakar, a.; Lesley, S. a.; Mathews, I. I.; Kohen, a. *Proc. Natl. Acad. Sci.* **2012**, *109* (39), 15722.

(20) Esra Önen, F.; Boum, Y.; Jacquement, C.; Spanedda, M. V.; Jaber, N.; Scherman, D.; Myllykallio, H.; Herscovici, J. *Bioorganic Med. Chem. Lett.* **2008**, *18* (12), 3628.

(21) Basta, T.; Boum, Y.; Briffotaux, J.; Becker, H. F.; Lamarre-Jouenne, I.; Lambry, J.-C.; Skouloubris, S.; Liebl, U.; Graille, M.; van Tilbeurgh, H.; Myllykallio, H. *Open Biol.* **2012**, *2* (10), 120120.

(22) Kögler, M.; Vanderhoydonck, B.; De Jonghe, S.; Rozenski, J.; Van Belle, K.; Herman, J.; Louat, T.; Parchina, A.; Sibley, C.; Lescrinier, E.; Herdewijn, P. *J. Med. Chem.* **2011**, *54* (13), 4847.

(23) Parchina, A.; Froeyen, M.; Margamuljana, L.; Rozenski, J.; DeJonghe, S.; Briers, Y.; Lavigne, R.; Herdewijn, P.; Lescrinier, E. *ChemMedChem* **2013**, *8*

(8), 1373.

(24) McGuigan, C.; Derudas, M.; Gonczy, B.; Hinsinger, K.; Kandil, S.; Pertusati, F.; Serpi, M.; Snoeck, R.; Andrei, G.; Balzarini, J.; McHugh, T. D.; Maitra, A.; Akorli, E.; Evangelopoulos, D.; Bhakta, S. *Bioorganic Med. Chem.* **2014**, *22* (9), 2816.

(25) Farber, S.; Diamond, L. K.; Mercer, R. D.; Sylvester, R. F.; Wolff, J. A. *N. Engl. J. Med.* **1948**, *238* (23), 787.

(26) Goldin, A.; Venditti, J. M.; Humphreys, S. R.; Dennis, D.; Mantel, N.; Greenhouse, S. W. *J. Natl. Cancer Inst.* **1955**, *15* (6), 1657.

(27) Chan, E. S. L.; Cronstein, B. N. *Nat. Rev. Rheumatol.* **2010**, *6* (3), 175.

(28) Porcelli, L.; G. Assaraf, Y.; Azzariti, A.; Paradiso, A.; Jansen, G.; J. Peters, G. *Curr. Drug Metab.* **2011**, *12* (10), 975.

(29) Assaraf, Y. G. *Cancer Metastasis Rev.* **2007**, *26* (1), 153.

(30) Falco, E. A.; Goodwin, L. G.; Hitchings, G. H.; Rollo, I. M.; Russell, P. B. *Br. J. Pharmacol. Chemother.* **1951**, *6* (2), 185.

(31) Crowther, A. F.; Levi, A. A. *Br. J. Pharmacol. Chemother.* **1953**, *8* (1), 93.

(32) Hitchings, G. H.; Elion, G. B.; VanderWerff, H.; Falco, E. A. *J. Biol. Chem.* **1948**, *174* (2), 765.

(33) Roth, B.; Falco, E. A.; Hitchings, G. H.; Bushby, S. R. M. *J. Med. Pharm. Chem.* **1962**, *5* (6), 1103.

(34) Fleming, M. P.; Datta, N.; Grüneberg, R. N. *Br. Med. J.* **1972**, *1* (5802), 726.

(35) Towner, K. J.; Slack, R. C. B. *Eur. J. Clin. Microbiol.* **1986**, *5* (5), 502.

(36) Amyes, S. G. B.; Towner, K. J.; Goldstein, F. W.; Acar, J. F.; Tait, S.; Young,

H. K.; Thomson, C. J.; Burdeska, A.; Then, R. L.; Mee, B. J. *J. Med. Microbiol.* **1990**, *31* (1), 1.

(37) Huovinen, P.; Sundstrom, L.; Swedberg, G.; Skold, O. *Antimicrob. Agents Chemother.* **1995**, *39* (2), 279.

(38) Then, R. L.; Kohl, I.; Burdeska, A. *J. Chemother.* **1992**, *4* (2), 67.

(39) Huang, S. H.; Chen, Y. C.; Chuang, Y. C.; Chiu, S. K.; Fung, C. P.; Lu, P. L.; Wang, L. S.; Wu, T. L.; Wang, J. T. *J. Microbiol. Immunol. Infect.* **2015**, *49* (5), 701.

(40) Fridkin, S. K.; Hageman, J. C.; Morrison, M.; Sanza, L. T.; Como-Sabetti, K.; Jernigan, J. A.; Harriman, K.; Harrison, L. H.; Lynfield, R.; Farley, M. M. *N. Engl. J. Med.* **2005**, *352* (14), 1436.

(41) TS, N.; KH, L.; Como-Sabetti, K.; Al, E. *JAMA* **2003**, *290* (22), 2976.

(42) Dale, G. E.; Broger, C.; D'Arcy, a; Hartman, P. G.; DeHoogt, R.; Jolidon, S.; Kompis, I.; Labhardt, a M.; Langen, H.; Locher, H.; Page, M. G.; Stüber, D.; Then, R. L.; Wipf, B.; Oefner, C. *J. Mol. Biol.* **1997**, *266*, 23.

(43) Lyon, B. R.; May, J. W.; Skurray, R. A. *Antimicrob. Agents Chemother.* **1983**, *23* (6), 817.

(44) Lyon, B. R.; Tennent, J. M.; May, J. W.; Skurray, R. A. *FEMS Microbiol. Lett.* **1986**, *33* (2–3), 189.

(45) Young, H. K.; Skurray, R. A.; Amyes, S. G. B. *Biochem. J.* **1987**, *243* (1), 309.

(46) Dale, G. E.; Then, R. L.; Stuber, D. **1993**, *37* (7), 1400.

(47) Dale, G. E.; Broger, C.; Hartman, P. G.; Langen, H.; Page, M. G. P.; Then, R. L.; Stuber, D. *J. Bacteriol.* **1995**, *177* (11), 2965.

(48) Heaslet, H.; Harris, M.; Fahnoe, K.; Sarver, R.; Putz, H.; Chang, J.; Subramanyam, C.; Barreiro, G.; Miller, J. R. *Proteins Struct. Funct. Bioinforma.* **2009**, *76* (3), 706.

(49) Oefner, C.; Bandera, M.; Haldimann, A.; Laue, H.; Schulz, H.; Mukhija, S.; Parisi, S.; Weiss, L.; Lociuro, S.; Dale, G. E. *J. Antimicrob. Chemother.* **2009**, *63* (4), 687.

(50) Sekiguchi, J.; Tharavichitkul, P.; Miyoshi-Akiyama, T.; Chupia, V.; Fujino, T.; Araake, M.; Irie, A.; Morita, K.; Kuratsuji, T.; Kirikae, T. *Antimicrob. Agents Chemother.* **2005**, *49* (9), 3948.

(51) Holden, M. T. G.; Lindsay, J. A.; Corton, C.; Quail, M. A.; Cockfield, J. D.; Pathak, S.; Batra, R.; Parkhill, J.; Bentley, S. D.; Edgeworth, J. D. *J. Bacteriol.* **2010**, *192* (3), 888.

(52) Nurjadi, D.; Olalekan, A. O.; Layer, F.; Shittu, A. O.; Alabi, A.; Ghebremedhin, B.; Schaumburg, F.; Hofmann-Eifler, J.; Van Genderen, P. J. J.; Caumes, E.; Fleck, R.; Mockenhaupt, F. P.; Herrmann, M.; Kern, W. V.; Abdulla, S.; Grobusch, M. P.; Kremsner, P. G.; Wolz, C.; Zanger, P. *J. Antimicrob. Chemother.* **2014**, *69* (9), 2361.

(53) Kadlec, K.; Schwarz, S. *Antimicrob. Agents Chemother.* **2009**, *53* (2), 776.

(54) De Gopegui, E. R.; Juan, C.; Zamorano, L.; Pérez, J. L.; Oliver, A. *Antimicrob. Agents Chemother.* **2012**, *56* (4), 2139.

(55) Amyes, S. G. B.; Smith, J. T. *Biochem. Biophys. Res. Commun.* **1974**, *58* (2), 412.

(56) Skold, O.; Widh, A. *J. Biol. Chem.* **1974**, *249* (13), 4324.

(57) Young, H. K.; Amyes, S. G. *J. Biol. Chem.* **1986**, *261* (6), 2503.

(58) Young, H.-K.; Thomson, C. J.; Amyes, S. G. B. *J. Med. Microbiol.* **1993**, *38* (4), 256.

(59) White, P. A. *J. Antimicrob. Chemother.* **2001**, *47* (4), 495.

(60) Kumar, A.; Chakraborti, S.; Joshi, P.; Chakrabarti, P.; Chakraborty, R. *Ann. Clin. Microbiol. Antimicrob.* **2011**, *10* (1), 19.

(61) Blahna, M. T.; Zalewski, C. A.; Reuer, J.; Kahlmeter, G.; Foxman, B.; Marrs, C. F. *J. Antimicrob. Chemother.* **2006**, *57* (4), 666.

(62) Brolund, A.; Sundqvist, M.; Kahlmeter, G.; Grape, M. *PLoS One* **2010**, *5* (2), e9233.

(63) Medina, A. M.; Rivera, F. P.; Pons, M. J.; Riveros, M.; Gomes, C.; Bernal, M.; Meza, R.; Maves, R. C.; Huicho, L.; Chea-Woo, E.; Lanata, C. F.; Gil, A. I.; Ochoa, T. J.; Ruiz, J. *Trans. R. Soc. Trop. Med. Hyg.* **2015**, *109* (8), 493.

(64) Baca, A. M.; Sirawaraporn, R.; Turley, S.; Sirawaraporn, W.; Hol, W. G. . *J. Mol. Biol.* **2000**, *302* (5), 1193.

(65) Yun, M.-K.; Wu, Y.; Li, Z.; Zhao, Y.; Waddell, M. B.; Ferreira, A. M.; Lee, R. E.; Bashford, D.; White, S. W. *Science (80-. ).* **2012**, *335* (6072), 1110.

(66) Romano, K. P.; Ali, A.; Royer, W. E.; Schiffer, C. a. *Proc. Natl. Acad. Sci. U. S. A.* **2010**, *107* (49), 20986.

(67) Swedberg, G.; Castensson, S.; Skold, O. *J. Bacteriol.* **1979**, *137* (1), 129.

(68) Dallas, W. S.; Gowen, J. E.; Ray, P. H.; Cox, M. J.; Dev, I. K. *J Bacteriol* **1992**, *174* (18), 5961.

(69) Vedantam, G.; Nichols, B. P. *Microb. Drug Resist.* **1998**, *4* (2), 91.

(70) Vedantam, G.; Guay, G. G.; Austria, N. E.; Doktor, S. Z.; Nichols, B. P. *Antimicrob. Agents Chemother.* **1998**, *42* (1), 88.

(71) Hampele, I. C.; D'Arcy, A.; Dale, G. E.; Kostrewa, D.; Nielsen, J.; Oefner, C.; Page, M. G.; Schönfeld, H. J.; Stüber, D.; Then, R. L. *J. Mol. Biol.* **1997**, *268* (1), 21.

(72) Lopez, P.; Espinosa, M.; Greenberg, B.; Lacks, S. A. *J. Bacteriol.* **1987**, *169* (9), 4320.

(73) Maskell, J. P.; Sefton, A. M.; Hall, L. M. *Antimicrob. Agents Chemother.* **1997**, *41* (10), 2121.

(74) Padayachee, T.; Klugman, K. P. *Antimicrob. Agents Chemother.* **1999**, *43* (9), 2225.

(75) DS, D. *J. Am. Med. Assoc.* **1946**, *130* (3), 124.

(76) Swedberg, G.; Ringertz, S.; Sköld, O. *Antimicrob. Agents Chemother.* **1998**, *42* (5), 1062.

(77) Sköld, O. *Antimicrob. Agents Chemother.* **1976**, *9* (1), 49.

(78) Wise, E. M.; Abou-Donia, M. M. *Proc. Natl. Acad. Sci. U. S. A.* **1975**, *72* (7), 2621.

(79) Sundström, L.; Rådström, P.; Swedberg, G.; Sköld, O. *Mol. Gen. Genet.* **1988**, *213* (2–3), 191.

(80) Radstrom, P.; Swedberg, G. *Antimicrob. Agents Chemother.* **1988**, *32* (11), 1684.

(81) Grape, M.; Sundström, L.; Kronvall, G. *J. Antimicrob. Chemother.* **2003**, *52* (6), 1022.

(82) Manyahi, J.; Tellevik, M. G.; Ndugulile, F.; Moyo, S. J.; Langeland, N.; Blomberg, B. *Microb. Drug Resist.* **2016**, *0* (0), mdr. 2016.0074.

(83) Lever Jr., O. W.; Bell, L. N.; McGuire, H. M.; Ferone, R. *J. Med. Chem.* **1985**, *28* (12), 1870.

(84) Lever, O. W.; Bell, L. N.; Hyman, C.; McGuire, H. M.; Ferone, R. *J. Med. Chem.* **1986**, *29* (5), 665.

(85) Babaoglu, K.; Qi, J.; Lee, R. E.; White, S. W. *Structure* **2004**, *12* (9), 1705.

(86) Hevener, K. E.; Yun, M. K.; Qi, J.; Kerr, I. D.; Babaoglu, K.; Hurdle, J. G.; Balakrishna, K.; White, S. W.; Lee, R. E. *J. Med. Chem.* **2010**, *53* (1), 166.

(87) Zhao, Y.; Hammoudeh, D.; Yun, M. K.; Qi, J.; White, S. W.; Lee, R. E. *ChemMedChem* **2012**, *7* (5), 861.

(88) Zhao, Y.; Shadrick, W. R.; Wallace, M. J.; Wu, Y.; Griffith, E. C.; Qi, J.; Yun, M.-K.; White, S. W.; Lee, R. E. *Bioorg. Med. Chem. Lett.* **2016**, *26* (16), 3950.

(89) Qi, J.; Virga, K. G.; Das, S.; Zhao, Y.; Yun, M. K.; White, S. W.; Lee, R. E. *Bioorganic Med. Chem.* **2011**, *19* (3), 1298.

(90) Raffaello, M. Diaminopyrimidines, Pharmaceutical Compositions Containing Them and Their Use as Anitbacterial. WO9720839 (A1), 1997.

(91) Schneider, P.; Hawser, S.; Islam, K. *Bioorganic Med. Chem. Lett.* **2003**, *13* (23), 4217.

(92) Kohlhoff, S. A.; Roblin, P. M.; Reznik, T.; Hawser, S.; Islam, K.; Hammerschlag, M. R. *Antimicrob. Agents Chemother.* **2004**, *48* (5), 1885.

(93) Talbot, G. H.; Thye, D.; Das, A.; Ge, Y. *Antimicrob. Agents Chemother.* **2007**, *51* (10), 3612.

(94) Sincak, C. A.; Schmidt, J. M. *Ann. Pharmacother.* **2009**, *43* (6), 1107.

(95) Sader, H. S.; Fritsche, T. R.; Jones, R. N. *Antimicrob. Agents Chemother.* **2009**, *53* (5), 2171.

(96) Zhanel, G.; Karlowsky, J. A. *Antimicrob. Agents Chemother.* **2009**, *53* (4), 1690.

(97) Neuner, E. A.; Ritchie, D. J.; Micek, S. T. *Semin. Respir. Crit. Care Med.* **2009**, *30* (1), 92.

(98) Pelphrey, P. M.; Popov, V. M.; Joska, T. M.; Beierlein, J. M.; Bolstad, E. S. D.; Fillingham, Y. A.; Wright, D. L.; Anderson, A. C. *J. Med. Chem.* **2007**, *50* (5), 940.

(99) Popov, V. M.; Chan, D. C. M.; Fillingham, Y. A.; Atom Yee, W.; Wright, D. L.; Anderson, A. C. *Bioorganic Med. Chem. Lett.* **2006**, *16* (16), 4366.

(100) Bolstad, D. B.; Bolstad, E. S. D.; Frey, K. M.; Wright, D. L.; Anderson, A. C. *J. Med. Chem.* **2008**, 6839.

(101) Paulsen, J. L.; Liu, J.; Bolstad, D. B.; Smith, A. E.; Priestley, N. D.; Wright, D. L.; Anderson, A. C. *Bioorganic Med. Chem.* **2009**, *17* (14), 4866.

(102) Liu, J.; Bolstad, D. B.; Smith, A. E.; Priestley, N. D.; Wright, D. L.; Anderson, A. C. *Chem. Biol.* **2008**, *15* (9), 990.

(103) Frey, K. M.; Liu, J.; Lombardo, M. N.; Bolstad, D. B.; Wright, D. L.; Anderson, A. C. *J. Mol. Biol.* **2009**, *387* (5), 1298.

(104) Viswanathan, K.; Frey, K. M.; Scocchera, E. W.; Martin, B. D.; Swain, P. W.; Alverson, J. B.; Priestley, N. D.; Anderson, A. C.; Wright, D. L. *PLoS One* **2012**, *7* (2), 1.

(105) Keshipeddy, S.; Reeve, S. M.; Anderson, A. C.; Wright, D. L. *J. Am. Chem. Soc.* **2015**, *137* (28), 8983.

# 2 Charged Non-Classical Antifolates with Diverse Antibiotic Activity

## 2.1 Preface

The following chapter is taken from the following publications:

- Scocchera, E.,† Reeve, S. M.,† Keshipeddy, S., Lombardo, M. N., Hajian, B., Sochia, A. E., Alverson, J. B., Priestley, N. D., Anderson, A. C., Wright, D. L; Charged Nonclassical Antifolates with Activity Against Gram-Positive and Gram-Negative Pathogens. *ACS Med. Chem. Lett.* **2016**, *7*, 692. 10.1021/acsmedchemlett.6b00120
  †Authors contributed equally

- Reeve, S. M.,† Scocchera, E.,† Ferreira, J. J., G-Dayanandan, N., Keshipeddy, S., Wright, D. L., Anderson, A. C; Charged Propargyl-Linked Antifolates Reveal Mechanisms of Antifolate Resistance and Inhibit Trimethoprim-Resistant MRSA Strains Possessing Clinically Relevant Mutations. *J. Med. Chem.* **2016**, *59*, 6493. 10.1021/acs.jmedchem.6b00688
  †Authors contributed equally

- Hajian, B., Scocchera, E., Keshipeddy, S., G-Dayanandan, N., Shoen, C., Kruscinska, J., Reeve, S., Cynamon, M., Anderson, A. C., Wright, D. L; Propargyl-Linked Antifolates Are Potent Inhibitors of Drug-Sensitive and Drug-Resistant Mycobacterium tuberculosis. *PLoS ONE* **2016**, *11*, e0161740. 10.1371/journal.pone.0161740

**Contributions:** My contribution to the work was the design of the carboxylate C-rings intended to mimic MTX interactions, the synthesis of the propargyl unsubstituted inhibitors, and participation in writing the manuscripts. Stephanie Reeve provided the biological data and crystal structure data for *Staphylococcus aureus*. Michael Lombardo provided the biological data for *Escherichia coli*. Behnoush Hajian provided the $IC_{50}$ data and crystal structure data for *Mycobacterium tuberculosis*. Dr. Michael Cynamon provided the anti-tuberculosis data. Santosh Keshipeddy provided the asymmetric PLA-COOHs.

## 2.2 Charge Effects on Drug Penetration into Cells

The natural DHFR substrates, folic acid or dihydrofolate, possess a weakly basic pterin ring and a negatively charged glutamate extension that are critical for binding of the enzyme. Several crystal structures with different species of DHFR reveal that classical antifolates, such as MTX (Fig. 1) and PMX, mimic these motifs of the substrate with a basic nitrogenous headgroup that forms strong contacts with an acidic residue in the active site and a glutamate tail that forms extensive ionic interactions with a basic amino acid (eg. Arg 57 in *S. aureus* DHFR).[1-3] As substrate mimics, classical antifolates often possess very high affinity for DHFR. For example, MTX inhibits human, *Escherichia coli*, and *Staphylococcus aureus* DHFR with $K_i$ values of 3.4 pM, 1 pM and 1 nM,[4,5] respectively. However, as these classical antifolates carry high negative charge at physiological pH, passive diffusion is limited. Currently, all approved anticancer DHFR inhibitors are categorized as classical antifolates as they require active transport through human cell membranes to obtain physiologically relevant concentrations.

As bacteria rely on the *de novo* synthesis of folate cofactors, they do not possess folic acid transporters. Therefore, classical antifolates must enter bacterial cells via passive diffusion which is greatly limited due to its highly charged character at physiological pH. Accordingly, the MIC value of the potent enzyme inhibitor MTX against wild-type Gram-negative *E. coli* is over 1 mM. Even when efflux pumps are genetically deleted, the MIC value is 64-256 μM,[5] demonstrating that the compound has limited permeability and is subject to efflux. Similarly, against the Gram-positive methicillin-resistant *S. aureus* (MRSA), methotrexate has an $MIC_{50}$ of 20 μg/mL or

$MIC_{90}$ of 100 µg/mL.[7] In contrast, the weakly basic, non-classical antifolate trimethoprim (**Figure 2.1**) with attenuated DHFR inhibition ($IC_{50}$ values of 23 nM and 20 nM) is a potent antibacterial against both MRSA and *E. coli* (MIC values of 0.3125 µg/mL) and is a first-line agent with sulfamethoxazole against both Gram-negative and Gram-positive infections.[8-11]

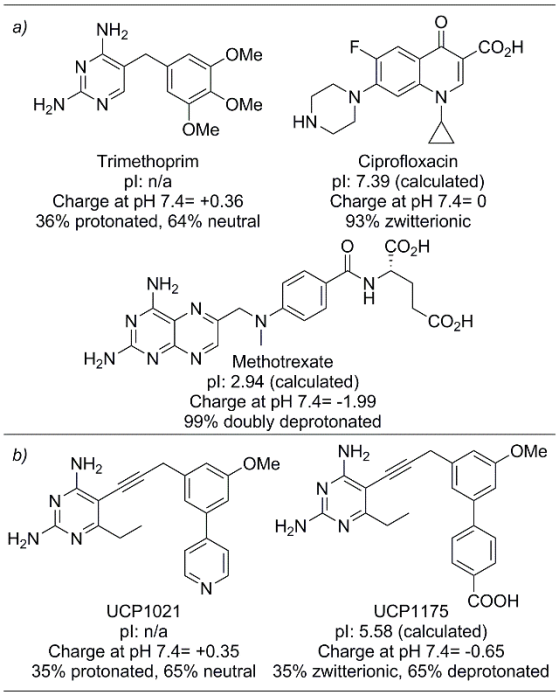


**Figure 2.1** A) Antibacterial Agents Effective against Gram-positive or Gram-negative Bacteria with Relevant Physiological Properties. B) A Previously Reported PLA, UCP1021,[6] is Compared to a PLA-COOH.

The inclusion of two acidic functional groups in MTX results in a highly negatively charged population at physiological pH with a net -2 charge. However, it has been appreciated that zwitterionic compounds possessing only a single acidic functional group, such as fluoroquinolones (Fig. 1) or tetracyclines, show utility against both Gram-positive and Gram-negative bacteria. For example, ciprofloxacin exists almost exclusively as the neutral charge-balanced form. The zwitterionic character

contributes to a lower clog$D_{7.4}$ value (-1.35 for ciprofloxacin), which has been shown to correlate with activity in Gram-negative bacteria[12].

## 2.3 PLA Design and Physical Properties

We have been developing the class of propargyl-linked antifolates (PLAs) as inhibitors of DHFR for both Gram-positive and Gram-negative bacteria. The PLAs, like trimethoprim, are characterized as weakly basic non-classical antifolates that passively diffuse through membranes and potently inhibit the DHFR enzyme,[6,13,14] often inhibiting the growth of bacterial cells with sub-micromolar MIC values. We have achieved very potent MIC values against MRSA and *Streptococcus pyogenes*[6,13,15] and good inhibition of *Klebsiella pneumoniae*[14] with compounds similar to UCP1021 (**Figure 2.1**).

We considered a hybrid design that would allow us to capture contacts typically made by the negatively charged glutamate tail in folate, while increasing bacterial cell permeability. This design would center on replacing the pyridyl function of UCP1021 with a carboxylic acid. Using Marvin (ChemAxon http://www.chemaxon.com), we calculated charges for the molecules in Figure 1 as well as designed PLAs. At neutral pH, the PLAs partition into two primary species: one is deprotonated at the carboxylate group with a neutral pyrimidine ring (65%); the other is deprotonated at the carboxylate group with a protonated pyrimidine ring, yielding a charge-neutral zwitterionic species (35%). The C-ring carboxylic acid functionality (see **Figure 2.1** for ring labels) is designed to form hydrogen bonds with a conserved basic residue (Arg 57 in SaDHFR or EcDHFR) in the active site, respectively. We synthesized eight PLA-COOHs with a

C6-ethyl diaminopyrimidine ring, either unsubstituted or methyl-substituted at the propargylic position, and a biphenyl system with either 2' or 3'-methoxy substituents. Any inhibitors synthesized with propargylic substitutions were prepared as enantiomerically pure compounds.

## 2.4 Synthesis

Alternate *t*-butyl benzoates were coupled via Suzuki reaction to suitable B-ring partners to produce biphenyl aldehydes **1a-d**. The formyl group was elaborated through Wittig homologation and acetylene formation to produce terminal alkynes **2a-d** that were coupled with the diaminopyrimidine headgroup under Sonagashira conditions. We were pleased to observe that final deblocking of the t-butyl ester under strong acidic conditions proceeded smoothly and in good yield to deliver the unbranched inhibitors **3a-d** (**Scheme 2.1**). As initial biological evaluation revealed that the para substitution was superior, non-racemic, methyl-branched homologs of **3c** and **3d** were prepared using our previously reported method.[13] Synthesis of PLA enantiomers began from the previously reported chiral thioesters (**4-5*R/S***) that were coupled to 4-methylbenzoate boronic acid via Suzuki coupling. Similar to the earlier synthesis, methyl ester cleavage could be achieved as the last synthetic step, affording compound **10-11*R/S***.

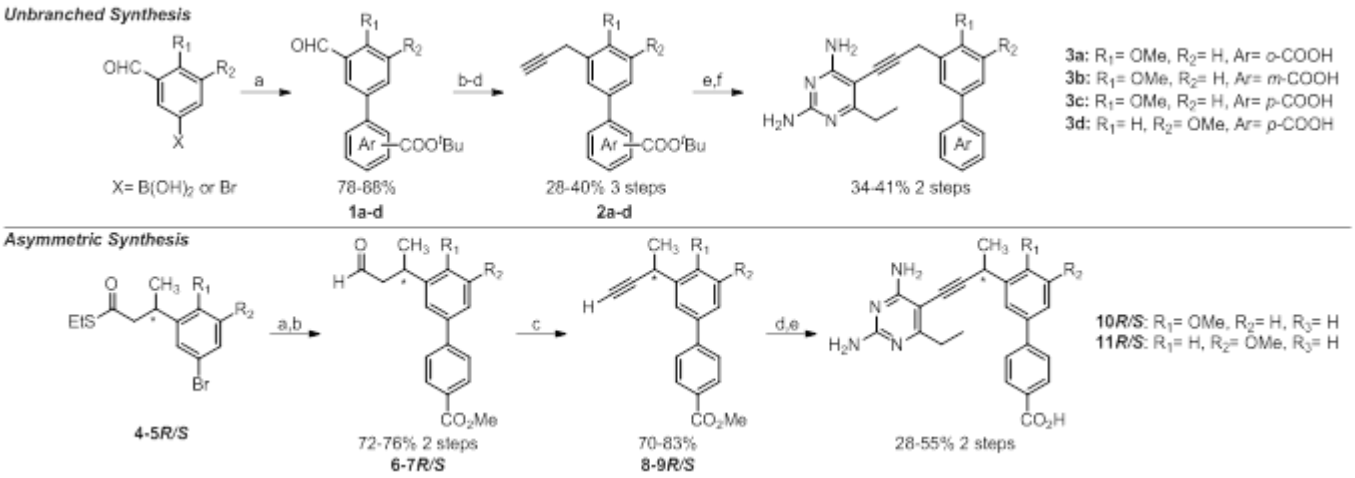


**Scheme 2.1.** Synthesis of Unbranched and Asymmetric PLAs. Reagents and Conditions: ***Unbranched Synthesis:*** (a) Ar-$B(OH)_2$ or Ar-Br, $Pd(PPh_3)_4$, $Cs_2CO_3$, Dioxane:$H_2O$, 90 °C; (b) methoxymethyl triphenylphosphonium chloride, $NaO^tBu$, THF, 0 °C; (c) NaI, TMSCl, MeCN, -20 °C; (d) dimethyl(1-diazo-2-oxopropyl)phosphonate, $K_2CO_3$, MeOH; (e) Iodoethyl diaminopyrimidine, $Pd(PPh_3)_2Cl_2$, CuI, KOAc, DMF, 50 °C; (f) TFA, DCM. ***Asymmetric Synthesis:*** (a) $PdCl_2(PPh_3)_2$, 4-Methoxycarbonylphenylboronic acid, Dioxane:$H_2O$, 90 °C; (b) 10% Pd/C, $Et_3SiH$, DCM; (c) Nonaflyl fluoride, $P_1$-t-Bu-tris(tetramethylene) phosphazene base, DMF, -15 °C to rt; (d) Iodoethyl diaminopyrimidine, $Pd(PPh_3)_2Cl_2$, CuI, KOAc, DMF, 50 °C; (e) LiOH, THF:$H_2O$, 32 °C.

## 2.1 Biological Evaluation

All eight compounds were evaluated for their inhibition ($IC_{50}$ values) of the *S. aureus* (Sa), *E. coli* (Ec) and human (Hu) DHFR enzymes (**Table 1**). Structure-activity analysis of the placement of the carboxylic acid group showed that, while the ortho and meta placement yielded the greatest selectivity over the human enzyme, placement in the para position yields the highest affinity to the pathogenic enzymes. In SaDHFR, moving the carboxylate from the para position to the meta or ortho position results in a 5- and 11-fold loss in activity, respectively. Activity against EcDHFR decreases 6-fold when the carboxylic acid is moved from the *para*- to *meta*-position but only 2.2-fold when moved to the *ortho*-position.

Further modifications were made to the *para*-COOH scaffold including methoxy substitution at the $R_2$ position as well as hydrogen and enantiomerically specific

methyl substitution at the $R_P$ position. Moving the methoxy from the $R_1$ (**3c**) to the $R_2$ (**3d**) position resulted in a three-fold increase in *Sa*DHFR activity, from 4.77 nM to 1.64 nM, respectively. The same change in methoxy position resulted in up to a 5.6-fold decrease in activity against the *Ec*DHFR enzyme. The placement of the methoxy group had little effect on activity against HuDHFR.

**Table 1**. PLA-COOH Enzyme Inhibition Values with Standard Deviations

| Cmpd | $R_P$ | $R_1$ | $R_2$ | Ar | Sa $IC_{50}$ (uM) | Ec $IC_{50}$ (uM) | Hu $IC_{50}$ (uM) |
|---|---|---|---|---|---|---|---|
| **3a** | H | $OCH_3$ | H | *o*-COOH | 0.359±0.03 | 0.195±0.008 | 3.5±0.064 |
| **3b** | H | $OCH_3$ | H | *m*-COOH | 0.157±0.008 | 0.526±0.02 | 1.5±0.056 |
| **3c** | H | $OCH_3$ | H | *p*-COOH | 0.032±0.01 | 0.090±0.006 | 0.817±0.028 |
| **3d** | H | H | $OCH_3$ | *p*-COOH | 0.011±0.0006 | 0.507±0.008 | 0.688±0.039 |
| **10*S*** | S-$CH_3$ | $OCH_3$ | H | *p*-COOH | 0.037±0.002 | 0.177±0.02 | 0.266±0.015 |
| **10*R*** | R-$CH_3$ | $OCH_3$ | H | *p*-COOH | 0.216±0.02 | 0.289±0.04 | 0.52±0.013 |
| **11*R*** | R-$CH_3$ | H | $OCH_3$ | *p*-COOH | 0.009±0.0007 | 0.084 ±0.002 | 0.254±0.015 |
| **11*S*** | S- $CH_3$ | H | $OCH_3$ | *p*-COOH | 0.014±0.001 | 0.166±0.01 | 0.502±0.030 |
| **TMP** | - | - | - | - | 0.023±0.003 | 0.020±0.002 | 198.2±0.1 |

**Table 2**. PLA-COOH Minimum Inhibitory Concentrations

| Cmpd | $R_P$ | $R_1$ | $R_2$ | Ar | ***S. aureus* 43300 (µg/mL)** | ***E. coli* 25922 (µg/mL)** | ***E. coli* NR698 (µg/mL)** |
|---|---|---|---|---|---|---|---|
| **3a** | H | $OCH_3$ | H | *o*-COOH | >20 | >32 | 20 |
| **3b** | H | $OCH_3$ | H | *m*-COOH | 0.625 | >20 | 0.0391 |
| **3c** | H | $OCH_3$ | H | *p*-COOH | 0.0195 | >20 | 0.0098 |
| **3d** | H | H | $OCH_3$ | *p*-COOH | 0.0195 | >20 | 0.0049 |
| **10S** | S-$CH_3$ | $OCH_3$ | H | *p*-COOH | 0.625 | >20 | 0.0391 |
| **10R** | R-$CH_3$ | $OCH_3$ | H | *p*-COOH | 0.0195 | 20 | 0.0012 |
| **11R** | R-$CH_3$ | H | $OCH_3$ | *p*-COOH | 0.0098 | 10 | 0.0024 |
| **11S** | S- $CH_3$ | H | $OCH_3$ | *p*-COOH | 0.0098 | 10 | 0.0024 |
| **TMP** | - | - | - | - | 0.3125 | 0.3125 | 0.0098 |
| **MTX** | - | - | - | - | >40 | >40 | 40 |

Previous studies have shown the importance of evaluating enantiomerically pure PLAs as the methyl configuration is important, not only for its noncovalent interactions but also for directing the binding position of the biaryl system and influencing the binding of alternative cofactor anomer.[13] A colleague, Dr. Santosh Keshipeddy, synthesized propargyl methyl enantiomer of compounds **3c** and **3d**. The *S*-enantiomer of **3c**, inhibitor **10*S***, exhibits no significant change in $IC_{50}$ value, unlike the *R*-enantiomer (**10*R***) that has a 7-fold loss in activity. The 3' methoxy *R*- and *S*-enantiomers, inhibitors **11*R*** and **11*S***, maintain similar activity as their hydrogen-substituted counterpart (**3d**), with $K_i$ values of 1.34, 2.09 and 1.64 nM, respectively.

## 2.2 Crystal Structure Analysis

Structures of SaDHFR bound to the PLA-COOH compounds **3c** and **3d** were determined by X-ray crystallography in order to validate the design principles. SaDHFR bound to **3c** shows the coordination of a water molecule between the carboxylic acid and the side chain of Arg 57 (**Figure 2.2**). SaDHFR bound to **3d** exhibits an extensive water network involving at least four water molecules, coordinated between the carboxylic acid of **3d**, both amino groups on Arg 57 as well as the carbonyl oxygen of Leu 28. The water network expands to include additional hydrogen bonding interactions with the side chains of Asn 56 and Thr 36 (**Figure 2.2**). The binding modes of the inhibitor represent significant differences in the crystal structures with inhibitors **3c** and **3d**. The methoxy substitution in the $R_1$ position of compound **3c** shifts the biaryl system 1.2 Å toward the solvent exposed surface, which

is likely responsible for differences in the observed water networks between compounds **3c** and **3d** (**Figure 2.2**).

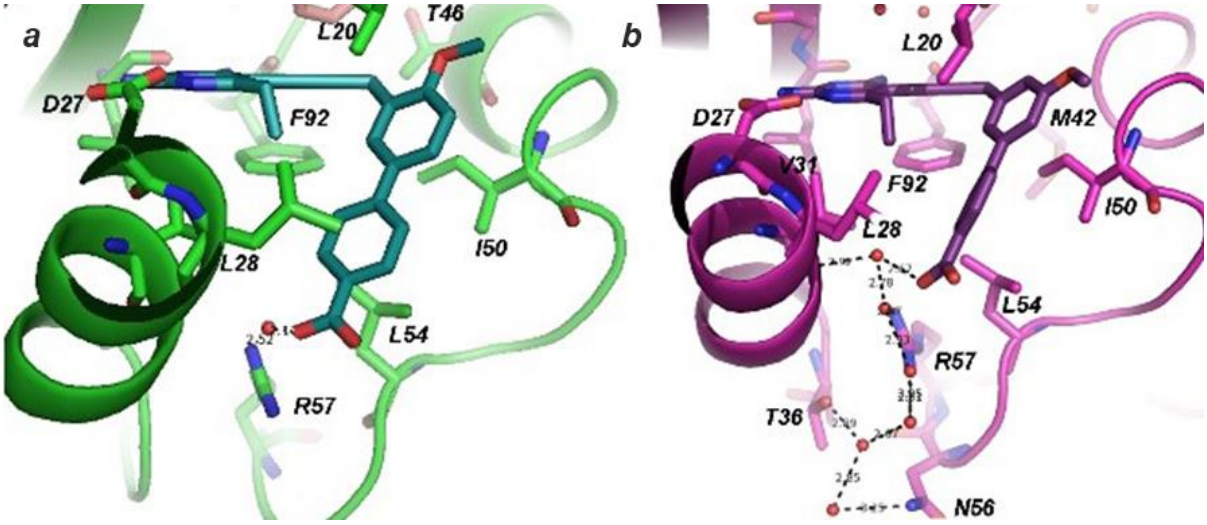


**Figure 2.2** Crystal Structures of Inhibitors **3c** (PDB ID: 5HF0) and **3d** (PDB ID: 5HF2) with SaDHFR and NADPH. A) Compound **3c** (dark green), a mixture of β–NADPH (salmon) and α–NADPH (yellow) and SaDHFR (green). B) Compound **3d** (dark purple), α-NADPH and SaDHFR (purple).

PLA-COOH inhibitors exhibit high levels of activity against the SaDHFR enzyme as well as against *S. aureus* with the majority of MIC values ranging from 0.0098-0.625 µg/mL (**Table 2**). Furthermore, inhibitors **3d**, **11*R*/*S*** were shown to be bactericidal with minimum bactericidal concentrations (MBC) less than four times the MIC (Table S3).[17] The compounds displayed reduced activity against wild-type *E. coli,* with compounds **11*R*** and **11*S*** exhibiting MIC values of 10 µg/mL. Two of the major barriers to activity against Gram-negative bacteria are permeability through the outer membrane and active removal of the inhibitor via efflux. MIC values were measured against NR698,[18] an engineered *E.coli* strain containing an in-frame deletion in the *imp* gene, which encodes a protein essential for outer membrane

assembly. This strain, with its compromised outer membrane, is used specifically to probe the role of compound permeability in antibacterial action.[19] Inhibition concentrations against the NR698 strain with compounds **3a-d** and **10-11*R/S*** showed an approximately 2,000-4,000 fold decrease, indicating that reduced penetration through the outer membrane is limiting PLA activity in *E. coli.* Efflux activity is unlikely as MIC values were not shifted in Δ*acrB,* Δ*macB,* Δ*emrB,* or Δ*acrF* strains (MIC values Δ*acrB* strain are shown in Supplemental Table S4, other data not shown). Similarly, MIC values were maintained between wild-type and porin knockout strains (Δ*ompF* and Δ*ompC*), validating that the compounds passively diffuse into the cells rather than gaining access through porins. MIC values for MTX for these strains were measured as ≥40 μg/mL (**Table 2**).

The extraordinary activity in the Gram-positive bacteria indicates that the design principles were successful, allowing the incorporation of negatively charged functionality to create key contacts with the enzyme without compromising cellular penetration, as with MTX. Alternatively in Gram-negative bacteria, the highly negative lipopolysaccharide barrier may mitigate the penetration of the negatively charged population of PLAs by electrostatic repulsion. This work motivates a further analysis of key physicochemical properties as outlined in **Figure 2.1** to potentially reduce the population of negatively charged species to favor charge-neutral zwitterions and enhance Gram-negative penetration.

## 2.3 Toxicity and Pharmacokinetic Properties

To examine the drug-like potential of the PLA-COOHs, a series of in vitro assays probed their effects on human cells, their inhibition of critical CYP isoforms and their lifetime in microsomal stability assays. The PLA-COOHs had no measurable cytotoxicity toward mammalian cells at concentrations of at least 100 μM. For example, compound **3c** had an $IC_{50}$ value greater than 500 μM toward HepG2, MCF-10A and human dermal fibroblast cells. Coupling the potent activity against Gram-positive bacterial cells with low cytotoxicity yields a high therapeutic index (>500,000). We have also been following cytochrome P450 inhibition for the PLA series and therefore measured the activity of compound **3c** against CYP3A4 and CYP2D6, two of the most prevalent isoforms. Inhibition of both enzymes required concentrations greater than 50 μM, indicating the compound may not interfere with the metabolism of other drugs. Finally, we tested the lifetime of compound **3c** in microsomal stability assays. Compound half-life was measured by following the parent compound using UPLC. The phase I half-life was 99 min and for phase II was approximately 87 min. The results of these in vitro experiments point toward an excellent drug-like profile for the PLA-COOHs.

## *2.4* PLA-COOH Activity against *Mycobacterium tuberculosis*

Tuberculosis (TB) is responsible for one million deaths every year and is one of the top deadly infections worldwide.[20] It is caused by *Mycobacterium tuberculosis* (Mtb), an acid-fast bacteria with an impermeable cell wall. Mtb is able to lie dormant

in macrophages for years in its latent form before multiplying, often in immune-compromised patients such as HIV patients.[21] The current treatment regimen is a combination therapy of four medications, isoniazid, rifampicin, ethambutol, and pyrazinamide, for two months followed by four months of isoniazid and rifampicin treatment. This regimen is often incompatible with HIV and diabetes medications, making treatment difficult. Also, the emergence of multi drug-resistant (MDR) TB and extensively drug-resistant (XDR) TB has limited treatment options further. MDR-TB strains are resistant to isoniazid and rifampicin. Current treatment consists of eight to ten drugs administered over one to two years. XDR-TB strains, in addition to isoniazid and rifampicin resistance, are also resistant to fluoroquinolones and one of the second-line injectables, amikacin, kanamycin, and capreomycin. New therapies, capable of shortening treatment duration, capable of targeting MDR- and XDR-TB, and compatible with other commonly concurrently administered drugs are urgently needed.[20,22-27]

Antifolates are not a currently exploited drug target in TB therapy. Clinically used antifolates, methotrexate, pyrimethamine, and trimetrexate (TMX), are potent inhibitors of Mtb DHFR but have little anti-TB activity, likely due to the inability to permeate the Mtb cell wall. One of the inspirations for synthesizing the COOH-PLAs was the zwitterionic character of the compound aiding in penetration through Gram-negative bacteria. Despite the failure of our rationale, we tested these compounds against Mtb in the hope of penetrating a much different cell wall.

**Table 3**. PLA-COOH MtbDHFR Activity and Anti-TB Activity against MDR-TB and XDR-TB Strains

| | $IC_{50}$ (nM) | | MIC (μg/mL) | | | | | | |
|---|---|---|---|---|---|---|---|---|---|
| **Cmpd** | **MtbDHFR** | **HuDHFR** | **Mtb Erdman** | **Mtb 5** | **Mtb 365** | **Mtb 276** | **Mtb 352** | **Mtb 56** | **Mtb C-31** |
| **3c** | 173 ± 15 | 870 ± 33 | 4 | 8 | 4 | 16 | 16 | 16 | >32 |
| **3b** | 311 ± 24 | 1577 ± 61 | 1 | ND | ND | ND | ND | ND | ND |
| **10R** | 111 ± 7 | 1955 ± 46 | 0.5 | ND | ND | ND | ND | ND | ND |
| **11R** | 177 ± 25 | 1015 ± 60 | <0.03 | 0.25 | <0.03 | ND | 0.06 | 0.06 | 8 |
| **3d** | 460 ± 50 | 688 ± 40 | 0.125 | 2 | 0.125 | ND | 0.5 | 0.5 | 8 |
| TMX | 17 | ND | 4 | ND | ND | ND | ND | ND | ND |
| TMP | 19,560 ± 200 | 97,179 ± 500 | 256 | ND | ND | ND | ND | ND | ND |
| INH | - | - | 0.03 | 4 | 2 | ND | 1 | 1 | 4 |

TMX – Trimetrexate; TMP – Trimethoprim; INH – Isoniazid

We were delighted that PLA-COOHs exhibited good anti-mycobaterium activity (**Table 2**). The best compound **11R** was <0.03 μg/mL, more active in fact than isoniazid, a clinically-used TB drug. Enzyme activity revealed good nanomolar inhibition, with **10R** being the best MtbDHFR inhibitor at 111 nM. However trimetrexate was nearly 10-fold more active against MtbDHFR with an $IC_{50}$ of 17 nM, despite its MIC value of 4 μg/mL. We believe this discrepancy can be explained by our COOH-PLAs being better able to permeate the Mtb cell.

We tested our COOH-PLAs against various clinically isolated MDR- and XDR-TB strains (in Table X, MDR strains are Mtb 365, Mtb 276, MTb 352, Mtb 56 and Mtb C-31; the single XDR strain is Mtb 5). The best compound **11R** showed excellent activity against three of the MDR-TB strains tested, with an MIC value no higher than 0.06 μg/mL. Against XDR-TB **11R** saw a 16-fold increase in activity compared to isoniazid, 0.25 μg/mL vs. 4 μg/mL respectively.

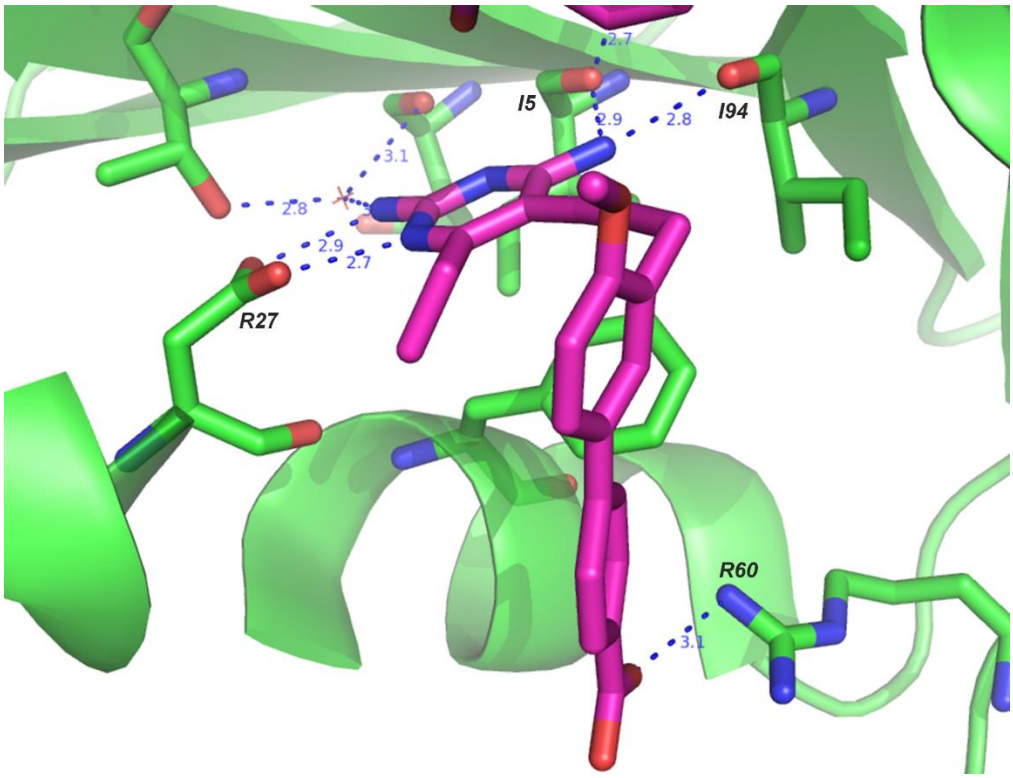


**Figure 2.3** Crystal Structure of **3c** Bound to MtbDHFR. (PDB: 5JA3)

In order to investigate the molecular interactions between MtbDHFR and the PLA-COOHs, MtbDHFR was crystallized with **3c**, an earlier PLA with promising Mtb activity, albeit less than **11R**. Structure analysis revealed that the 2,4-diaminopyrimidine ring makes the expected hydrogen bonds with Asp27, the carbonyls of I5 and I94, and a water-mediated hydrogen bond with the carbonyl of Glu111 and Thr113 (**Figure 2.3**). MtbDHFR carries a Tyr100 in a similar position of the TMP-resistant F98Y *S. aureus* mutant; however, it does not appear to disrupt hydrogen bonding. Phe31 appears to make pi-stacking interactions with the diaminopyrimidine and alkyne. The C-ring acid in **3c** makes a hydrogen bond with Arg60; however, it is not an idealized interaction between carboxylic acid and Arg60 because the rigid PLA structure doesn't allow for proper orientation.

## 2.5 Conclusion

In summary, this work presents a new series of hybrid antifolates that demonstrates how the incorporation of a carboxylate moiety to mimic one of the key interactions common to classical antifolates can be incorporated into the propargyl-linked antifolate architecture without compromising the ability to gain access to the target enzyme, DHFR. The evaluation of eight inhibitors showed that they have high enzyme affinity and increased antibacterial activity against MRSA, *E. coli*, and *M. tuberculosis* relative to earlier PLAs. High resolution crystal structures of two compounds with *S. aureus* DHFR reveal that affinity is enhanced by water-mediated contacts between the carboxylate and Arg 57 in the active site. Against M. tuberculosis DHFR, high resolution crystal structure analysis reveals a non-idealized interaction between the C-ring carboxylate and Arg 60. Additional profiling supports the development of these compounds as antibacterial candidates.

## 2.6 Experimental

All reactions, unless specified, were conducted under an atmosphere of argon in glassware that had been flame dried. Methylene chloride ($CH_2Cl_2$) was used from Baker Cycle-Tainers, anhydrous toluene, *tert*-butyl methyl ether (MTBE), dioxane, triethylamine and dimethylformamide (DMF) were purchased from Sigma-Aldrich. Josiphos was purchased from STREM, pyridine boronic acid from Frontier Scientific, MeMgBr (3.0 M in diethyl ether); $CuBr{\cdot}SMe_2$ from Sigma-Aldrich and was recrystallized from $Me_2S$ prior to use. Where appropriate, control of temperature was achieved with a Neslab Cryocool CC-100 II immersion cooler, ice-bath or a heated oil bath. $^1H$ NMR spectra were recorded at 400 MHz, and/or at 500 MHz and calibrated to the $CDCl_3$ peak at 7.28 ppm. $^{13}C$ NMR spectra were recorded at 100MHz, and/or at 125 MHz and calibrated to the $CDCl_3$ peak at 77.23 ppm. Chemical shifts are reported in units of parts per million (ppm). High-resolution mass spectra were obtained on the JMS-AX505HA instruments and/or on an AccuTOF instrument at the University of Connecticut. Flash chromatography was performed on Silica Gel, 40 microns, 32-63 flash silica and/or $-NH_2$ capped spherical silica gel. Thin layer chromatography was performed on silica gel (Silica Gel 60 $F_{254}$) glass plates and the compounds were visualized by UV and/or potassium permanganate stain.

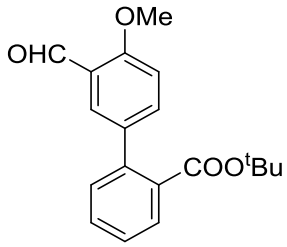


**3'-Formyl-4'-methoxybiphenyl-2-carboxylic acid *tert*-butyl ester (1a)**. In a screw cap pressure vessel fitted with a stir bar was added 2-(tert-butoxycarbonylphenyl) boronic acid (1.00 g, 4.98 mmol), 3-bromo-5-methoxybenzaldehyde (1.28 g, 4.98 mmol), $Pd(PPh_3)_4$ (0.29 g, 0.25 mmol, 5% Pd), $Cs_2CO_3$ (4.09 g, 12.45 mmol), anhydrous dioxane (20 mL), and water (2 mL). The mixture was degassed by bubbling argon through for 15 min, sealed, and heated to 100 °C for 4 h, when TLC showed consumption of aryl bromide. The reaction was diluted with saturated brine and extracted 3x with EtOAc. The combined organic layers were dried over $NaSO_4$ and filtered. The filtrate was concentrated and purified by flash column chromatography ($SiO_2$, 40 g, 5% EtOAc/hexanes) to afford bicyclic ester **1a** as a slightly yellow solid (1.34 g, 86%); $^1$H NMR (500 MHz, $CDCl_3$) $\delta$ 10.55 (s, 1H), 7.86 (d, $J$ = 2.4 Hz, 1H), 7.84 (dd, $J$ = 7.7, 1.4 Hz, 1H), 7.57 (dd, $J$ = 8.5, 2.4 Hz, 1H), 7.53 (td, $J$ = 7.6, 1.5 Hz, 1H), 7.44 (td, $J$ = 7.6, 1.3 Hz, 1H), 7.35 (dd, $J$ = 7.7, 1.3 Hz, 1H), 7.08 (d, $J$ = 8.5 Hz, 1H), 4.03 (s, 3H), 1.38 (s, 9H); $^{13}$C NMR (126 MHz, $CDCl_3$) δ 189.5, 167.6, 161.1, 140.5, 136.0, 134.5, 132.7, 130.9, 130.6, 129.9, 128.7, 127.3, 124.4, 111.4, 81.5, 55.9, 27.8; HRMS (DART $[M+H]^+$) *m/z* 313.1433 (calculated for $C_{19}H_{21}O_4$, 313.1440).

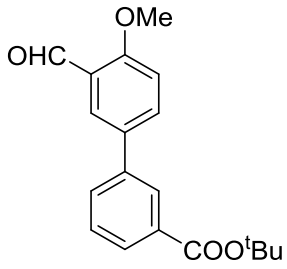


**3'-Formyl-4'-methoxybiphenyl-3-carboxylic acid *tert*-butyl ester (1b)**. According to the general Suzuki coupling procedure, 3-(tert-butoxycarbonylphenyl) boronic acid (0.50 g, 2.25 mmol), 3-bromo-5-methoxybenzaldehyde (0.48 g, 2.25 mmol), $Pd(PPh_3)_4$ (0.13 g, 0.11 mmol, 5% Pd), $Cs_2CO_3$ (1.47 g, 4.5 mmol), anhydrous dioxane (10 mL), and water (1 mL) were added to a 50 mL screw cap pressure vessel. The mixture was degassed by bubbling argon through for 15 min, sealed, and heated to 100 °C for 4 h, when TLC showed consumption of aryl bromide. The reaction was diluted with saturated brine and extracted 3x with EtOAc. The combined organic layers were dried over $NaSO_4$ and filtered. The filtrate was concentrated and purified by flash column chromatography ($SiO_2$, 20 g, 5% EtOAc/hexanes) to afford bicyclic ester **1b** as a slightly yellow solid (0.52 g, 74%); $^1$H NMR (500 MHz, $CDCl_3$) $\delta$ 10.57 (s, 1H), 8.23 (t, $J$ = 1.9 Hz, 1H), 8.14 (d, $J$ = 2.5 Hz, 1H), 8.00 (dt, $J$ = 7.7, 1.4 Hz, 1H), 7.87 (dd, $J$ = 8.6, 2.5 Hz, 1H), 7.77 (dt, $J$ = 7.7, 1.4 Hz, 1H), 7.52 (t, $J$ = 7.7 Hz, 1H), 7.14 (d, $J$ = 8.6 Hz, 1H), 4.03 (s, 3H), 1.67 (s, 9H); $^{13}$C NMR (126 MHz, $CDCl_3$) $\delta$ 189.7, 165.7, 161.5, 139.7, 134.4, 133.0, 132.7, 130.7, 128.8, 128.3, 127.6, 127.0, 125.0, 112.3, 112.3, 81.3, 55.9, 28.2, 28.2; HRMS (DART $[M+H]^+$) *m/z* 313.1434 (calculated for $C_{19}H_{21}O_4$, 313.1440).

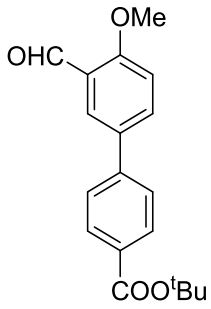


**3'-Formyl-4'-methoxybiphenyl-4-carboxylic acid *tert*-butyl ester (1c)**. According to the general Suzuki coupling procedure, 4-(tert-butoxycarbonylphenyl) boronic acid (1.00 g, 4.98 mmol), 3-bromo-5-methoxybenzaldehyde (1.28 g, 4.98 mmol), $Pd(PPh_3)_4$ (0.29 g, 0.25 mmol, 5% Pd), $Cs_2CO_3$ (4.09 g, 12.45 mmol), anhydrous dioxane (20 mL), and water (2 mL) were added to a 50 mL screw cap pressure vessel. The mixture was degassed by bubbling argon through for 15 min, sealed, and heated to 100 °C for 4 h, when TLC showed consumption of aryl bromide. The reaction was diluted with saturated brine and extracted 3x with EtOAc. The combined organic layers were dried over $NaSO_4$ and filtered. The filtrate was concentrated and purified by flash column chromatography ($SiO_2$, 40 g, 5% EtOAc/hexanes) to afford bicyclic ester **1c** as a slightly yellow solid (1.23 g, 79%); $^{1}$H NMR (500 MHz, $CDCl_3$) $\delta$ 10.53 (s, 1H), 8.12 (d, $J$ = 1.9 Hz, 1H), 8.06 (d, $J$ = 8.1 Hz, 2H), 7.83 (d, $J$ = 10.5 Hz, 1H), 7.63 (d, $J$ = 8.1 Hz, 2H), 7.10 (d, $J$ = 8.7 Hz, 1H), 4.00 (s, 3H), 1.63 (s, 9H); $^{13}$C NMR (126 MHz, $CDCl_3$) $\delta$ 189.5, 165.5, 161.7, 143.3, 134.4, 132.7, 130.8, 130.0, 126.9, 126.3, 125.0, 112.3, 81.1, 55.9, 28.2; HRMS (DART $[M+H]^+$) $m/z$ 313.1412 (calculated for $C_{19}H_{21}O_4$, 313.1440).

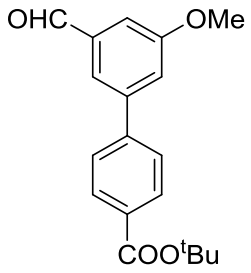


**5'-Formyl-3'-methoxybiphenyl-4-carboxylic acid *tert*-butyl ester (1d)**. According to the general Suzuki coupling procedure, 4-(tert-butoxycarbonylphenyl) boronic acid (0.50 g, 2.25 mmol), 3-bromo-4-methoxybenzaldehyde (0.48 g, 2.25 mmol), $Pd(PPh_3)_4$ (0.13 g, 0. 11 mmol, 5% Pd), $Cs_2CO_3$ (1.47 g, 4.5 mmol), anhydrous dioxane (10 mL), and water (1 mL) were added to a 50 mL screw cap pressure vessel. The mixture was degassed by bubbling argon through for 15 min, sealed, and heated to 100 °C for 4 h, when TLC showed consumption of aryl bromide. The reaction was diluted with saturated brine and extracted 3x with EtOAc. The combined organic layers were dried over $NaSO_4$ and filtered. The filtrate was concentrated and purified by flash column chromatography ($SiO_2$, 20 g, 5% EtOAc/hexanes) to afford bicyclic ester **1d** as a slightly yellow solid (0.54 g, 77%); $^{1}$H NMR (500 MHz, $CDCl_3$) $\delta$ 10.09 (s, 1H), 8.12 (d, $J$ = 8.4 Hz, 2H), 7.74 (m, 1H), 7.70 (d, $J$ = 8.4 Hz, 2H), 7.45 (d, $J$ = 1.7 Hz, 2H), 3.97 (s, 3H), 1.66 (s, 9H); $^{13}$C NMR (126 MHz, $CDCl_3$) $\delta$ 191.9, 165.4, 160.7, 143.4, 142.5, 138.4, 131.7, 130.1, 126.9, 122.3, 120.2, 111.7, 81.3, 55.8, 55.7, 28.2; HRMS (DART $[M+H]^+$) *m/z* 313.1450 (calculated for $C_{19}H_{21}O_4$, 313.1440).

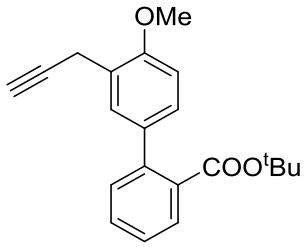


**4'-Methoxy-3'-prop-2-ynylbiphenyl-2-carboxylic acid *tert*-butyl ester (2a)**. In a dried RB flask fitted with a stir bar under argon atmosphere, methoxymethyl triphenylphosphonium chloride (1.37 g, 4.0 mmol) was dissolved in dry THF (10 mL) and cooled to 0 °C. Sodium *tert*-butoxide (0.39 g, 4.0 mmol) was added (reaction turned dark red) and stirred for 20 min. Aldehyde **1a** (0.50 g, 1.6 mmol) was added in dry THF (5 mL, reaction turned orange). TLC analysis showed consumption of **1a** after 30 min. The reaction was quenched with saturated $NH_4Cl$ and extracted with EtOAc (3 x 15 mL). The combined organic layers were washed with brine, dried over $NaSO_4$, and filtered. The filtrate was passed through a column of silica gel (10% EtOAc in hexanes) to afford a mixture of enol ether isomers, which were immediately hydrolyzed in the subsequent step.

In a dried RB flask fitted with a stir bar under argon atmosphere was added enol ether (0.48 g, 1.41 mmol) in MeCN (20 mL). Sodium iodide (0.23 g, 1.55 mmol) was added and the reaction mixture was cooled to -20 °C. TMSCl (0.17 g, 1.55 mmol) was added and stirred at -20 °C for 30 min, when TLC showed SM consumption. The reaction was diluted with EtOAc (20 mL) and $Na_2S_2O_3$ (10 mL) and stirred as reaction warmed to rt. The organic layer was separated and the aqueous phase was extracted with EtOAc (3 x 20 mL). The combined organic layers were washed with brine, dried over

$NaSO_4$, and filtered. The filtrate was concentrated and used without further purification.

In a dried RB flask fitted with a stir bar under argon atmosphere was added aldehyde (0.28 g, 0.86 mmol) in MeOH (5 mL). The Ohira-Bestmann reagent (0.33 g, 1.72 mmol) was added (turned yellow/green) and cooled to 0 °C. Powdered $K_2CO_3$ (0.36 g, 2.58 mmol) was added and stirred at 0 °C for 2 h, when TLC showed consumption of SM. The reaction was diluted with brine (5 mL) and extracted with EtOAc (3 x 15 mL). The combined organic layers were washed with brine, dried over $NaSO_4$ and filtered. The filtrate was concentrated and purified by flash column chromatography ($SiO_2$, 10 g, 5% EtOAc/hexanes) to afford bicyclic alkyne **2a** as a white solid (0.20 g, 39% yield 3 steps); $^1$H NMR (500 MHz,$CDCl_3$) $\delta$ 7.81 (dd, $J$ = 7.7, 1.4 Hz, 1H), 7.54 (dd, $J$ = 2.4, 1.2 Hz, 1H), 7.52 (td, $J$ = 7.5, 1.3, 1H), 7.42 (td, $J$ = 7.5, 1.3 Hz, 1H), 7.38 (dd, $J$ = 7.5, 1.3 Hz, 1H), 7.25 (dd, $J$ = 8.3, 2.3 Hz, 1H), 6.93 (d, $J$ = 8.3 Hz, 1H), 3.93 (s, 3H), 3.66 (d, $J$ = 2.7 Hz, 2H), 2.19 (t, $J$ = 2.7 Hz, 1H), 1.37 (s, 9H); $^{13}$C NMR (126 MHz, $CDCl_3$) $\delta$ 168.2, 156.2, 141.8, 134.2, 133.1, 130.7, 130.6, 129.6, 129.3, 129.3, 127.9, 126.8, 124.0, 109.7, 81.7, 81.2, 70.7, 55.6, 55.6, 27.8, 19.3. HRMS (DART $[M]^+$) $m/z$ 322.1573 (calculated for $C_{21}H_{23}O_3$ 322.1569).

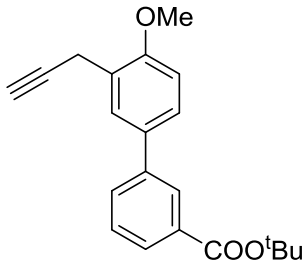

**4'-Methoxy-3'-prop-2-ynylbiphenyl-3-carboxylic acid *tert*-butyl ester (2b)**. In a dried RB flask fitted with a stir bar under argon atmosphere, methoxymethyl triphenylphosphonium chloride (0.88 g, 2.56 mmol) was dissolved in dry THF (8 mL) and cooled to 0 °C. Sodium *tert*-butoxide (0.25 g, 2.56 mmol) was added (reaction turned dark red) and stirred for 20 min. Aldehyde **1b** (0.40 g, 1.28 mmol) was added in dry THF (4 mL, reaction turned orange). TLC analysis showed consumption of **1b** after 30 min. The reaction was quenched with saturated $NH_4Cl$ and extracted with EtOAc (3 x 15 mL). The combined organic layers were washed with brine, dried over $NaSO_4$ and filtered. The filtrate was passed through a column of silica gel (10% EtOAc in hexanes) to afford a mixture of enol ether isomers, which were immediately hydrolyzed in the subsequent step.

In a dried RB flask fitted with a stir bar under argon atmosphere was added enol ether (0.39 g, 1.15 mmol) in MeCN (15 mL). Sodium iodide (0.21 g, 1.38 mmol) was added and the reaction mixture was cooled to -20 °C. TMSCl (0.15 g, 1.38 mmol) was added, stirred at -20 °C for 30 min, when TLC showed SM consumption. The reaction was diluted with EtOAc (20 mL) and $Na_2S_2O_3$ (10 mL) and stirred as reaction warmed to rt. The organic layer was separated and the aqueous phase was extracted with EtOAc (3 x 20 mL). The combined organic layers were washed with brine, dried over $NaSO_4$ and filtered. The filtrate was concentrated and used without further purification.

In a dried RB flask fitted with a stir bar under argon atmosphere was added aldehyde (0.30 g, 0.92 mmol) in MeOH (5 mL). The Ohira-Bestmann reagent (0.35 g, 1.84 mmol) was added (turned yellow/green) and cooled to 0 °C. Powdered $K_2CO_3$ (0.38 g, 2.76 mmol) was added and stirred at 0 °C for 2 h, when TLC showed consumption

of SM. The reaction was diluted with brine (5 mL) and extracted with EtOAc (3 x 15 mL). The combined organic layers were washed with brine, dried over $NaSO_4$ and filtered. The filtrate was concentrated and purified by flash column chromatography ($SiO_2$, 10 g, 5% EtOAc/hexanes) to afford bicyclic alkyne **2b** as a white solid (0.13 g, 31% yield 3 steps); $^1$H NMR (500 MHz, $CDCl_3$) $\delta$ 8.25 (s, 1H), 7.96 (d, $J$ = 7.8 Hz, 1H), 7.82 (d, $J$ = 2.2 Hz, 1H), 7.79 – 7.74 (m, 1H), 7.53 (dd, $J$ = 8.4, 2.2 Hz, 1H), 7.50 (t, $J$ = 7.7 Hz, 1H), 6.96 (d, $J$ = 8.5 Hz, 1H), 3.91 (s, 3H), 3.67 (d, $J$ = 2.6 Hz, 2H), 2.24 (t, $J$ = 2.6 Hz, 1H), 1.66 (s, 9H); $^{13}$C NMR (126 MHz, $CDCl_3$) $\delta$ 165.9, 156.6, 140.9, 132.7, 132.5, 130.7, 130.7, 130.7, 128.6, 127.8, 127.7, 127.7, 127.6, 127.6, 126.6, 125.0, 110.4, 81.8, 81.1, 70.7, 55.6, 28.2, 19.3; HRMS (DART $[M]^+$) *m/z* 322.1578 (calculated for $C_{21}H_{23}O_3$ 322.1569).

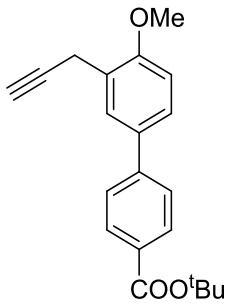


**4'-Methoxy-3'-prop-2-ynylbiphenyl-4-carboxylic acid *tert*-butyl ester (2c)**. In a dried RB flask fitted with a stir bar under argon atmosphere, methoxymethyl triphenylphosphonium chloride (1.37 g, 4.0 mmol) was dissolved in dry THF (10 mL) and cooled to 0 °C. Sodium *tert*-butoxide (0.39 g, 4.0 mmol) was added (reaction turned dark red) and stirred for 20 min. Aldehyde **1c** (0.50 g, 1.6 mmol) was added in dry THF (5 mL, reaction turned orange). TLC analysis showed consumption of **1c** after 30 min. The reaction was quenched with saturated $NH_4Cl$ and extracted with

EtOAc (3 x 15 mL). The combined organic layers were washed with brine, dried over $NaSO_4$ and filtered. The filtrate was passed through a column of silica gel (10% EtOAc in hexanes) to afford a mixture of enol ether isomers, which were immediately hydrolyzed in the subsequent step.

In a dried RB flask fitted with a stir bar under argon atmosphere was added enol ether (0.50 g, 1.47 mmol) in MeCN (20 mL). Sodium iodide (0.26 g, 1.76 mmol) was added and the reaction mixture was cooled to -20 °C. TMSCl (0.19 g, 1.76 mmol) was added, stirred at -20 °C for 30 min, when TLC showed SM consumption. The reaction was diluted with EtOAc (20 mL) and $Na_2S_2O_3$ (10 mL and stirred as the reaction warmed to rt. The organic layer was separated and the aqueous phase was extracted with EtOAc (3 x 20 mL). The combined organic layers were washed with brine, dried over $NaSO_4$ and filtered. The filtrate was concentrated and used without further purification.

In a dried RB flask fitted with a stir bar under argon atmosphere was added aldehyde (0.34 g, 1.03 mmol) in MeOH (7 mL). The Ohira-Bestmann reagent (0.40 g, 2.06 mmol) was added (turned yellow/green) and cooled to 0 °C. Powdered $K_2CO_3$ (0.43 g, 3.09 mmol) was added and stirred at 0 °C for 2 h, when TLC showed consumption of SM. The reaction was diluted with brine (5 mL) and extracted with EtOAc (3 x 15 mL). The combined organic layers were washed with brine, dried over $NaSO_4$ and filtered. The filtrate was concentrated and purified by flash column chromatography ($SiO_2$, 12 g, 5% EtOAc/hexanes) to afford bicyclic alkyne **2c** as a white solid (0.23 g, 45% yield 3 steps); $^1$H NMR (500 MHz, $CDCl_3$) $\delta$ 8.09 (d, $J$ = 8.2 Hz, 2H), 7.85 (d, 1H), 7.66 (d, $J$ = 8.2 Hz, 2H), 7.52 (dd, $J$ = 8.6, 2.4 Hz, 1H), 6.93 (d, $J$ = 8.5 Hz, 1H), 3.89 (s, 3H), 3.67 (d, $J$ = 2.7 Hz, 2H), 2.27 (t, $J$ = 2.5 Hz, 1H), 1.66 (s, 9H); $^{13}$C NMR (126

MHz, $CDCl_3$) $\delta$ 165.8, 156.9, 156.9, 144.8, 132.4, 130.2, 129.9, 129.9, 127.8, 126.7, 126.4, 125.0, 125.0, 110.4, 81.7, 77.4, 77.1, 76.9, 70.9, 55.5, 28.3, 19.4; HRMS (DART $[M]^+$) *m/z* 322.1539 (calculated for $C_{21}H_{23}O_3$ 322.1569).

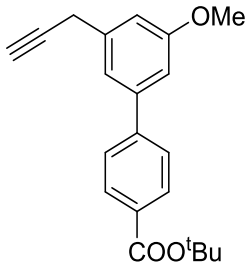


**3'-Methoxy-5'-prop-2-ynylbiphenyl-4-carboxylic acid *tert*-butyl ester (2d)**. In a dried RB flask fitted with a stir bar under argon atmosphere, methoxymethyl triphenylphosphonium chloride (1.76 g, 5.12 mmol) was dissolved in dry THF (12 mL) and cooled to 0 °C. Sodium *tert*-butoxide (0.49 g, 5.12 mmol) was added (reaction turned dark red) and stirred for 20 min. Aldehyde **1d** (0.64 g, 2.05 mmol) was added in dry THF (7 mL, reaction turned orange). TLC analysis showed consumption of **1d** after 30 min. The reaction was quenched with saturated $NH_4Cl$ and extracted with EtOAc (3 x 15 mL). The combined organic layers were washed with brine, dried over $NaSO_4$ and filtered. The filtrate was passed through a column of silica gel (10% EtOAc in hexanes) to afford a mixture of enol ether isomers, which were immediately hydrolyzed in the subsequent step.

In a dried RB flask fitted with a stir bar under argon atmosphere was added enol ether (0.56 g, 1.64 mmol) in MeCN (20 mL). Sodium iodide (0.27 g, 1.8 mmol) was added and the reaction mixture was cooled to -20 °C. TMSCl (0.20 g, 1.8 mmol) was added, stirred at -20 °C for 30 min, when TLC showed SM consumption. The reaction was

diluted with EtOAc (20 mL) and $Na_2S_2O_3$ (10 mL), and stirred as reaction warmed to rt. The organic layer was separated and the aqueous phase was extracted with EtOAc (3 x 20 mL). The combined organic layers were washed with brine, dried over $NaSO_4$ and filtered. The filtrate was concentrated and used without further purification.

In a dried RB flask fitted with a stir bar under argon atmosphere was added aldehyde (0.38 g, 1.15 mmol) in MeOH (7 mL). The Ohira-Bestmann reagent (0.44 g, 2.3 mmol) was added (turned yellow/green) and cooled to 0 °C. Powdered $K_2CO_3$ (0.48 g, 3.45 mmol) was added and stirred at 0 °C for 2 h, when TLC showed consumption of SM. The reaction was diluted with brine (5 mL) and extracted with EtOAc (3 x 15 mL). The combined organic layers were washed with brine, dried over $NaSO_4$ and filtered. The filtrate was concentrated and purified by flash column chromatography ($SiO_2$, 12 g, 5% EtOAc/hexanes) to afford bicyclic alkyne **2d** as a white solid (0.22 g, 34% yield 3 steps); $^1$H NMR (500 MHz, $CDCl_3$) $\delta$ 8.09 (d, $J$ = 8.5 Hz, 2H), 7.67 (d, $J$ = 8.5 Hz, 2H), 7.23 (s, 1H), 7.07 (s, 1H), 7.00 (s, 1H), 3.92 (s, 3H), 3.71 (d, $J$ = 2.6 Hz, 2H), 2.27 (t, $J$ = 2.7 Hz, 1H), 1.66 (s, 9H); $^{13}$C NMR (126 MHz, $CDCl_3$) $\delta$ 165.7, 160.3, 144.9, 141.9, 138.3, 131.1, 129.9, 127.0, 119.4, 113.1, 111.6, 81.6, 81.1, 70.9, 55.5, 28.3, 25.0. HRMS (DART $[M]^+$) $m/z$ 322.1572 (calculated for $C_{21}H_{23}O_3$ 322.1569).

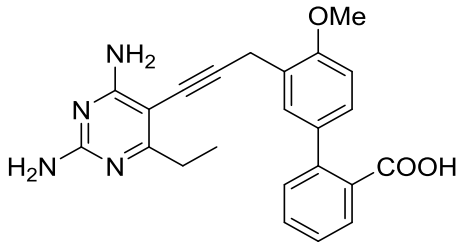

**6-Ethyl-5-[3-(2-methoxy-5-(2-carboxyphenyl)-phenyl)-prop-1-ynyl]-pyrimidine-2,4-diamine (3a)**. In a screw cap vial fitted with a stir bar and a septum, was added alkyne (0.10 g, 0.31 mmol), iodo-ethylpyrimidine (0.06 mg, 0.24 mmol), $Pd(PPh_3)_2Cl_2$ previously doped with 10% CuI by weight (0.01 g, 0.02 mmol), and KOAc (0.23 g, 2.38 mmol). DMF (3 mL) was added and argon was bubbled through the stirring solution for 10 min. The vial was sealed and heated to 50 °C until the reaction was complete by TLC (2-3 h). The reaction was dried in vacuo using toluene as an azeotrope. The residue was washed with saturated sodium bicarbonate, extracted 3x with EtOAc. The organic layer was washed with brine, dried over sodium sulfate, and filtered. The filtrate was concentrated and purified by flash column chromatography (coupled product eluted with 90% EtOAc in hexanes). The coupled *t*butyl ester was carried forward with no further purification.

TFA (0.5 mL) was added to the *t*butyl ester dissolved in DCM (1 mL). The reaction was stirred until complete by TLC (30 min). The reaction was dried in vacuo to remove excess TFA. The carboxylic acid was purified by flash column chromatography (eluted with 8% MeOH in DCM) to give a white solid (0.043 g, 42% 2 step yield); $^1$H NMR (500 MHz, DMSO-$d_6$) δ 7.71 (d, *J* = 7.3 Hz, 1H), 7.56 (t, *J* = 7.5 Hz, 1H), 7.50 – 7.46 (m, 1H), 7.43 (t, *J* = 7.5 Hz, 1H), 7.36 (d, *J* = 7.6 Hz, 1H), 7.23 (dd, *J* = 8.3, 2.0 Hz, 1H), 7.06 (d, *J* = 8.4 Hz, 1H), 6.38 (bs, 2H), 6.21 (bs, 2H), 3.88 (s, 3H), 3.85 (s, 2H), 2.55 (q, *J* = 7.5 Hz, 2H), 1.04 (t, *J* = 7.5 Hz, 3H). $^{13}$C NMR (126 MHz, DMSO) δ 170.3, 164.9, 156.4, 141.2, 133.5, 132.8, 131.2, 130.8, 129.5, 129.2, 128.2, 127.3, 125.1, 110.7, 95.7, 88.6, 76.7, 56.0, 29.1, 21.1, 12.8; HRMS (DART $[M+H]^+$) *m/z* 403.1744 (calculated for $C_{23}H_{23}N_4O_3$ 403.1770).

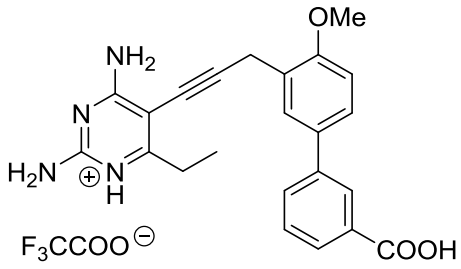


**6-Ethyl-5-[3-(2-methoxy-5-(3-carboxyphenyl)-phenyl)-prop-1-ynyl]-pyrimidine-2,4-diamine-trifluoroacetate salt (3b)**. In a screw cap vial fitted with a stir bar and a septum, was added alkyne (0.10 g, 0.31 mmol), iodo-ethylpyrimidine (0.06 mg, 0.24 mmol), $Pd(PPh_3)_2Cl_2$ previously doped with 10% CuI by weight (0.01 g, 0.02 mmol), and KOAc (0.23 g, 2.38 mmol). DMF (3 mL) was added and argon was bubbled through the stirring solution for 10 min. The vial was sealed and heated to 50 °C until complete by TLC (2-3 h). The reaction was dried in vacuo using toluene as an azeotrope. The residue was washed with saturated sodium bicarbonate, extracted 3x with EtOAc. The organic layer was washed with brine, dried over sodium sulfate, and filtered. The filtrate was concentrated and purified by flash column chromatography (coupled product eluted with 90% EtOAc in hexanes). The coupled *t*butyl ester was carried forward with no further purification.

TFA (0.5 mL) was added to the *t*butyl ester dissolved in DCM (1 mL). The reaction was stirred until complete by TLC (30 min). The reaction was dried in vacuo to remove excess TFA. The carboxylic acid was purified by flash column chromatography (eluted with 8% MeOH in DCM) to give a white solid (0.48 g, 53% yield 2 steps). Compound isolated as the TFA salt; $^1$H NMR (500 MHz, DMSO-$d_6$) δ 8.48 (s, 1H), 8.16 (s, 1H), 7.91 (d, $J$ = 7.7 Hz, 1H), 7.88 (d, $J$ = 7.8 Hz, 1H), 7.78 – 7.75 (m, 1H),

7.73 (s, 1H), 7.67 – 7.63 (m, 1H), 7.59 (t, *J* = 7.7 Hz, 1H), 7.17 (d, *J* = 8.5 Hz, 1H), 3.93 (s, 2H), 3.91 (s, 3H), 2.71 (q, *J* = 7.5 Hz, 2H), 1.18 (t, *J* = 7.6 Hz, 3H)**;** $^{13}$C NMR (126 MHz, DMSO) δ 167.7, 164.9, 164.9, 159.0 (q, *J* = 31.3), 157.0, 154.5, 140.6, 131.9, 131.0, 129.8, 128.1, 127.6, 127.2, 127.0, 125.3, 111.8, 98.6, 91.8, 72.2, 56.2, 25.6, 21.0, 12.4; HRMS (DART $[M+H]^+$) *m/z* 403.1748 (calculated for $C_{23}H_{23}N_4O_3$ 403.1770).

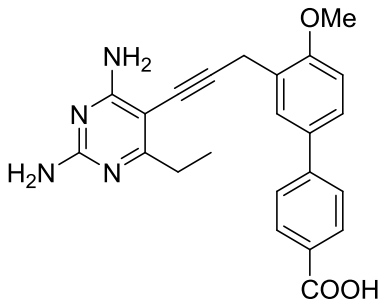


**6-Ethyl-5-[3-(2-methoxy-5-(4-carboxyphenyl)-phenyl)-prop-1-ynyl]-pyrimidine-2,4-diamine (3c)**. In a screw cap vial fitted with a stir bar and a septum, was added alkyne (0.10 g, 0.31 mmol), iodo-ethylpyrimidine (0.06 mg, 0.24 mmol), $Pd(PPh_3)_2Cl_2$ previously doped with 10% CuI by weight (0.01 g, 0.02 mmol), and KOAc (0.23 g, 2.38 mmol). DMF (3 mL) was added and argon was bubbled through the stirring solution for 10 min. The vial was sealed and heated to 50 °C until complete by TLC (2-3 h). The reaction was dried in vacuo using toluene as an azeotrope. The residue was washed with saturated sodium bicarbonate and extracted 3x with EtOAc. The organic layer was washed with brine, dried over sodium sulfate, and filtered. The filtrate was concentrated and purified by flash column chromatography (coupled product eluted with 90% EtOAc in hexanes). The coupled *t*butyl ester was carried forward with no further purification.

TFA (0.5 mL) was added to the *t*butyl ester dissolved in DCM (1 mL). The reaction was stirred until complete by TLC (30 min). The reaction was dried in vacuo to remove excess TFA. The carboxylic acid was purified by flash column chromatography (eluted with 8% MeOH in DCM) to give a white solid (0.039 g, 43% yield 2 steps); $^{1}$H NMR (500 MHz, $CDCl_3$: Methanol-$d_4$) δ 8.08 (d, *J* = 8.4 Hz, 2H), 7.76 (d, *J* = 2.3 Hz, 1H), 7.68 (d, *J* = 8.4 Hz, 2H), 7.61 (dd, *J* = 8.5, 2.4 Hz, 1H), 7.10 (d, *J* = 8.6 Hz, 1H), 3.95 (s, 3H), 3.95 (s, 2H), 2.79 (q, *J* = 7.6 Hz, 2H), 1.28 (t, *J* = 7.6 Hz, 3H); $^{13}$C NMR (126 MHz, DMSO) δ 171.8, 165.0, 161.6, 157.3, 144.2, 131.7, 130.4, 127.9, 127.7, 127.0, 126.5, 126.3, 111.7, 95.7, 88.5, 76.9, 56.2, 29.3, 21.1, 11.0**;** HRMS (DART $[M+H]^+$) *m/z* 403.1746 (calculated for $C_{23}H_{23}N_4O_3$ 403.1770).

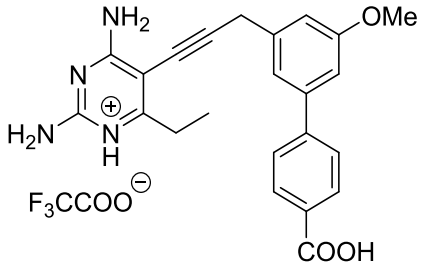


**6-Ethyl-5-[3-(3-methoxy-5-(4-carboxyphenyl)-phenyl)-prop-1-ynyl]-pyrimidine-2,4-diamine-trifluoroacetate salt (3d)**. In a screw cap vial fitted with a stir bar and a septum, was added alkyne (0.10 g, 0.31 mmol), iodo-ethylpyrimidine (0.06 mg, 0.24 mmol), $Pd(PPh_3)_2Cl_2$ previously doped with 10% CuI by weight (0.01 g, 0.02 mmol), and KOAc (0.23 g, 2.38 mmol). DMF (3 mL) was added and argon was bubbled through the stirring solution for 10 min. The vial was sealed and heated to 50 °C until complete by TLC (2-3 h). The reaction was dried in vacuo using toluene as an azeotrope. The residue was washed with saturated sodium bicarbonate and extracted

3x with EtOAc. The organic layer was washed with brine, dried over sodium sulfate, and filtered. The filtrate was concentrated and purified by flash column chromatography (coupled product eluted with 90% EtOAc in hexanes). The coupled *t*butyl ester was carried forward with no further purification.

TFA (0.5 mL) was added to the *t*butyl ester dissolved in DCM (1 mL). The reaction was stirred until complete by TLC (30 min). The reaction was dried in vacuo to remove excess TFA. The carboxylic acid was purified by flash column chromatography (eluted with 8% MeOH in DCM) to give as a white solid (0.045 g, 49% yield 2 steps). Compound isolated as the TFA salt; $^{1}$H NMR (500 MHz, DMSO-$d_6$) δ 7.5-7.0 (bs, 4H), 8.04 (d, $J$ = 7.7 Hz, 2H), 7.81 (d, $J$ = 7.7 Hz, 2H), 7.36 (s, 1H), 7.18 (s, 1H), 7.06 (s, 1H), 4.01 (s, 2H), 3.86 (s, 3H), 2.75 – 2.61 (m, 2H), 1.18 (t, $J$ = 7.4 Hz, 3H)**;** $^{13}$C NMR (126 MHz, DMSO) δ 167.6, 164.9, 160.5, 158.6 (q, $J$ = 31.3), 144.6, 141.1, 139.5, 130.4, 127.4, 119.5, 114.1, 111.1, 98.0, 90.8, 73.4, 55.8, 26.5, 26.0, 12.6**;** HRMS (DART $[M+H]^+$) *m/z* 403.1777 (calculated for $C_{23}H_{23}N_4O_3$ 403.1770).

**HPLC Purity Analysis**

Purity analysis were performed with a reversed phase high performance liquid chromatography on a Shimadzu Prominence 20 instrument fitted with a Luna 5µ C18(2) 100 Å column (5 µM, 4.6 mm x 250 mm, Phenomenex) and using UV diode array detection at 254 nm. Two separate determinations (Method A: isocratic: 40/60/0.1 MeCN/$H_2O$/TFA and Method B: isocratic: 60/40/0.1 MeOH/$H_2O$/TFA or 80/20/0.1 MeOH/$H_2O$/TFA) were made to determine compound purity. Flow rate was 1.0 mL/min for Method A and 1.0 mL/min for Method B. Compounds were diluted in

HPLC grade methanol and filtered prior to analysis. Sample concentrations were 1 mg/ml. All final tested compounds were at least 95% pure according to both methods.

## 2.7 References


(1) Bennett, B.; Wan, Q.; Ahmad, M.; Langan, P.; Dealwis, C. *Structure* **2009,** *166*, 162.

(2) Sawaya, M.; Kraut, J. *Biochemistry* **1997,** *36*, 586.

(3) Li, R.; Sirawaraporn, R.; Chitnumsub, P.; Sirawaraporn, W.; Wooden, J.; Athappilly, F.; Turley, S.; Hol, W. *J. Mol. Biol.* **2000,** *295*, 307.

(4) Burchall, J.; Hitchings, G. *Mol. Pharmacol.* **1965,** *1*, 126.

(5) Kopytek, S.; Dyer, J.; Knapp, G.; Hu, J. *Antimicrob. Agents and Chem.* **2000,** *44*, 3210.

(6) Viswanathan, K.; Frey, K.; Scocchera, E.; Martin, B.; Swain, P.; Alverson, J.; Priestley, N.; Anderson, A.; Wright, D. *PLoS ONE* **2012,** *7*, (2), e29434.

(7) Kruszewska, H.; Zareba, T.; Tyski, S. *Acta Pol. Pharm.* **2000,** *57S*, 117.

(8) Frei, C.; Miller, M.; Lewis, J.; Lawson, K.; Hunter, J.; Oramasionwu, C.; Talbert, R. *J. Am. Board Fam. Med.* **2010,** *23*, 714.

(9) Khawcharoenporn, T.; Tice, A. *Am. J. Med.* **2010,** *123*, 942.

(10) Le, J.; Lieberman, J. *Pharmacotherapy* **2006,** *26*, 1758.

(11) Wood, J.; Smith, D.; Baker, E.; Brecher, S.; Gupta, K. *Antimicrob Agents Chemother.* **2012,** *56*, 5655.

(12) O'Shea, R.; Moser, H. *J. Med. Chem.* **2008,** *51*, 2871.

(13) Keshipeddy, S.; Reeve, S.; Anderson, A.; Wright, D. *J. Am. Chem. Soc.* **2015,** *137*, 8983.

(14) Lamb, K.; Lombardo, M.; Alverson, J.; Priestley, N.; Wright, D.; Anderson, A. *Antimicrob. Agents and Chem.* **2014,** *58*, 7484.

(15) Frey, K.; Viswanathan, K.; Wright, D.; Anderson, A. *Antimicrob. Agents and Chemother.* **2012,** *56*, 3556.

(16) Zhou, W.; Viswanathan, K.; Hill, D.; Anderson, A.; Wright, D. *Drug Metab. Distrib.* **2012,** *40*, 2002.

(17) Pankey, G.; Sabath, L. *Clin Infect Dis* **2004,** *38*, 864.

(18) Jakeman, D.; Sadeghi-Khomami, A. *Biochemistry* **2011,** *50*, 10359.

(19) Ruiz, N.; Falcone, B.; Kahne, D.; Silhavy, T. *Cell* **2005,** *121*, 307.

(20) Koul, A.; Arnoult, E.; Lounis, N.; Guillemont, J.; Andries, K. Nature **2011**, 469 (7331), 483.

(21) Galagan, J. E. Nat. Rev. Genet. **2014**, 15 (5), 307.

(22) Gandhi, N. R.; Nunn, P.; Dheda, K.; Schaaf, H. S.; Zignol, M.; van Soolingen, D.; Jensen, P.; Bayona, J. Lancet **2010**, 375 (9728), 1830.

(23) Gillespie, S. Antimicrob. Agents Chemother. **2002**, 46 (2), 267.

(24) Khachi, H.; O'Connell, R.; Ladenheim, D.; Orkin, C. J. Antimicrob. Chemother. **2009**, 64 (4), 871.

(25) L'homme, R. F.; Nijland, H. M.; Gras, L.; Aarnoutse, R. E.; van Crevel, R.; Boeree, M.; Brinkman, K.; Prins, J. M.; Juttmann, J. R.; Burger, D. M. AIDS **2009**, 27 (7), 863.

(26) Andries, K. Science. **2005**, 307 (5707), 223.

(27) Ruslami, R.; Nijland, H. M. J.; Adhiarta, I. G. N.; Kariadi, S. H. K. S.; Alisjahbana, B.; Aarnoutse, R. E.; van Crevel, R. Antimicrob. Agents Chemother. **2010**, 54 (3), 1068.

(28) Nixon, M. R.; Saionz, K. W.; Koo, M. S.; Szymonifka, M. J.; Jung, H.; Roberts, J. P.; Nandakumar, M.; Kumar, A.; Liao, R.; Rustad, T.; Sacchettini, J. C.; Rhee, K. Y.; Freundlich, J. S.; Sherman, D. R. Chem. Biol. **2014**, 21 (7), 819.

# 3 Design and Development of a New PLA Scaffold: B-ring deleted chain PLAs as Effective Non-Classical Antifolates

## 3.1 Preface

**Contributions:** My contributions to this chapter were the design and synthesis of the chain PLAs. Michael Lombardo provided the biological activity data against *E. coli* and the crystal structure of UCP1103 bound to *E. coli*. Stephanie Reeve provided biological activity data against *S. aureus*.

## 3.2 PLAs and Gram-negative Pathogens

Infections by Gram-negative bacteria pose a significant challenge to drug discovery programs tasked with finding new therapies to treat them. While discovering new drugs to treat Gram-positive bacteria is difficult, Gram-negative bacteria pose a greater challenge largely due to the inability of many Gram-positive antibacterials to enter the Gram-negative cell.[1] Combined with an ever present threat of acquired resistance, it is no surprise that two of the three microorganisms classified by the CDC as 'urgent' are Gram-negative bacteria.[2]

Antifolates, such as Trimethoprim (TMP) and sulfamethoxazole (SMX, administered as Bactrim), are used clinically to treat skin and soft tissue infections and uncomplicated urinary tract infections caused by *Escherichia coli* and *Klebsiella pneumoniae*. TMP inhibits dihydrofolate reductase (DHFR) and SMX inhibits dihydropteroate synthase (DHPS). Both are essential enzymes in the folate pathway responsible for converting dihydrofolate (DHF) to tetrahydrofolate (THF).[3] Recently, Bactrim resistance has reduced its use clinically in favor of nitrofurantoin and fluoroquinolones.[4] Unsurprisingly, fluoroquinolone resistance has followed, complicating its use in treating more serious infections.[5] With Enterobacteriaceae resistance growing and TMP use declining, antifolates represent an opportunity for new therapies.

We have been developing a new class of propargyl-linked antifolates (PLA) as DHFR inhibitors based on modifications to TMP's structure. We have observed excellent enzyme and growth inhibition against methicillin-resistant *Staphyloccocus aureus* (MRSA),[6,7] as well as against clinically relevant TMP-resistant DHFR mutants.[8]

We have also observed excellent MIC activity against *Mycobacterium tuberculosis*, both multi-dug resistant (MDR) and extensively drug resistant (XDR).[9] Unfortunately, we have seen a dramatic reduction in MIC activity against Enterobacteriaceae. We have previously reported PLAs with good MIC activity against *K. pneumoniae*[10,11] however *E. coli* activity is reduced due to the problems associated with antibacterial entry into the Gram-negative cell.

### 3.3 Entry into Gram-negative Bacterial Cells

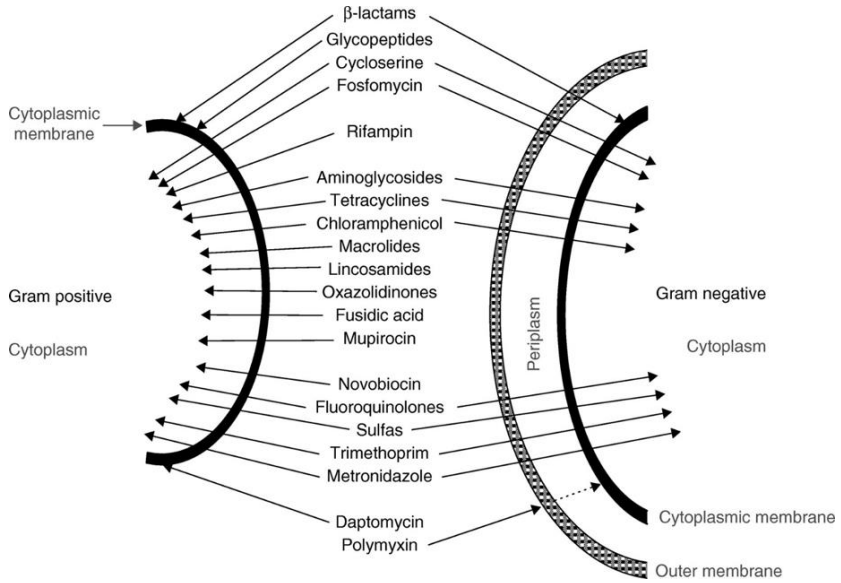


**Figure 3.1** Gram-negative Outer Membrane Restricts Entry of Many Drugs Capable of Targeting Gram-positive Bacteria[1]

It is well known that antibacterial penetration into Gram-negative bacteria is a notoriously difficult problem in drug discovery.[12] While Gram-positive bacteria possess a cytoplasmic membrane that acts as a filter to highly charged compounds, Gram-negative bacteria possess an additional outer membrane (OM) that acts to slow penetration of lipophilic compounds into the cell (**Figure 3.1**). This orthogonal filtering mechanism is significant for the loss in activity of many clinically used Gram-positive antibacterials against Gram-negative pathogens.

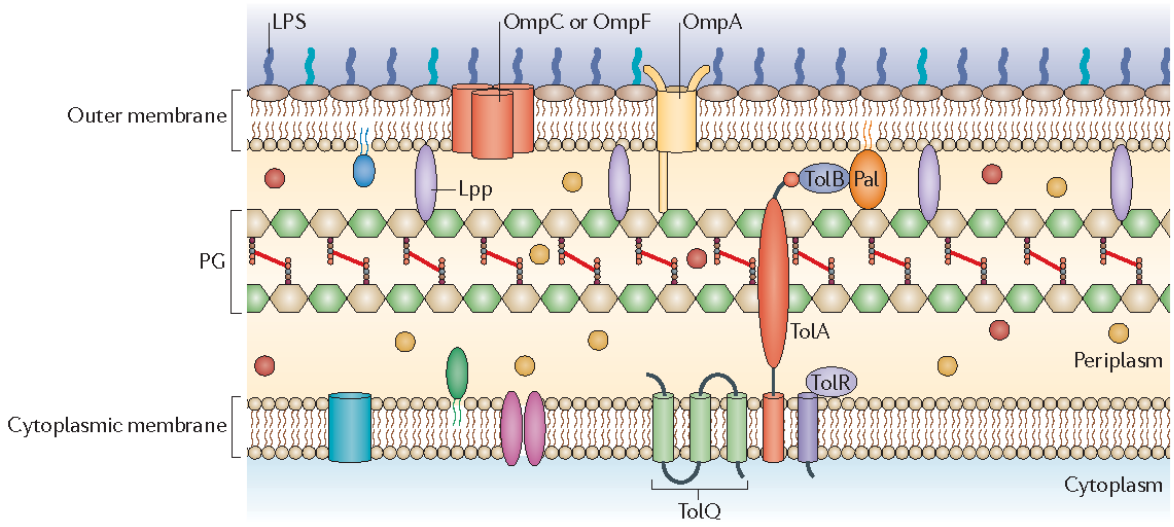


**Figure 3.2** Gram-negative Bacterial Outer Membrane (OM) Architecture[19]

The OM structure is made of a lipid bilayer with ordered lipopolysaccharide (LPS) making up the outer leaflet (**Figure 3.2**). The LPS layer is highly negatively charged, making passive diffusion through the OM difficult compared to a typical lipid bilayer.[13] While passive diffusion is possible, many clinically used antibacterials penetrate the OM through porins, small channels that traverse the OM. Porins allow small, highly charged solutes to enter into the periplasmic space between the OM and inner

membrane (IM). Efflux pumps, multi-protein complexes that span from the OM, through the perisplasm, and anchor to the IM, are working to eject solutes into the extracellular space. Together, the OM and efflux pumps work synergistically to limit accumulation of drug concentration in the cell.[12,14-15]

To overcome the difficulties presented by Gram-negative OM penetration, many have examined the physicochemical properties of clinically used Gram-negative antibacterials to identify structure-activity relationships (SAR). Molecular weight and lipophilicity, measured by the octanol water partition coefficient (logP), have been identified as physical properties that diverge from Gram-positive antibacterials and other clinically used therapeutics (**Figure 3.3**). Nikaido reported the size exclusion limit of the OM was 600 daltons, an often cited number that is not absolute.[16] Nikaido also reported that much larger but more flexible polyethyleneglycols were able to penetrate the OM, meaning that flexibility and shape must play a role in penetration as well.

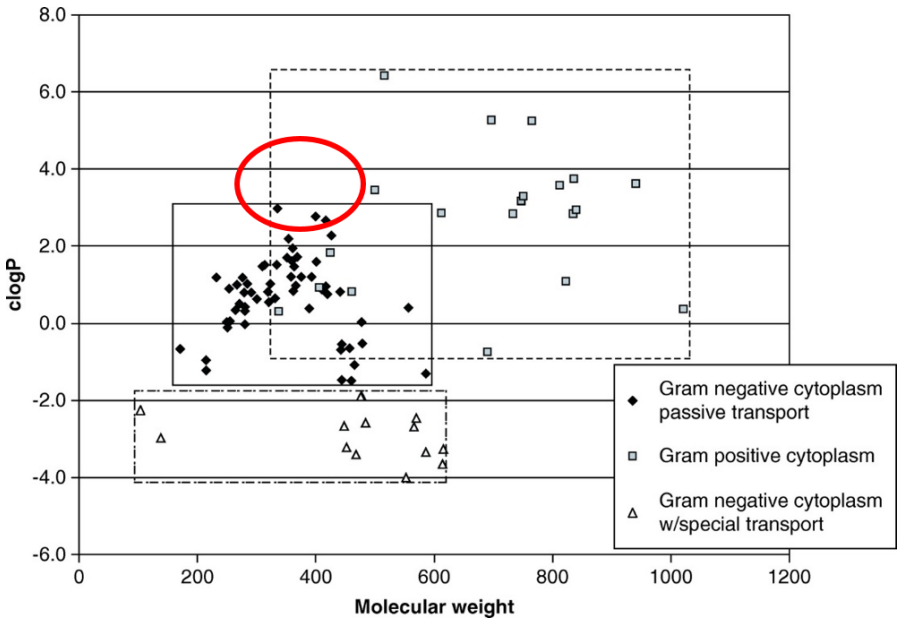


**Figure 3.3** Physical Properties Play a Significant Role in Entry Through the OM. The red circle denotes where traditional PLAs fall on the chart

PLAs have traditionally been highly lipophilic, inflexible compounds with molecular weights above 400 daltons. Here, we report the design, synthesis, and biological activity of chain PLAs. By removing the B-ring, we can retain the necessary enzyme interactions of the diaminopyrimidine and the varied C-rings, while removing a large, hydrophobic, and rigid benzene in favor of a carbon chain. This will have the effect of bringing the physicochemical properties of this new generation of PLAs closer to what is believed to be ideal for Gram-negative cellular penetration.

### 3.4 Design and Synthesis of Chain PLAs

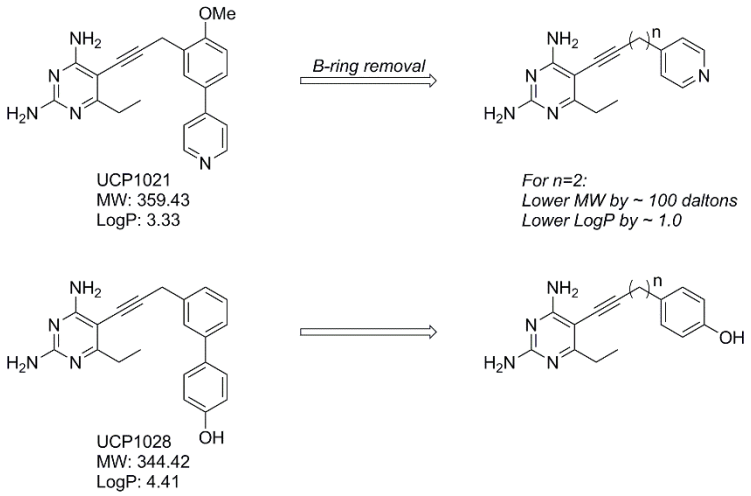


**Scheme 3.1** Design of Chain PLAs from Parent PLAs

We began by modifying a previously reported PLA with nanomolar Gram-positive antibacterial activity and poor Gram-negative antibacterial activity, UCP1021 (**Scheme 3.1**). We envisioned removing the methoxybenzene B-ring and leaving the carbon chain connecting the diaminopyrimidine to a distal pyridine. To determine the ideal chain length three compounds bearing butynyl-, pentynyl-, and hexynyl-linked chains were synthesized. For the truncated butynyl compound **7**, we performed a

Horner-Wadsworth-Emmons reaction to generate the ester with the proper chain length (**Scheme 3.2**). Catalytic hydrogenation, ester reduction, and subsequent re-oxidation gave aldehyde **5**. Typical Ohira-Bestmann alkyne synthesis gave **6**, which was coupled to the diaminopyrimidine via Sonogashira coupling to give **7**. For pentynyl-linked **4a** and butynyl-linked **9**, we knew we could access both from the common aldehyde **2a**. From **1a**, Wittig homologation installed the aldehyde functionality directly via the protected acetal. Catalytic hydrogenation and acetal cleavage gave the desired aldehyde **2a**. Alkyne synthesis gave **3a** which subsequently underwent Sonogashira coupling to generate pentynyl-linked **4a.** From **2a**, a one carbon Wittig homolgation and enol ether cleavage yielded the extended aldehyde which was subjected to Ohira-Bestmann homologation to give alkyne **8**. Sonogashira coupling yielded the desired hexynyl-linked **9**. Biological evaluation determined that the pentynyl-linked **4a** was the most active compound (**Table 3**). Subsequent compounds **4b-c** were synthesized exclusively as the pentynyl-linked variants.

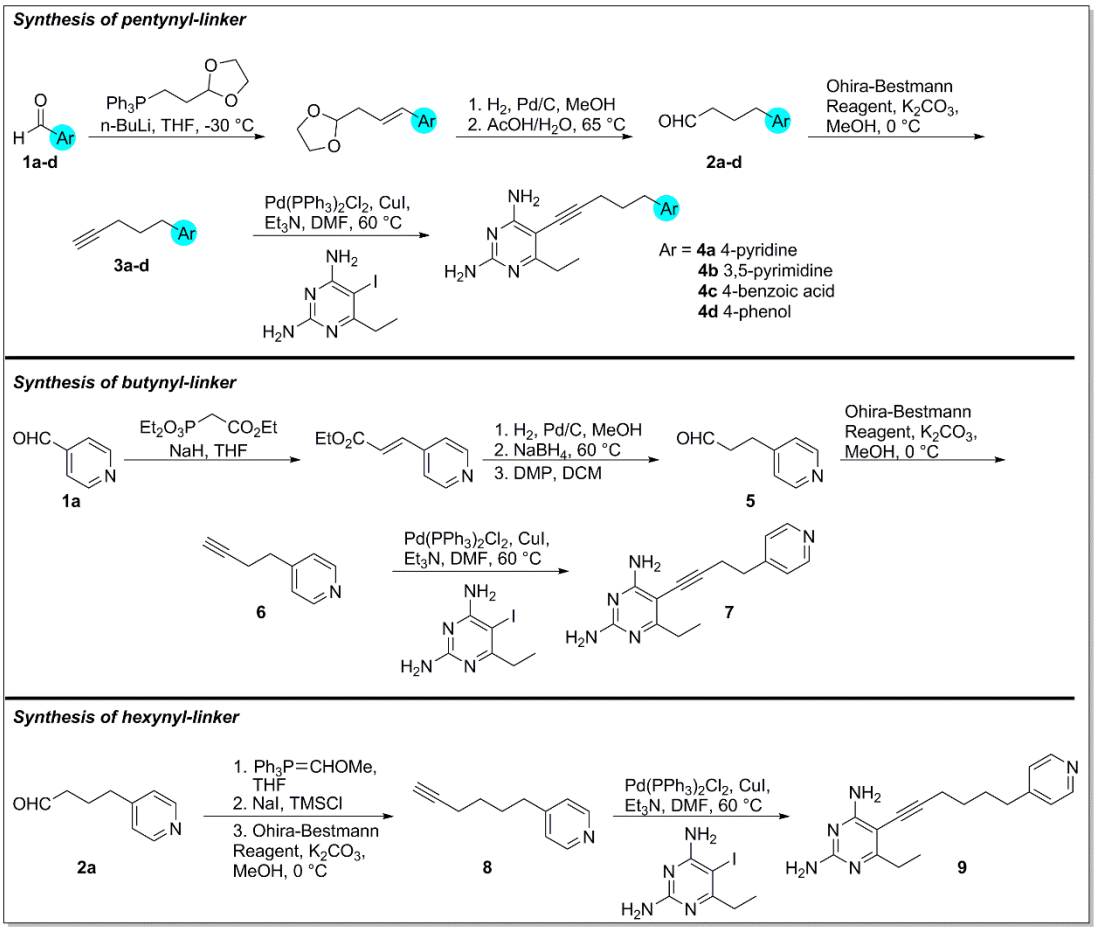


**Scheme 3.2** Synthesis of Chain PLAs

## 3.5 Chain PLA Biological Activity

We were pleased that all three compounds maintained potent enzyme activity (**Table 3**), with **4a** being as potent as UCP1021, 19 nm and 21 nm respectively. However, we saw a significant loss in growth inhibition activity of all three compounds compared to UCP1021. Compound **4a** was the most potent of the three chain compounds as a 0.625 µg/ml inhibitor, compared to UCP1021 which is a 0.023 µg/ml inhibitor.

Against EcDHFR, all three chain compounds showed increased enzyme activity relative to UCP1021, an 830 nM inhibitor. Compounds **9** and **7** showed a 4-fold increase in activity, 211 nm and 204 nm respectively, while **4a** saw a 15-fold increase in activity. Compound **4a** also showed the best growth inhibition activity against Ec25922 at 6.25 µg/ml, at least a 3.2-fold increase compared to UCP1021. Compound **7** showed moderate activity with an MIC of 10 µg/ml, while **9** showed no activity at >50 µg/ml. The data suggested that going forward, we should pursue three atom linkages between the acetylene and the C-ring.

To determine if the chain compounds were penetrating through the outer membrane of *E. coli*, we tested them against a wild-type *E. coli* strain, BW25113, a ΔacrB strain, JW0451, and an engineered strain with a deletion in the *imp gene*, that encodes a protein necessary for outer membrane assembly, NR698. This panel of strains offers insight into the mechanism most responsible for the loss in activity of our compounds against *E. coli*. A large activity loss between NR698 and JW0451 would lead us to believe that compound permeability through the outer membrane is responsible. A compound with a large activity loss between JW0451 and BW25113 would indicate that the compound is an efflux substrate.

When comparing **4a** to UCP1021 we see that they have similar activity against NR698 (0.0391 µg/ml vs 0.07813 µg/ml); however, there is a significant difference between the two compounds against JW045 (0.3125 µg/ml vs. 2.5 µg/ml). This indicates that **4a** is penetrating the outer membrane more than its B-ring counterpart, UCP1021. This is further confirmed when comparing the BW25113 parent strain activity (15 µg/ml vs. 20 µg/ml). The fact that these two compounds have similar

activity in the LPS knockout strain, and the WT BW25113 strain, indicates that the difference observed in the JW0451 strain is likely due to the ability of **4a** to penetrate the outer membrane of *E.coli* better than UCP1021. Comparing their physicochemical properties we see that **4a** has a lower MW than UCP1021 (281.36 vs. 359.43) and also a lower cLogP (2.47 vs. 3.33), supporting our initial hypothesis.

**Table 4**. Chain PLA Scaffold and Biological Activity

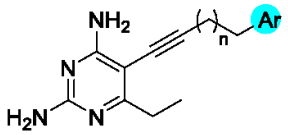


| | | | | *E. coli* | | | | *S. aureus* | |
|---|---|---|---|---|---|---|---|---|---|
| **Cmpd** | **n** | **Ar** | **EcIC$_{50}$** | **BW25113** | **JW0451** | **NR698** | **Ec25922** | **SaIC$_{50}$** | **SaMIC** |
| **7** | 1 | 4-Pyridine | 0.204±0.005 | 20 | 2.5 | 0.0625 | 10 | 0.033±0.003 | 5 |
| **4a** | 2 | 4-Pyridine | 0.055±0.001 | 15 | 0.3125 | 0.0391 | 6.25 | 0.019±0.003 | 0.625 |
| **9** | 3 | 4-Pyridine | 0.211±0.007 | >20 | 5 | 0.0391 | >50 | 0.030±0.002 | 1.25 |
| **4b** | 2 | 3,5-Pyrimidine | 0.100±0.008 | >20 | 20 | 0.313 | >20 | nd | 5 |
| **4c** | 2 | 4-Benzoic acid | 0.105±0.010 | >20 | 5 | 0.3125 | >20 | 0.028±0.001 | 2.5 |
| **4d** | 2 | 4-Phenol | nd | 10 | 1.25 | 0.0195 | >20 | 0.010±0.002 | 0.1563 |

Compound **4d**, with a three-carbon linker between the alkyne and a distal phenol, was synthesized as a direct comparator against UCP1128, its B-ring counterpart. While both were inactive against the ATCC test strain, **4d** showed increased activity against BW25113 compared to UCP1128 (10 µg/ml vs. >20 µg/ml). Little difference was seen between the two compounds in the JW0451 strain, indicating there is likely no difference in their ability to penetrate the outer membrane of *E.coli*. However, an almost 10-fold difference was seen in the NR698 strain (0.0195 µg/ml vs. 0.156 µg/ml). This could be due to **4d** being a better EcDHFR inhibitor than UCP1128; however, incomplete data leaves this conclusion unconfirmed.

Both **4a** and **4d** showed that removal of the B-ring in traditional PLAs led to better enzyme inhibition and an increase in cellular potency against *E.coli*, as measured by MIC. Compound **4a** in particular gave substance to our original hypothesis that reducing MW and cLogP of our traditional PLAs could increase *E. coli* penetration and growth inhibition. Compounds **4a** and **4d** also showed promising activity against *S. aureus*, with **4d** having a superior $IC_{50}$ and MIC with value of 10 nM and MIC of 0.156 µg/ml, respectively.

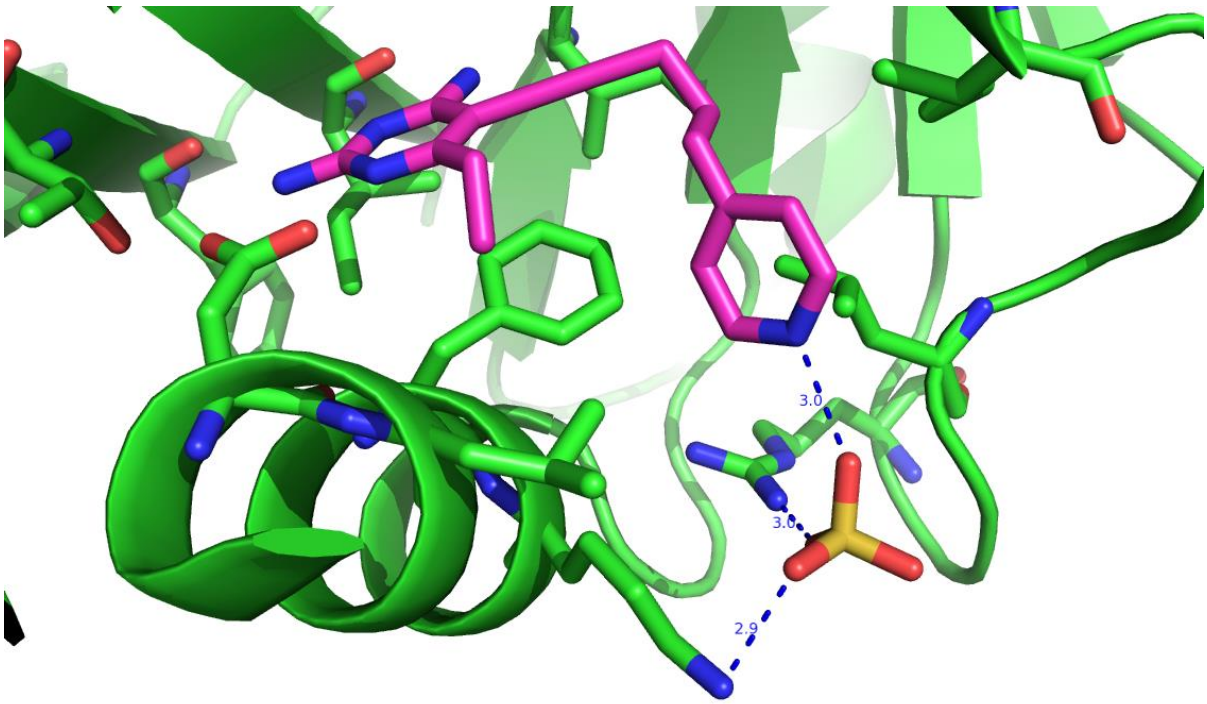


**Figure 3.4** Crystal Structure of **4a** (magenta) Bound to wt *E.coli* DHFR.

Compound **4a** is shown bound to WT E.coli DHFR displaying the common diaminopyrimidine motif (**Figure 3.4**). Asp27 makes hydrogen bonding contacts with two nitrogens of the ring, while the protonated nitrogen makes a hydrogen bonding interaction with a water molecule. Lys38 and the carbonyl of Ile5 make hydrogen-

bonding contacts with the other two nitrogen atoms in the diaminopyrimidine ring. Phe31 makes a π-π interaction with the acetylenic linker. No electron density is seen in the NADPH binding pocket which sits above the propargylic position of the inhibitor. The absence of NADPH could be an artifact of the crystallization conditions, however it could also give insight into the activity of **4a**. If **4a** can bind without NADPH being present, it is possible that its activity is owed to the removal of the natural co-factor from the active site. Interestingly, the distal pyridine ring makes a hydrogen bonding interaction with a sulfate anion, which is stabilized by further hydrogen bonding contacts with Lys32 and Arg57. This is certainly unusual and has implications for further drug design. By incorporating functionality at this extended position that can accompany multiple hydrogen bond contacts we could design better enzyme inhibitors and ultimately better leads.

We have shown a modified scaffold, based on our previously reported PLA lead compounds, consisting of a removed B-ring, with either all-carbon or heteroatom-containing chain connecting the acetylenic linker to the variable "C-ring". We determined the optimal atom length of the chain, which is possibly variable depending on the C-ring substitution. Our hypothesis of reducing LogP and MW to increase penetration into the Gram-negative bacterial cell was supported when comparing chain compounds **4a** and **4d** to their B-ring parent compounds. These inhibitors show moderate activity against *E. coli* and could be improved upon going forward.

## 3.6 Experimentals

The $^{1}H$ and $^{13}C$ NMR spectra were recorded on Bruker instruments at 500 MHz. Chemical shifts are reported in ppm and are referenced to residual $CHCl_3$ solvent; 7.24 and 77.23 ppm for $^{1}H$ and $^{13}C$, residual solvent MeOH; 4.78, 3.31 and 49.15 ppm respectively. The high-resolution mass spectrometry was provided by the University of Connecticut Mass Spectrometry Laboratory using AccuTOF mass spectrometer and/or using DART source. TLC analyses were performed on Sorbent Technologies silica gel HL TLC plates. All glassware was oven-dried and allowed to cool under an argon atmosphere. Anhydrous dichloromethane, and tetrahydrofuran were used directly from Baker Cycle-Tainers. All reagents were used directly from commercial sources unless otherwise stated.

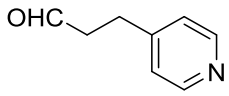


**3-(Pyridin-4-yl)propanal (5).** A 25-mL flask was flame dried under argon. Once at rt, NaH (18.67 mmol, 0.45 g) was suspended in THF (25 mL) and cooled to 0 °C. Triethylphosphonoacetate (9.34 mmol, 2.09 g) was added and stirred at 0 °C for 15 minutes. A solution of 4-pyridinecarboxaldehyde (4.67 mmol, 0.50 g) in THF (2 mL) was added dropwise and stirred at 0 °C for 30 minutes before slowly warming to rt. The reaction was complete by TLC after 1 hour. The reaction was quenched by addition of saturated $NH_4Cl$ and extracted with EtOAc (3x15 mL). The organic layer was dried and the solvent was removed to give a crude oil that was used without further purification.

In a 50 mL flask, the crude oil was dissolved in MeOH (15 mL) and added to a RB flask containing 10% Pd/C (0.33 mmol, 0.036 g). The flask was evacuated and back-filled with $H_2$ for five cycles. The reaction was allowed to stir until complete by TLC. The reaction was filtered through celite, washed with EtOAc, and the solvent was removed to give a crude oil that was used without further purification.

In a 50 mL flask, the crude oil was dissolved in MeOH (20 mL) and $NaBH_4$ (5.02 mmol, 0.19 g) added. The reaction was stirred at 60 °C until complete by TLC (be sure to appropriately vent flask to allow for $H_2$ evolution). Saturated $NH_4Cl$ was added and the mixture was extracted with EtOAc (3x20 mL). The organic layer was dried, the solvent was removed, and the crude oil was used without further purification.

In a 50 mL flask, the crude oil dissolved in DCM (20 mL) and Dess-Martin periodinane (3.33 mmol, 1.41 g) was added with stirring until complete by TLC. Saturated sodium thiosulfate was added and extracted with EtOAc (3x15 mL). The organic layer was dried, the solvent was removed, and the aldehyde was purified via column chromatography (eluted in 50:50 EtOAc:Hexanes) to give a slight yellow oil (0.31 g, 50% yield over 4 steps). NMR data agreed with previous reports.[17]

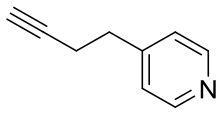


**4-(But-3-ynyl)pyridine (6). General Ohira-Bestmann Homologation Method**

To a dried 25 mL flask under argon was added $K_2CO_3$ (0.86 mmol, 0.12 g) and 5 mL MeOH and cooled to 0 °C. Dimethyl (1-diazo-2-oxopropyl)phosphonate (0.60 mmol, 0.12 g) was added and stirred for 15 minutes. Pyridine-4-propanal **5** (0.57 mmol, 0.08 g) was added and stirred until complete by TLC. Brine was added to quench the

reaction and the aqueous layer was extracted with EtOAc (3x10 mL). The organic layer was dried, the solvent was removed, and the alkyne was purified via column chromatography (eluted in 30:70 EtOAc:Hexanes) to give a yellow oil (0.06 g, 75%). $^{1}$H NMR (500 MHz, $CDCl_3$) δ 8.64 – 8.42 (m, 2H), 7.16 (d, J = 5.2 Hz, 2H), 2.83 (t, J = 7.3 Hz, 2H), 2.51 (td, J = 7.3, 2.5 Hz, 2H), 1.99 (t, J = 2.5 Hz, 1H); $^{13}$C NMR (126 MHz, CDCl3) δ 149.9, 149.2, 124.0, 82.9, 69.8, 34.0, 19.5.

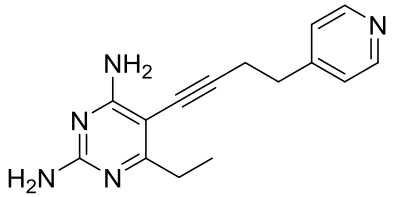


**6-Ethyl-5-(4-(pyridin-4-yl)but-1-ynyl)pyrimidine-2,4-diamine (7). General Method for Sonogashira Coupling.**

In a 20 mL vial, pyridine-4-propyne (0.35 mmol, 0.05 g), 6-ethyl,5-iodo 2,4-diaminopyrimidine (0.26 mmol, 0.07 g), $Pd(PPh_3)_4Cl_2$ (0.026 mmol, 0.018 g), and CuI (0.052 mmol, 0.010 g) were added. To the solids was added DMF (2 mL) and $Et_3N$ (1 mL), followed by degassing via 3 freeze-pump-thaw cycles. The reaction was heated to 65 °C for 16 h. Once complete by TLC, DMF was removed via multiple toluene azeotropes. Once dried, the reaction mixture was pre-absorbed onto a 1:1 mixture of $SiO_2$ and $NH_2$-capped $SiO_2$. PLA **7** was purified via column chromatography (eluted in 2% MeOH in DCM) to give a slight yellow solid (0.025 g, 35%). $^{1}$H NMR (500 MHz, MeOD:$CDCl_3$) δ 8.45 (s, 2H), 7.33 (d, J = 5.2 Hz, 2H), 2.97 (t, J = 6.9 Hz, 2H), 2.88 (t, J = 6.8 Hz, 2H), 2.49 (q, J = 7.6 Hz, 2H), 1.10 (t, J = 7.6 Hz, 3H); $^{13}$C

NMR (126 MHz, MeOD:$CDCl_3$) δ 172.6, 164.5, 160.6, 151.0, 148.9, 124.6, 97.0, 90.1, 74.2, 34.2, 29.2, 20.3, 12.4.

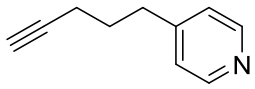


**4-(Pent-4-ynyl)pyridine (3a). General method for pentynyl – chain synthesis**

A 25-mL flask was flame dried under argon. Once at rt, 2(1,3-dioxolan-2-yl) ethyl-triphenylphosphonium chloride (9.66 mmol, 4.28 g) was dissolved in THF (6 mL) and cooled to -30 °C. *n*BuLi (9.66 mmol, 3.86 mL, 2.5 M in hexanes) was added dropwise and allowed to stir for 30 minutes. A solution of 4-pyridinecarboxaldehyde (8.40 mmol, 0.90 g) in THF (1 mL) was added dropwise and stirred at -30 °C for 30 minutes before slowly warming to rt. The reaction was complete by TLC after 2 hours. The reaction was quenched by addition of saturated $NH_4Cl$. The aqueous layer was extracted with EtOAc (3x10 mL). The combined organic layers were dried and the solvent was removed to give a crude oil that was used without further purification.

In a 50 mL flask, the crude oil was dissolved in MeOH (30 mL) and added to flask containing 10% Pd/C (1.00 mmol, 0.108 g). The flask was evacuated and back-filled with $H_2$ for five cycles. The reaction was allowed to stir until complete by TLC. The reaction was filtered through celite, washed with EtOAc, and the solvent was removed to give a crude oil that was used without further purification.

In a 100 mL flask, the crude oil was dissolved in AcOH:$H_2O$ (50 mL of 80:20) and heated to 65 °C until complete by TLC. Once complete, the solvent was removed and the material was purified by column chromatography (eluted in 50:50 Hexanes:EtOAc) to give a slight yellow oil (0.75 g, 60%). NMR characterization matched previous reports in the literature.[18]

The aldehyde was subjected to the General Ohira-Bestmann Homologation method to generate the title alkyne as a yellow oil (0.09 g, 62%). $^1$H NMR (500 MHz, $CDCl_3$) δ 8.43 (d, J = 5.5 Hz, 2H), 7.07 (d, J = 5.5 Hz, 2H), 2.72 – 2.65 (m, 2H), 2.15 (td, J = 6.9, 2.6 Hz, 2H), 1.98 (t, J = 2.6 Hz, 1H), 1.79 (p, J = 7.2 Hz, 2H); $^{13}$C NMR (126 MHz, $CDCl_3$) δ 150.5, 149.8, 124.0, 83.6, 69.4, 33.9, 28.9, 17.9.

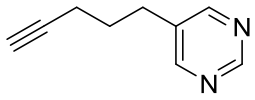


**5-(Pent-4-ynyl)pyrimidine (3b).** Synthesized according to the "General method for pentynyl-chain synthesis" to give title alkyne as a yellow oil (0.11 g, 35% from **4b**): $^1$H NMR (500 MHz, $CDCl_3$) δ 9.06 (s, 1H), 8.59 (s, 2H), 2.79 – 2.70 (m, 2H), 2.23 (td, J = 6.8, 2.6 Hz, 2H), 2.02 (t, J = 2.6 Hz, 1H), 1.85 (dt, J = 14.4, 6.9 Hz, 2H); $^{13}$C NMR (126 MHz, $CDCl_3$) δ 157.1, 156.9, 134.5, 83.1, 69.8, 53.2, 29.2, 17.8.

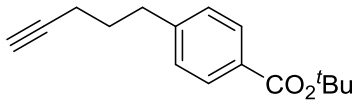


***tert*-Butyl 4-(pent-4-ynyl)benzoate (3c).** Synthesized according to the "General method for pentynyl-chain synthesis" to give title alkyne as a yellow oil (0.150 g, 32% from **4d**): $^1$H NMR (500 MHz, $CDCl_3$) δ 7.94 (d, J = 8.0 Hz, 2H), 7.26 (d, J = 7.9 Hz,

2H), 2.81 (t, J = 7.6 Hz, 2H), 2.21 (td, J = 6.9, 2.6 Hz, 2H), 2.03 (t, J = 2.7 Hz, 1H), 1.87 (p, J = 7.1 Hz, 2H), 1.61 (s, 9H); $^{13}$C NMR (126 MHz, $CDCl_3$) δ 165.8, 146.4, 129.9, 129.6, 128.4, 83.8, 80.7, 69.0, 34.5, 29.7, 28.2, 17.8.

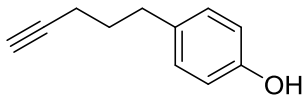


**4-(Pent-4-ynyl)phenol (3d).** Synthesized according to the "General method for pentynyl-chain synthesis" to give title alkyne as a yellow oil (0.150 g, 32% from **4c**): $^{1}$H NMR (500 MHz, $CDCl_3$) δ 7.11 (d, J = 8.3 Hz, 2H), 6.81 (d, J = 8.4 Hz, 2H), 2.71 (t, J = 7.5 Hz, 2H), 2.23 (td, J = 7.0, 2.6 Hz, 2H), 2.04 (t, J = 2.6 Hz, 1H), 1.85 (p, J = 7.1 Hz, 2H); $^{13}$C NMR (126 MHz, $CDCl_3$) δ 153.7, 133.8, 129.6, 115.2, 84.3, 68.7, 33.7, 30.3, 17.7.

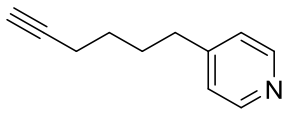


**4-(Hex-5-ynyl)pyridine (8).** To a 0 °C suspension of methoxymethyl-triphenylphosphonium chloride (2.68 mmol, 0.92 g,) in THF (10 mL) under an argon atmosphere was added NaO$^{t}$Bu (2.68 mmol, 0.26 g) in one portion. The red-orange suspension was stirred for 30 minutes at 0 °C. Pyridine-4-butanal **2a** (1.34 mmol, 0.20 g) was added in THF (2 mL) and stirred at 0 °C until complete by TLC. The reaction was quenched with $H_2O$ and extracted with EtOAc (3x15 mL). The organic layer was dried and the solvent was removed to give a crude oil that was used without further purification.

The crude oil was dissolved in MeCN (8 mL) under an argon atmosphere. Sodium iodide (0.47 mmol, 0.70 g) was added and cooled to -20 °C. TMSCl (0.47 mmol, 0.06 mL) was added and stirred at -20 °C until complete by TLC. The reaction was diluted with EtOAc (10 mL) and saturated sodium thiosulfate was added. The reaction stirred as it warmed to rt. The mixture was extracted with EtOAc (3x15 mL), the combined organic layers were dried, and the solvent was removed to give a crude oil that was used without further purification.

The general Ohira-Bestmann alkyne homologation method was followed to synthesize the title alkyne **8** as a slightly yellow oil (0.07 g, 33% over 3 steps): $^{1}$H NMR (500 MHz, $CDCl_3$) δ 8.50 (d, J = 5.9 Hz, 2H), 7.13 (d, J = 5.9 Hz, 2H), 2.65 (t, J = 7.7 Hz, 2H), 2.25 (td, J = 7.0, 2.6 Hz, 2H), 1.98 (t, J = 2.6 Hz, 1H), 1.78 (p, J = 7.6 Hz, 2H), 1.59 (dt, J = 14.8, 7.1 Hz, 2H); $^{13}$C NMR (126 MHz, $CDCl_3$) δ 151.2, 149.9, 124.0, 82.2, 68.8, 34.8, 29.3, 28.0, 18.4.

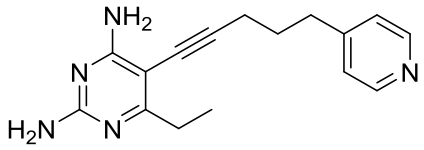


**6-Ethyl-5-(5-(pyridin-4-yl)pent-1-ynyl)pyrimidine-2,4-diamine (4a).** Synthesized according to the “General method for Sonogashira Coupling” to give title compound as a pale yellow solid (0.018 g, 37%): $^{1}$H NMR (500 MHz, $CDCl_3$) δ 8.48 (d, J = 5.9 Hz, 2H), 7.16 (d, J = 5.8 Hz, 2H), 2.83 – 2.75 (m, 2H), 2.68 (q, J = 7.6 Hz, 2H), 2.51 (t, J = 6.9 Hz, 2H), 1.95 (p, J = 7.0 Hz, 2H), 1.24 (t, J = 7.7 Hz, 5H).

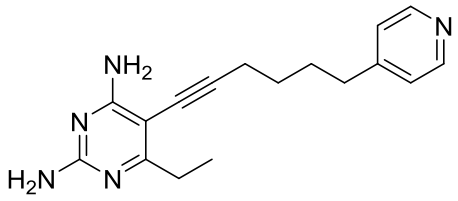

**6-Ethyl-5-(5-(pyridin-4-yl)hex-1-ynyl)pyrimidine-2,4-diamine (9).** Synthesized according to the “General method for Sonogashira Coupling” to give title compound as a pale yellow solid (0.014 g, 24%): NMR data not available

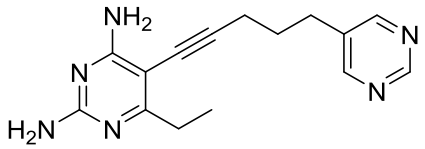

**6-Ethyl-5-(5-(pyrimidin-5-yl)pent-1-ynyl)pyrimidine-2,4-diamine (4b).** Synthesized according to the “General method for Sonogashira Coupling” to give title compound as a yellow solid (0.022 g, 31%): $^{1}$H NMR (500 MHz, $CDCl_3$) δ 9.12 (s, 1H), 8.65 (s, 2H), 5.19 (s, 2H), 4.93 (s, 2H), 2.82 (t, J = 7.7 Hz, 2H), 2.71 (q, J = 7.6 Hz, 2H), 2.56 (t, J = 6.9 Hz, 2H), 1.98 (p, J = 7.0 Hz, 2H), 1.26 (t, J = 7.6 Hz, 3H).

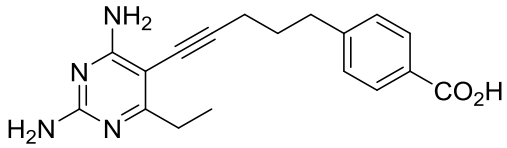

**4-(5-(2,4-Diamino-6-ethylpyrimidin-5-yl)pent-4-ynyl)benzoic acid (4c).** Synthesized according to the “General method for Sonogashira Coupling” to give title compound as a yellow solid (0.025 g, 38%): $^{1}$H NMR (500 MHz, DMSO-d6) δ 7.88 (d,

J = 8.1 Hz, 2H), 7.36 (d, J = 8.1 Hz, 2H), 2.79 (t, J = 7.6 Hz, 2H), 2.67 (q, J = 7.5 Hz, 2H), 2.49 (d, J = 7.1 Hz, 2H), 1.90 (p, J = 7.2 Hz, 2H), 1.21 (d, J = 7.6 Hz, 3H).

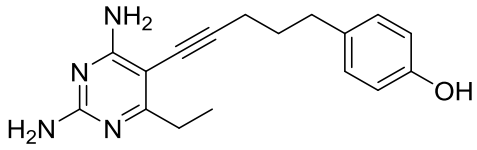


**4-(5-(2,4-Diamino-6-ethylpyrimidin-5-yl)pent-4-ynyl)phenol (4d).** Synthesized according to the “General method for Sonogashira Coupling” to give title compound as a yellow solid (0.027 g, 44%): $^{1}$H NMR (500 MHz, $CDCl_3$) δ 7.06 (d, J = 8.3 Hz, 2H), 6.78 (d, J = 8.3 Hz, 2H), 2.70 (dt, J = 12.2, 7.5 Hz, 4H), 2.48 (t, J = 7.0 Hz, 2H), 1.90 (p, J = 7.1 Hz, 2H), 1.25 (t, J = 7.6 Hz, 3H).

## 3.7 References


(1) Silver, L. L. *Expert Opin. Drug Discov* **2008**, *3* (5), 487.

(2) CDC. *Current* **2013**, 114.

(3) Zhou, W.; Scocchera, E. W.; Wright, D. L.; Anderson, A. C. *Medchemcomm* **2013**, *4*, 908.

(4) Gupta, K.; Hooton, T. M.; Naber, K. G.; Wullt, B.; Colgan, R.; Miller, L. G.; Moran, G. J.; Nicolle, L. E.; Raz, R.; Schaeffer, A. J.; Soper, D. E. *Clin. Infect. Dis.* **2011**, *52* (5), 103.

(5) Dalhoff, A. *Infection* **2012**, *40* (3), 239.

(6) Viswanathan, K.; Frey, K. M.; Scocchera, E. W.; Martin, B. D.; Swain, P. W.; Alverson, J. B.; Priestley, N. D.; Anderson, A. C.; Wright, D. L. *PLoS One* **2012**, *7* (2), 1.

(7) Scocchera, E.; Reeve, S. M.; Keshipeddy, S.; Lombardo, M. N.; Hajian, B.; Sochia, A. E.; Alverson, J. B.; Priestley, N. D.; Anderson, A. C.; Wright, D. L. *ACS Med. Chem. Lett.* **2016**, *7* (7), 692.

(8) Reeve, S. M.; Scocchera, E.; Ferreira, J. J.; G-Dayanandan, N.; Keshipeddy, S.; Wright, D. L.; Anderson, A. C. *J. Med. Chem.* **2016**, *59* (13), 6493.

(9) Hajian, B.; Scocchera, E.; Keshipeddy, S.; G-Dayanandan, N.; Shoen, C.; Krucinska, J.; Reeve, S.; Cynamon, M.; Anderson, A. C.; Wright, D. L. *PLoS One* **2016**, *11* (8), e0161740.

(10) Lamb, K. M.; Lombardo, M. N.; Alverson, J.; Priestley, N. D.; Wright, D. L.; Anderson, A. C. *Antimicrob. Agents Chemother.* **2014**, *58* (12), 7484.

(11) Lombardo, M. N.; G-Dayanandan, N.; Wright, D. L.; Anderson, A. C. *ACS Infect. Dis.* **2016**, *2* (2), 149.

(12) Pages, J. M.; James, C. E.; Winterhalter, M. *Nat Rev Microbiol* **2008**, *6* (12), 893.

(13) Plésiat, P.; Nikaido, H. *Mol. Microbiol.* **1992**, *6* (10), 1323.

(14) Nikaido, H. *Microbiol. Mol. Biol. Rev.* **2003**, *67* (4), 593.

(15) Nikaido, H. *J. Bacteriol.* **1996**, *178* (20), 5853.

(16) Decad, G. M.; Nikaido, H. *J. Bacteriol.* **1976**, *128* (1), 325.

(17) Vassiliou, S.; Węglarz-Tomczak, E.; Berlicki; Pawełczak, M.; Nocek, B.; Mulligan, R.; Joachimiak, A.; Mucha, A. *J. Med. Chem.* **2014**, *57* (19), 8140.

(18) Massaro, A.; Mordini, A.; Mingardi, A.; Klein, J.; Andreotti, D. *European J. Org. Chem.* **2011**, No. 2, 271.

(19) Schwechheimer, C.; Kuehn, M. J. *Nat. Rev. Microbiol.* **2015**, *13* (10), 605.

# 4 Direct Substitution of Arylalkynyl Carbinols Provides Convenient Access to Diverse Terminal Acetylene Building Blocks

## 4.1 Preface

The following chapter is taken from the following publication:

G-Dayanandan, N.,† Scocchera, E. W.,† Keshipeddy, S., Jones, H. F., Anderson, A. C., Wright, D. L.; Direct Substitution of Arylalkynyl Carbinols Provides Access to Diverse Terminal Acetylene Building Blocks. *Org*. *Lett*. **2016**, acs.orglett.6b03438. †Authors contributed equally

**Contributions:** My contribution to the work is the idea of a divergent synthesis from a common propargyl alcohol intermediate, the implementation of the Reetz chemistry, and the synthesis of the geminal dimethyl substituted compounds as well as two of the singly-methylated propargyl compounds. Narendran G-Dayanandan implemented the deoxygenation of propargyl alcohols and synthesized the propargyl unsubstituted compounds and the other singly-methylated compounds.

## 4.2 Introduction and Alkyne Utility

The incorporation of alkyne functionality in screening libraries,[1-4] biological probes,[5,6] and therapeutic agents[7,8] is becoming increasingly prevalent. This is due to both the relative ease of their incorporation into complex molecules, through cross-coupling chemistry[9-12] and azide "click" cycloadditions[13] and their distinct topological features. While aryl alkynes are often observed in the literature, alkyl alkynes bearing a propargyl position capable of functionalization are less common. This is likely due to the propensity of alkynes to isomerize to allenes under mild conditions. In fact, a Scifinder literature survey showed a plethora of arylalkynyl carbinols in biologically relevant molecules. This motif is likely generated from nucleophilic alkyne addition to carbonyls without subsequent alteration of the resulting propargyl alcohol. It is worthwhile to ask whether there is a biological importance to the propargyl alcohol functionality or if it is included simply due to synthetic ease. Nicholas developed a method to mask alkyne functionality using dicobalt octacarbonyl ($Co_2(CO_8)$)[14,15] while the propargyl position underwent functionalization, with a subsequent deprotection once the propargyl functionality was set. While it has been utilized to synthesize bioactive molecules,[16,17] it is far from an ideal solution from a synthetic perspective.

## 4.3 PLAs and Their Synthesis

A structure-based drug design approach has led to a series of propargyl-linked antifolates (PLAs) characterized by the insertion of a propargylic linker[18-20] between a 2,4-diaminopyrimidine A ring and a hydrophobic B-ring (**Scheme 4.1**). The acetylenic linker offers unique advantages as it projects the B-ring deeper into a large hydrophobic cavity in PLA's target, DHFR, while the small, linear projection of the alkyne allows it to pass through a narrow channel in the enzyme.

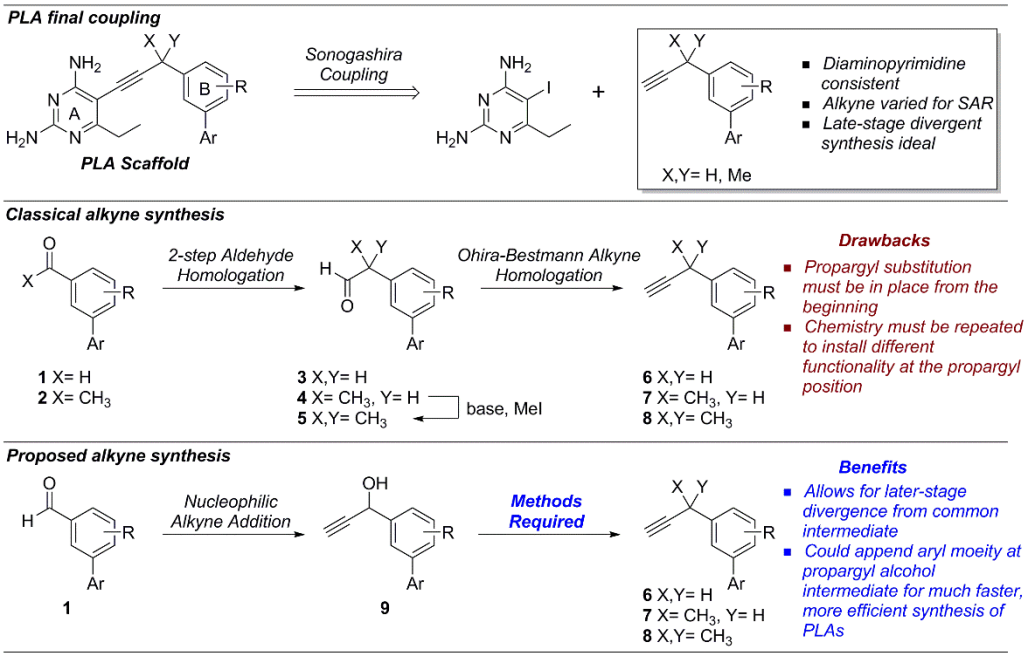


**Scheme 4.1.** PLA Synthesis: Benefits of an Updated Synthesis

In developing this class of inhibitors, the importance of propargyl substitution has shown itself to be critical with unsubstituted, mono-methylated, and di-methylated derivatives showing strong effects on organism-specific potency,[21] selectivity over the human DHFR,[22] metabolic stability,[23] and NADPH binding.[24] Various propargyl

substitutions are required to probe the hydrophobic pocket of DHFR to properly determine structure-activity relationships (SAR).

We had previously developed[25] a route (**Scheme 4.1**) to the acetylenic component of PLAs based on a Wittig homologation of biaryl aldehydes **1** or methyl ketones **2** to produce the unsubstituted or mono-methylated intermediates **3** and **4** respectively; the geminal-dimethyl substitution **5** was prepared via subsequent enolate alkylation. Homologation of the phenylacetaldehydes with the Ohira-Bestmann[26] reagent generated terminal alkyne building blocks **6-8** that were subjected to Sonogashira coupling with the 2,4-diaminopyrimidine A ring to generate PLAs. There are several drawbacks to the homologation method: 1) Divergence occurs at the beginning of the synthesis leading to synthetic redundancies to generate slightly modified PLAs for SAR, 2) use of the expensive Ohira-Bestmann reagent required to build alkynes, instead of intermolecular alkyne addition, and 3) alkyne homologation often leads to base-mediated alkyne isomerization to allene, lowering yields.

We have been interested in developing an alternative route to terminal acetylenes that would allow access to various propargyl substitutions from a common starting material. We desired a route that would begin with nucleophilic alkyne addition to biaryl aldehydes **1** to produce propargyl alcohols **9** (**Scheme 4.1**). Divergence from **9** via propargyl alcohol displacement would generate the unbranched PLAs **6** via deoxygenation and the mono-methyl (**7**) and dimethyl PLAs (**8**) via nucleophilic methylation.

## 4.4 Previous Methods for Deoxygenation of Propargyl Alcohols

Trifluoroacetic acid is often used to activate the propargyl alcohols with hydride as the reductant; however isomerization of the propargyl cation to the allenyl cation often complicates the reaction.[27,28] Nicholas employed $Co_2(CO_8)$ to stabilize the propargyl cation and reduce allene formation.[14,15,17] Lewis-acid mediated deoxygenation of propargyl alcohols typically utilizes boron trifluoride etherate and triethylsilane as the hydride source.[29] Other Lewis acids have included $Bi(OTf)_3$, $Ca(Ntf_2)_2$,[31] $InBr_3$,[32] and $NaAuCl_4$.[33] Heterocycles and silyl-protected terminal alkynes are uncommon functionalities in the reported examples.

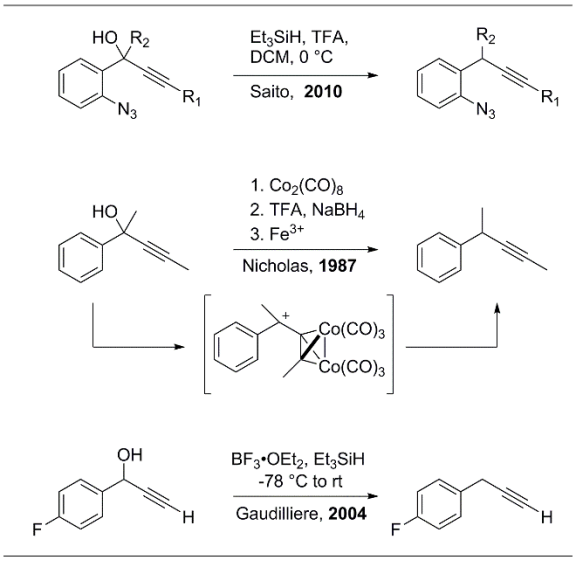


**Scheme 4.2** Selected Examples of Propargyl Alcohol Deoxygenation

## 4.5 Previous Methods for Methylation of Propargyl Alcohols

Nucleophilic methyl additions to propargyl alcohols are sparse in the literature, and complicated by a lack of substrate diversity and the need for various ligands (**Scheme 4.3**).[34,35] Moreover, nucleophilic methyl additions to arylalkynyl carbinols are

practically unknown in the literature. A single report described methyl magnesium bromide displacement of an arylalkynyl carbinol previously reacted with a ruthenium-based fullerene ligand to generate a stable ruthenium- allenylidene complex (**Scheme 4.3**).[36] Additionally, PLAs often possess a basic heterocyclic C-ring that could limit the ability to effect such direct methylations. Previous members of the Wright lab had utilized methodology first reported by Reetz[37,38] to effect a late-stage geminal dimethylation in the total synthesis of Frondosin B.[39] We were interested in repurposing Reetz's reagent, a pre-mixed solution of dimethyl zinc and titanium tetrachloride, for our propargyl methylation needs. Herein, we describe an efficient series of propargylic substitution reactions compatible with the heterocyclic functionality that can be used to generate a homologous series of propargylic variants from a common starting material.

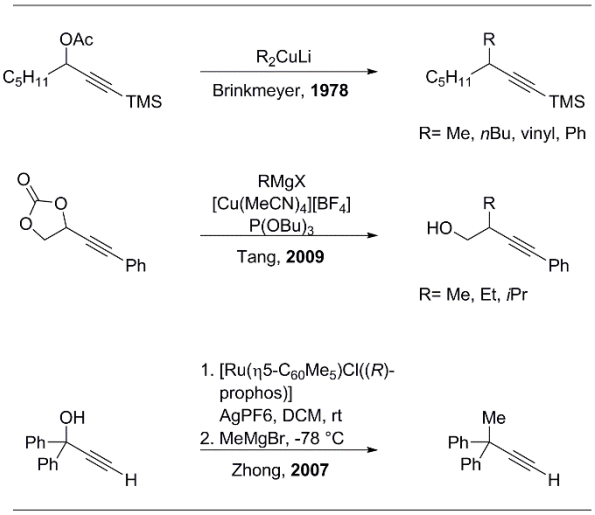


**Scheme 4.3** Selected Examples of Propargyl Alcohol Methylation

## 4.6 Modified Synthesis Results

Several commercially or readily available *m*-bromobenzaldehydes were directly converted to a variety of heterobiaryl aldehydes by Suzuki cross-coupling with a suitable boronic acid. The aryl propargyl alcohols **10a-k** were prepared by nucleophilic addition of trimethylsilylacetylene to the aryl aldehyde. Treatment of the alcohols with an excess of boron trifluoride etherate and triethylsilane led to the reduced methylene derivatives as an unexpected mixture of TMS-, TES- and desilylated terminal acetylenes (**Scheme 4.4**). The reaction was compatible with several nitrogenous heterocycles with the exception of pyrimidine (**11f**, **11h**), where there was competitive hydride reduction of the heterocycle. In the cases of silyl-alkyne mixtures of deoxygenated products the crude reaction mixture was subjected to a mild deprotection involving either a silver/cyanide mediated[40] hydrolysis or a less toxic equimolar mixture[41] of *n*-$Bu_4NF$ and $CH_3COOH$ to convert all species to the desired terminal alkyne. There is no precedent, to our knowledge, for the silyl exchange reaction that occurs in the reduction process.

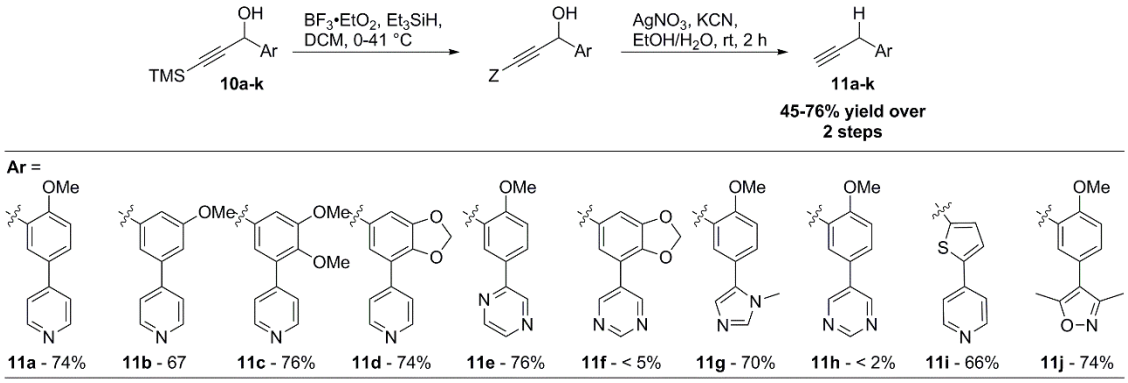


**Scheme 4.4** Deoxygenation of Propargyl Alcohols

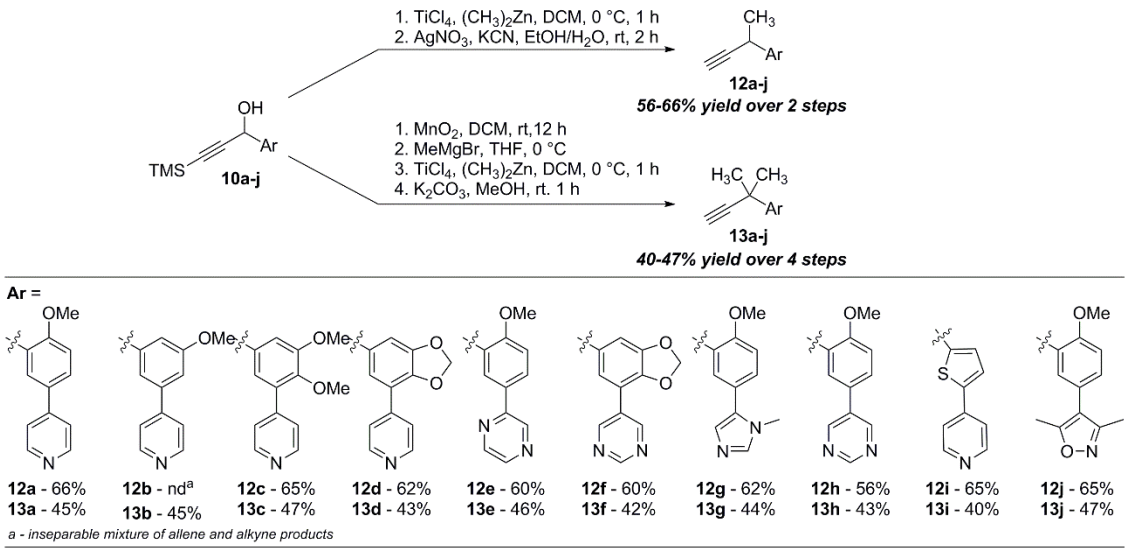


**Scheme 4.5** Methylation of Propargyl Alcohols

Treatment of the secondary alcohols with dimethylzinc[42] (**Scheme 4.5**) in the presence of titanium tetrachloride led to direct formation of the methyl branched systems in good overall yields. Surprisingly, only the *o*-methoxy substituted **12b** saw significant allene formation, possibly due to the lack of aryl stabilization of the propargyl cation intermediate. Desilylations of the terminal acteylenes were accomplished using silver nitrate and potassium cyanide. To generate geminal dimethyl substitution at the propargyl position the secondary propargyl alcohols were oxidized to their corresponding ketones with manganese dioxide. Methyl magnesium bromide addition to propargyl ketones generated tertiary alcohols which were subjected to the same Reetz chemistry to give geminal dimethyl variants. Desilylation was accomplished using potassium carbonate in alcoholic solvent. These conditions were not amenable to the mono-methylated compounds as allene isomerization was observed.

In summary, these methods allow for ready access to a series of 3-aryl propynes with both unsubstituted and branched propargylic carbons. Additional stabilization of the putative aryl substituted propargyl cation by suitably placed donor groups on the aromatic ring improves the overall efficiency of the reaction. These direct substitution reactions were sufficiently mild to allow the incorporation of the wide range of nitrogenous heterocycles in the substrate. In addition, there is evidence that the basic heterocycle plays a role in the facility of the reduction process, an effect that can be mimicked by the addition of exogenous pyridine to the reaction. These direct methods provide for the preparation of the series of differentially substituted 1-aryl propynes from readily available propargyl alcohols by direct reduction or substitution of the readily ionized hydroxyl group.

## 4.7 Experimental Data

The $^{1}H$ and $^{13}C$ NMR spectra were recorded on Bruker instruments at 500 MHz. Chemical shifts are reported in ppm and are referenced to residual $CHCl_3$ solvent; 7.24 and 77.23 ppm for $^{1}H$ and $^{13}C$, residual solvent MeOH; 4.78, 3.31 and 49.15 ppm respectively. The high-resolution mass spectrometry was provided by the Notre Dame Mass Spectrometry Laboratory and University of Connecticut Mass Spectrometry Laboratory using AccuTOF mass spectrometer and/or using DART source. IR data were obtained using Alpha diamond ATR probe. TLC analyses were performed on Sorbent Technologies silica gel HL TLC plates. All glassware was oven-dried and allowed to cool under an argon atmosphere. Anhydrous dichloromethane, and tetrahydrofuran were used directly from Baker Cycle-Tainers. All reagents were used directly from commercial sources unless otherwise stated. Boronic acids for Suzuki coupling were purchased from Frontier Scientific, Inc.

### General Procedure for Alkyne Addition

A 50 mL flask with stir bar was flame dried under argon. Ethynyltrimethyl silane was added to THF (2M) at 0 °C and stirred for two minutes. Isopropyl magnesium chloride was added dropwise and stirred initially at 0 °C for 30 minutes followed by another 30 minutes at room temperature. The grey colored Grignard reagent was cooled to 0 °C and the aldehyde in THF (0.1M) was added dropwise for 5 minutes. The reaction was followed by TLC and quenched with sat. $NH_4Cl$. The aqueous layer was extracted with ether (3x). The combined organic layers were dried with $MgSO_4$, filtered, and evaporated. The crude compound was pre-absorbed onto silica gel and purified by column chromatography.

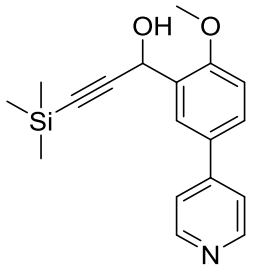


**1-(2-methoxy-5-(pyridin-4-yl) phenyl)-3-(trimethylsilyl) prop-2-yn-1-ol (10a)**

According to the general nucleophilic addition, ethynyltrimethyl silane (6.6mmol, 0.93mL) in THF (2M, 3.29 mL) and isopropyl magnesium chloride (2M, 3.3mL) was stirred. At 0 °C was added the aldehyde (5.06 mmol, 1.07 g) in THF (0.1M, 50.6mL). Following the general workup and flash chromatography ($SiO_2$, 40 g, 3%MeOH/$CH_2Cl_2$), the title alkynol was obtained as a white solid (1.48 g, 94%): TLC $R_f$ = 0.1 (3%MeOH/$CH_2Cl_2$); $^1$H NMR (500 MHz, $CDCl_3$) δ 8.58 (d, *J* = 5.7 Hz, 2H), 7.91 (d, *J* = 2.2 Hz, 1H), 7.58 (dd, *J* = 8.5, 2.2 Hz, 1H), 7.44 (d, *J* = 6.0 Hz, 2H), 6.98 (d, *J* = 8.5 Hz, 1H), 5.77 (s, 1H), 3.92 (s, 3H), 0.19 (s, 9H); $^{13}$C NMR (125 MHz, $CDCl_3$) δ 158.0, 150.3, 148.0, 130.5, 129.8, 128.3, 127.0, 121.2, 111.6, 104.7, 91.5, 61.0, 56.0, 0.1.; IR (neat $cm^{-1}$) 3139, 2977, 2868, 2165, 1562, 1504, 1228, 1011; HRMS (DART, $M^+$ + H) *m/z* 312.1393 (calculated for $C_{18}H_{21}NO_2Si$, 312.1420).

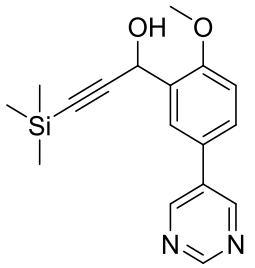


**1-(2-methoxy-5-(pyrimidin-5-yl) phenyl)-3-(trimethylsilyl) prop-2-yn-1-ol (10b)**

According to the general nucleophilic addition, ethynyltrimethyl silane (3.55mmol, 0.50 mL) in THF (2M, 1.78 mL) and isopropyl magnesium chloride (2M, 3.55 mmol, 1.78 mL) was stirred. At 0 °C was added the aldehyde (2.37 mmol, 0.51g) in THF (0.1M, 23.6 mL). Following the general workup and flash chromatography ($SiO_2$, 20 g, 3%MeOH/$CH_2Cl_2$), the title alkynol was obtained as a white solid (0.7 g, 95%): TLC $R_f$ = 0.1 (3%MeOH/$CH_2Cl_2$); $^1$H NMR (500 MHz, $CDCl_3$) δ 9.14 (s, 1H), 8.90 (s, 2H), 7.85 (s, 1H), 7.52 (d, *J* = 10.7 Hz, 1H), 7.03 (d, *J* = 8.5 Hz, 1H), 5.77 (s, 1H), 3.93 (s, 3H), 0.18 (s, 9H); $^{13}$C NMR (125 MHz, $CDCl_3$) δ 157.9, 157.2, 154.6, 134.0, 130.1, 128.4, 126.9, 126.9, 112.0, 104.2, 91.9, 61.1, 56.1, 0.1; IR (neat $cm^{-1}$) 3177, 3010, 2837, 2164, 1608, 1308, 1059; HRMS (DART, $M^+$ + H) *m/z* 313.1391 (calculated for $C_{17}H_{20}N_2O_2Si$, 312.1372).

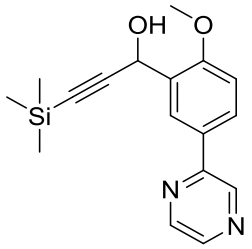


**1-(2-methoxy-5-(pyrazin-2-yl) phenyl)-3-(trimethylsilyl) prop-2-yn-1-ol (10c)**

According to the general nucleophilic addition, ethynyltrimethyl silane (1.45 mmol, 0.2 mL) in THF (2M, 0.72 mL) and isopropyl magnesium chloride (2M, 0.72 mL) was stirred. At 0 °C was added the aldehyde (0.9 mmol, 0.2 g) in THF (0.1M, 9.7mL). Following the general workup and flash chromatography ($SiO_2$, 10 g, 3%MeOH/$CH_2Cl_2$), the title alkynol was obtained as a white solid (0.27 g, 95%): TLC $R_f$ = 0.1 (3%MeOH/$CH_2Cl_2$); $^1$H NMR (500 MHz, $CDCl_3$) δ 8.96 (s, 1H), 8.57 (s, 1H), 8.43 (d, *J* = 2.4 Hz, 1H), 8.28 (d, *J* = 2.2 Hz, 1H), 8.01 (dd, *J* = 8.6, 2.3 Hz, 1H), 7.01 (d, *J* = 8.6 Hz, 1H), 5.75 (s, 1H), 3.94 (s, 3H), 0.20 (s, 9H). $^{13}$C NMR (125 MHz, $CDCl_3$) δ 158.6, 152.5, 144.3, 142.4, 141.7, 129.6, 129.1, 128.7, 127.0, 111.6, 104.5, 91.7, 61.5, 56.1, 0.1. IR (neat $cm^{-1}$) 3055, 2980, 2884, 2847, 1913, 1675, 1604, 1414, 1272, 1166, 1112, 1010, 825; HRMS (DART, $M^+$ + H) *m/z* 313.1394 (calculated for $C_{17}H_{20}N_2O_2Si$, 312.1372).

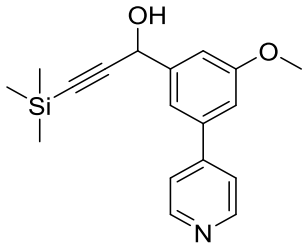


**1-(3-methoxy-5-(pyridin-4-yl) phenyl)-3-(trimethylsilyl) prop-2-yn-1-ol (10d)**

According to the general nucleophilic addition, ethynyltrimethyl silane (2.1 mmol, 0.3 mL) in THF (2M, 1.0 mL) and isopropyl magnesium chloride (2M, 1.0 mL) was stirred. At 0 °C was added the aldehyde (1.7 mmol, 0.4 g) in THF (0.1M, 17.4 mL). Following the general workup and flash chromatography ($SiO_2$, 20 g, 3%MeOH/$CH_2Cl_2$), the title alkynol was obtained as a brownish oil (0.51 g, 94%): TLC $R_f$ = 0.1 (3%MeOH/$CH_2Cl_2$); $^1$H NMR (500 MHz, $CDCl_3$) δ 8.59 (s, 2H), 7.46 (d, $J$ = 4.5 Hz, 2H), 7.38 (s, 1H), 7.19 (s, 1H), 7.07 (s, 1H), 5.50 (s, 1H), 3.85 (s, 3H), 0.18 (s, 9H); $^{13}$C NMR (125 MHz, $CDCl_3$) δ 160.5, 150.1, 148.5, 143.5, 139.7, 122.0, 118.0, 113.1, 112.7, 105.4, 91.7, 64.7, 55.7, 0.0; IR (neat $cm^{-1}$) 3153, 2958, 2899, 2837, 2170, 1648, 1550, 1325, 1217, 1049; HRMS (DART, $M^+$ + H) *m/z* 312.1434 (calculated for $C_{18}H_{21}NO_2Si$, 312.1420).

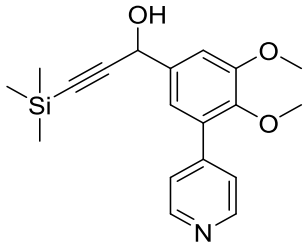


**1-(3,4-dimethoxy-5-(pyridin-4-yl) phenyl)-3-(trimethylsilyl) prop-2-yn-1-ol (10e)**

According to the general nucleophilic addition, ethynyltrimethyl silane (3.79 mmol, 0.54 mL,) in THF (2M, 1.9 mL) and isopropyl magnesium chloride (2M, 1.9 mL) was

stirred. At 0 °C was added the aldehyde (2.5 mmol, 0.6g) in THF (0.1M, 25.2 mL). Following the general workup and flash chromatography ($SiO_2$, 30 g, 50% 3%MeOH/$CH_2Cl_2$), the title alkynol was obtained as a colorless oil (0.82g, 95%): TLC $R_f$ = 0.1 (3%MeOH/$CH_2Cl_2$); $^1$H NMR (500 MHz, $CDCl_3$) δ 8.57 (d, *J* = 4.9 Hz, 2H), 7.45 (d, *J* = 6.0 Hz, 2H), 7.21 (d, *J* = 1.7 Hz, 1H), 7.09 (d, *J* = 1.8 Hz, 1H), 5.45 (s, 1H), 3.91 (s, 3H), 3.59 (s, 3H), 0.18 (s, 9H); $^{13}$C NMR (125 MHz, $CDCl_3$) δ 153.4, 149.5, 146.7, 146.4, 137.3, 132.6, 124.3, 120.4, 111.7, 105.5, 91.8, 64.6, 61.0, 56.2, 0.0; IR (neat $cm^{-1}$) 3085, 3009, 2964, 2821, 2162, 1642, 1410, 1241, 1134, 1049, 828; HRMS (DART, $M^+$ + H) *m/z* 342.1516 (calculated for $C_{19}H_{23}NO_3Si$, 342.1525).

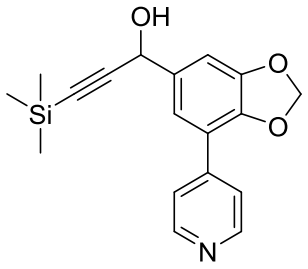


**1-(7-(pyridin-4-yl) benzo[d][1,3] dioxol-5-yl)-3-(trimethylsilyl) prop-2-yn-1-ol (10f)**

According to the general nucleophilic addition, ethynyltrimethyl silane (3.78 mmol, 0.53 mL) in THF (0.53 mL) and isopropyl magnesium chloride (2M, 1.9 mL) was stirred. At 0 °C was added the aldehyde (1.26 mmol, 0.3g) in THF (0.1M, 12.6 mL). Following the general workup and flash chromatography ($SiO_2$, 15 g, 3%MeOH/$CH_2Cl_2$), the title alkynol was obtained as a yellow hygroscopic solid (0.41 g, 99%): TLC $R_f$ = 0.1 (3%MeOH/$CH_2Cl_2$); $^1$H NMR (500 MHz, $CDCl_3$) δ 8.58 (d, *J* = 4.3 Hz, 2H), 7.61 (d, *J* = 5.8 Hz, 2H), 7.28 (s, 1H), 7.09 (s, 1H), 6.05 (s, 2H), 5.42 (s, 1H), 0.18 (s, 9H); $^{13}$C NMR (125 MHz, $CDCl_3$) δ 150.0, 148.8, 145.6, 143.6, 135.9,

122.3, 119.2, 119.0, 108.3, 105.4, 101.8, 91.6, 64.5, 0.0; IR (neat $cm^{-1}$) 3140, 2958, 2896, 2170, 1639, 1600, 1402, 1248, 1195, 1044, 1002, 824; HRMS (DART, $M^+ + H$) *m/z* 326.1223 (calculated for $C_{18}H_{19}NO_3Si$, 326.1212).

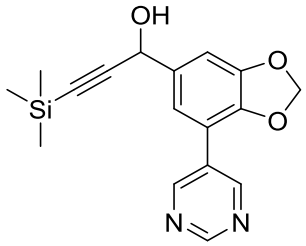


**1-(7-(pyrimidin-5-yl) benzo[d][1,3] dioxol-5-yl)-3-(trimethylsilyl) prop-2-yn-1-ol (10g)**

According to the general nucleophilic addition, ethynyltrimethyl silane (0.9 mmol, 0.14 mL) in THF (2M, 0.5 mL) and isopropyl magnesium chloride (2M, 0.99 mmol, 0.5 mL was stirred. At 0 °C was added the aldehyde (0.66 mmol, 0.15 g) in THF (0.1M, 6.6 mL). Following the general workup and flash chromatography ($SiO_2$, 10 g, 3%MeOH/$CH_2Cl_2$), the title alkynol was obtained as a light yellow solid (0.21 g, 96%): TLC $R_f$ = 0.1 (3%MeOH/$CH_2Cl_2$); $^1$H NMR (500 MHz, $CDCl_3$) δ 9.14 (s, 1H), 9.05 (s, 2H), 7.24 (s, 1H), 7.10 (s, 1H), 6.07 (s, 2H), 5.42 (s, 1H), 0.20 (s, 9H); $^{13}$C NMR (125 MHz, $CDCl_3$) δ 157.5, 155.5, 148.9, 145.5, 136.0, 129.8, 118.8, 115.3, 108.3, 104.8, 102.0, 92.3, 64.7, 0.0; IR (neat $cm^{-1}$) 3189, 2955, 2899, 2172, 1606, 1409, 1249, 1041, 1006, 837; HRMS (DART, $M^+ + H$) *m/z* 327.1190 (calculated for $C_{17}H_{18}N_2O_3Si$, 327.1165).

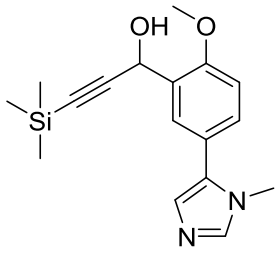


**1-(2-methoxy-5-(1-methyl-1H-imidazol-5-yl) phenyl)-3-(trimethylsilyl) prop-2-yn-1-ol (10h)**

According to the general nucleophilic addition, ethynyltrimethyl silane (2.0 mmol, 0.28 mL) in THF (1.0 mL) and isopropyl magnesium chloride (2M, 2.0 mmol, 1.0 mL) was stirred. At 0 °C was added the aldehyde (1.66 mmol, 0.36 g) in THF (0.1M, 16.6 mL). Following the general workup and flash chromatography ($SiO_2$, 10 g, 3%MeOH/$CH_2Cl_2$), the title alkynol was obtained as a light yellow solid (0.49 g, 94%): TLC $R_f$ = 0.03 (3%MeOH/$CH_2Cl_2$); $^1$H NMR (500 MHz, $CDCl_3$) δ 7.62 (d, *J* = 2.1 Hz, 1H), 7.45 (s, 1H), 7.27 (dd, *J* = 8.4, 2.2 Hz, 1H), 6.98 (s, 1H), 6.93 (d, *J* = 8.5 Hz, 1H), 5.76 (s, 1H), 3.88 (s, 3H), 3.60 (s, 3H), 0.15 (s, 9H); $^{13}$C NMR (125 MHz, $CDCl_3$) δ 156.7, 138.8, 133.2, 129.9, 129.6, 128.5, 127.5, 122.3, 111.3, 105.0, 90.9, 60.5, 55.9, 32.6, 0.1; IR (neat $cm^{-1}$) 3113, 2957, 2899, 2837, 2167, 1488, 1279, 1040, 838; HRMS (DART, $M^+$ + H) *m/z* 315.1532 (calculated for $C_{17}H_{22}N_2O_2Si$, 315.1529).

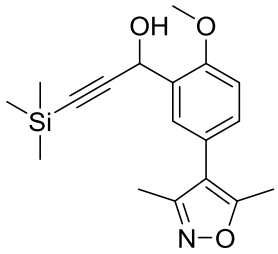


**1-(5-(3,5-dimethylisoxazol-4-yl)-2-methoxyphenyl)-3-(trimethylsilyl) prop-2-yn-1-ol (10i)**

According to the general nucleophilic addition, ethynyltrimethyl silane (4.1 mmol, 0.6 mL) in THF (2M, 2.0 mL) and isopropyl magnesium chloride (2M, 4.1mmol, 2.0 mL) was stirred. At 0 °C was added the aldehyde (2.72 mmol, 0.63 g) in THF (0.1M, 27.2 mL). Following the general workup and flash chromatography ($SiO_2$, 20 g, 3%MeOH/$CH_2Cl_2$), the title alkynol was obtained as a colorless oil (0.86 g, 96%): TLC $R_f$ = 0.4 (3%MeOH/$CH_2Cl_2$); $^1$H NMR (500 MHz, $CDCl_3$) δ 7.53 (s, 1H), 7.17 (d, *J* = 8.1 Hz, 1H), 6.95 (d, *J* = 8.1 Hz, 1H), 5.76 (d, *J* = 5.4 Hz, 1H), 3.90 (s, 3H), 2.38 (s, 3H), 2.24 (s, 3H), 0.18 (s, 9H); $^{13}$C NMR (125 MHz, $CDCl_3$) δ 164.9, 158.7, 156.2, 130.2, 129.2, 128.9, 122.7, 116.1, 111.3, 104.6, 91.0, 60.5, 55.8, 11.5, 10.8, -0.1; IR (neat $cm^{-1}$) 3038, 2923, 2862, 2724, 1682, 1601, 1245, 1176, 1120, 1014, 825; HRMS (DART, $M^+ + H$) *m/z* 330.1528 (calculated for $C_{18}H_{23}NO_3Si$, 330.1525).

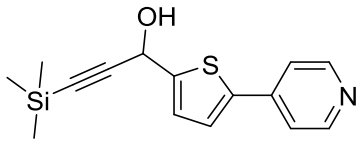


**1-(5-(pyridin-4-yl) thiophen-2-yl)-3-(trimethylsilyl) prop-2-yn-1-ol (10j)**

According to the general nucleophilic addition, ethynyltrimethyl silane (2.6 mmol, 0.4 mL) in THF (2M, 1.3 mL) and isopropyl magnesium chloride (2M, 2.6 mmol, 1.3 mL) was stirred. At 0 °C was added the aldehyde (2.2 mmol, 0.41g) in THF (0.1M, 21.6 mL). Following the general workup and flash chromatography ($SiO_2$, 20 g, 3%MeOH/$CH_2Cl_2$), the title alkynol was obtained as a brown solid (0.6 g, 95%): TLC $R_f$ = 0.2 (3%MeOH/$CH_2Cl_2$); $^1$H NMR (500 MHz, $CDCl_3$) δ 8.49 (d, *J* = 6.2 Hz, 2H), 7.41 (d, *J* = 6.2 Hz, 2H), 7.33 (d, *J* = 3.7 Hz, 1H), 7.14 (d, *J* = 4.4 Hz, 1H), 5.65 (s, 1H), 0.19 (s, 9H); $^{13}$C NMR (125 MHz, $CDCl_3$) δ 150.1, 147.7, 141.9, 141.1, 126.7, 125.3, 119.9, 104.4, 91.3, 60.6, -0.1; IR (neat $cm^{-1}$) 3181, 3017, 2112, 1592, 1494, 1414, 1219, 991, 800; HRMS (DART, $M^+$ + H) *m/z* 288.0901 (calculated for $C_{15}H_{17}NOSSi$, 288.0878).

**General Procedure for Propargyl Methylation**

To a 100 mL flame dried flask under argon was added $CH_2Cl_2$ (1M) at room temperature and cooled to 0 °C. $TiCl_4$ (1M in toluene, 1 eq) was added followed by dimethyl zinc (1.2 M in toluene, 2 eq) and stirred at 0 °C for 30 minutes. To the yellow heterogeneous mixture, alkynol (1eq, in 0.1 M $CH_2Cl_2$) was added dropwise for 10 min. TLC analysis was performed on a small aliquot quenched with MeOH. After ~1 h, the reaction was stopped by a slow dropwise addition of MeOH. Care should be

taken to avoid frothing and addition of MeOH continued until the reaction turns into a homogeneous yellow solution. The crude mixture was stirred at room temperature for 5 minutes and pushed through a plug of silica gel and the solvent was evaporated. To deprotect the TMS alkyne, the crude mixture was dissolved in EtOH (0.2M) and stirred for 30 min with $AgNO_3$ (3 eq, in 1.5M water). KCN (10 eq) dissolved in $H_2O$ (10M) was added slowly and stirred for 1h. The reaction mixture was diluted with EtOAc, washed with water, and dried with $MgSO_4$. The solvent was evaporated, the crude mixture was pre-absorbed onto silica gel, and column chromatography was carried out with 3% MeOH in $CH_2Cl_2$ to afford propargyl-methylated alkynes.

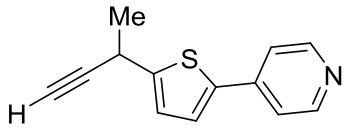


**4-[5-(1-Methyl-prop-2-ynyl)-thiophen-2-yl]-pyridine (12j)**

According to the general methylation protocol, alkynol (0.52 mmol, 0.15 g) in $CH_2Cl_2$ (0.1M) was added to the pre-mixed solution of $TiCl_4$ (0.52 mmol, 1.0 mL) and dimethylzinc (1.04 mmol, 1.60 mL) in $CH_2Cl_2$ (1M). Following the general workup and deprotection, the crude mixture was purified by flash chromatography ($SiO_2$, 5 g, 1:1 EtoAc/hexane) to give the methylated alkyne as a yellow solid (0.17 g, 65%): TLC $R_f$ = 0.8 (1:1 EtoAc/hexane); $^1$H NMR (500 MHz, $CDCl_3$) δ 8.58 (d, J = 4.6 Hz, 2H), 7.48 – 7.41 (m, 2H), 7.35 (d, J = 3.7 Hz, 1H), 7.03 (dd, J = 3.6, 1.0 Hz, 1H), 4.06 (qd, J = 6.9, 2.1 Hz, 1H), 2.36 (d, J = 2.5 Hz, 1H), 1.65 (d, J = 7.1 Hz, 3H). $^{13}$C NMR (125 MHz, $CDCl_3$) δ 150.3, 148.5, 141.4, 139.5, 125.3, 125.0, 119.5, 85.6, 70.5, 27.4, 24.0; IR

(neat $cm^{-1}$) 3198, 2984, 2934, 1594, 1460, 1414, 1220, 991, 802, 690, 525; HRMS (DART, $M^+ + H$) *m/z* 214.0705 (calculated for $C_{13}H_{12}NS$, 214.0690).

**Tertiary propargyl alcohol formation from secondary propargyl alcohol.** The secondary propargyl alcohol was added in dichloromethane to a dried round bottom flask fitted with a stir bar and dried $MnO_2$ (20 equiv). Once complete by TLC, the reaction mixture was filtered through celite and solvent removed in vacuo. The residue was brought up in THF, placed under argon, and methyl magnesium bromide (3.0 M in $Et_2O$, 1.5 equiv) was added via syringe. Once complete by TLC, saturated ammonium chloride was added. The product was extracted 3x with EtOAc, washed with brine, dried over sodium sulfate, filtered, and dried in vacuo. The tertiary alcohol was used with no further purification.

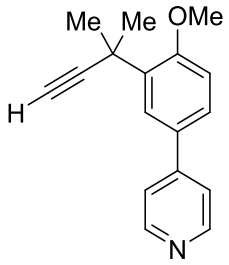


**4-[3-(1,1-Dimethyl-prop-2-ynyl)-4-methoxy-phenyl]-pyridine (13a)**

The tertiary alcohol (0.15 g, 0.461 mmol) was subjected to the general procedure for methylation. Once completed, the dried residue isolated from silica plug was dissolved in MeOH and $K_2CO_3$ (2 equiv) added. The reaction was stirred until complete by TLC. The title compound was purified via column chromatography ($SiO_2$, 1:1 ethyl acetate/hexanes) and isolated as a white solid (0.08 g, 53% 2 steps); $^1H$ NMR (500 MHz, Chloroform-*d*) δ 8.66 (s, 2H), 8.07 (s, 1H), 7.56 (d, *J* = 8.4 Hz, 1H),

7.55 – 7.48 (m, 2H), 7.02 (d, *J* = 8.4 Hz, 1H), 3.94 (s, 3H), 2.47 (s, 1H), 1.77 (s, 6H). $^{13}$C NMR (126 MHz, $CDCl_3$) δ 158.9, 150.3, 148.3, 133.9, 130.1, 126.8, 121.4, 112.5, 91.4, 70.4, 55.6, 36.1, 29.0; IR (neat $cm^{-1}$) 3295, 2972, 2934, 1597, 1487, 1283, 1253, 1221, 1081, 1024, 808, 637; HRMS (DART) calcd for $C_{17}H_{17}NO$ $[M+H]^+$: 252.1368, obs. 252.1326.

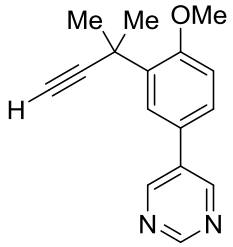


**5-[3-(1,1-Dimethyl-prop-2-ynyl)-4-methoxy-phenyl]-pyrimidine (13b)**

The tertiary alcohol (0.15 g, 0.459 mmol) was subjected to the general procedure for methylation. Once completed, the dried residue isolated from silica plug was dissolved in MeOH and $K_2CO_3$ (2 equiv) added. The reaction was stirred until complete by TLC. The title compound was purified via column chromatography ($SiO_2$, 1:1 ethyl acetate/hexanes) and isolated as a white solid (0.07 g, 47% 2 steps); $^1$H NMR (500 MHz, Chloroform-*d*) δ 9.30 – 9.16 (m, 1H), 9.01 (s, 2H), 8.00 (d, *J* = 2.3 Hz, 1H), 7.49 (dd, *J* = 8.4, 2.3 Hz, 1H), 7.06 (d, *J* = 8.4 Hz, 1H), 3.95 (s, 3H), 2.47 (s, 1H), 1.77 (s, 6H). $^{13}$C NMR (126 MHz, $CDCl_3$) δ 158.7, 156.9, 154.6, 134.4, 126.9, 126.8, 126.3, 112.8, 91.3, 70.7, 70.7, 55.6, 36.2, 29.0; IR (neat $cm^{-1}$) 3290, 2970, 2931, 1606, 1550, 1500, 1389, 1358, 1286, 1252, 1223, 1080, 1022, 895, 815, 726, 627; HRMS (DART) calcd for $C_{16}H_{16}N_2O$ $[M+H]^+$: 253.1341, obs. 253.1316.

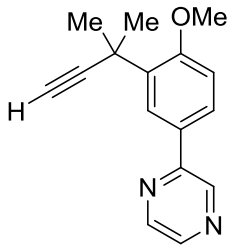


**2-[3-(1,1-Dimethyl-prop-2-ynyl)-4-methoxy-phenyl]-pyrazine (13c)**

The tertiary alcohol (0.15 g, 0.459 mmol) was subjected to the general procedure for methylation. Once completed, the dried residue isolated from silica plug was dissolved in MeOH and $K_2CO_3$ (2 equiv) added. The reaction was stirred until complete by TLC. The title compound was purified via column chromatography ($SiO_2$, 1:1 ethyl acetate/hexanes) and isolated as a white solid (0.08 g, 55% 2 steps); $^1$H NMR (500 MHz, Chloroform-*d*) δ 9.03 (s, 1H), 8.62 (s, 1H), 8.47 (s, 1H), 8.42 (d, *J* = 2.0 Hz, 1H), 7.95 (dd, *J* = 8.5, 2.0 Hz, 1H), 7.05 (d, *J* = 8.5 Hz, 1H), 3.96 (s, 3H), 2.46 (s, 1H), 1.78 (s, 6H). $^{13}$C NMR (126 MHz, $CDCl_3$) δ 159.5, 153.1, 144.2, 142.2, 134.0, 128.6, 127.1, 126.7, 112.4, 91.4, 70.2, 55.6, 36.0, 29.1; IR (neat $cm^{-1}$) 3292, 2971, 2932, 1605, 1503, 1427, 1279, 1252, 1143, 1078, 1025, 816, 634; HRMS (DART) calcd for $C_{16}H_{16}N_2O$ $[M+H]^+$: 253.1341, obs. 253.1322.

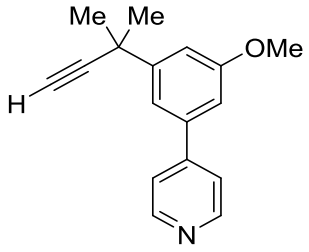


**4-[3-(1,1-Dimethyl-prop-2-ynyl)-5-methoxy-phenyl]-pyridine (13d)**

The tertiary alcohol (150 mg, 0.461 mmol) was subjected to the general procedure for methylation. Once completed, the dried residue isolated from silica plug was dissolved in MeOH and $K_2CO_3$ (2 equiv) added. The reaction was stirred until complete by TLC. The title compound was purified via column chromatography ($SiO_2$, 1:1 ethyl acetate/hexanes) and isolated as a white solid (0.08 g, 50% 2 steps); $^1$H NMR (500 MHz, Chloroform-*d*) δ 8.85 – 8.54 (m, 2H), 7.63 – 7.48 (m, 2H), 7.44 (d, *J* = 1.6 Hz, 1H), 7.23 (d, *J* = 2.0 Hz, 1H), 7.03 (d, *J* = 1.9 Hz, 1H), 3.91 (s, 3H), 2.42 (s, 1H), 1.67 (s, 6H). $^{13}$C NMR (126 MHz, $CDCl_3$) δ 160.3, 150.4, 149.1, 148.7, 139.8, 122.0, 117.1, 112.7, 110.6, 90.7, 70.5, 55.6, 36.2, 31.7; IR (neat cm$^{-1}$) 3288, 2974, 2932, 1592, 1549, 1451, 1405, 1322, 1264, 1049, 818, 642; HRMS (DART) calcd for $C_{17}H_{17}NO$ $[M+H]^+$: 252.1368, obs. 252.1407.

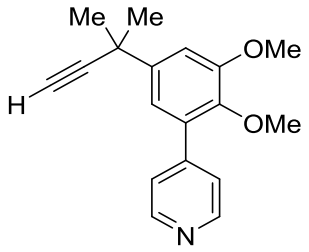


**4-[5-(1,1-Dimethyl-prop-2-ynyl)-2,3-dimethoxy-phenyl]-pyridine (13e)**

The tertiary alcohol (150 mg, 0.422 mmol) was subjected to the general procedure for methylation. Once completed, the dried residue isolated from silica plug was dissolved in MeOH and $K_2CO_3$ (2 equiv) added. The reaction was stirred until complete by TLC. The title compound was purified via column chromatography ($SiO_2$, 1:1 ethyl acetate/hexanes) and isolated as a yellow solid (0.08 g, 56% 2 steps) (; $^1$H NMR (500 MHz, Chloroform-*d*) δ 8.68 (s, 2H), 7.52 (d, *J* = 4.2 Hz, 2H), 7.24 (d, *J* = 1.7 Hz, 1H), 7.12 (d, *J* = 1.8 Hz, 1H), 3.96 (s, 3H), 3.64 (s, 3H), 2.40 (s, 1H), 1.65 (s, 6H). $^{13}$C NMR (126 MHz, $CDCl_3$) δ 153.0, 149.7, 146.5, 145.4, 142.9, 132.6, 124.4, 118.9, 111.1, 90.8, 70.3, 61.0, 56.2, 36.0, 31.8; IR (neat $cm^{-1}$) 3286, 2973, 2933, 1594, 1547, 1481, 1462, 1405, 1278, 1240, 1146, 1042, 1005, 827, 645; HRMS (DART) calcd for $C_{18}H_{19}NO_2$ $[M+H]^+$: 282.1494, obs. 282.1504.

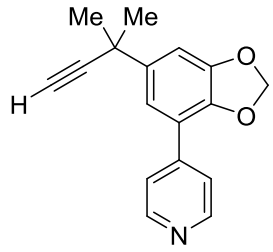


**4-[6-(1,1-Dimethyl-prop-2-ynyl)-benzo[1,3] dioxol-4-yl]-pyridine (13f)**

The tertiary alcohol (150 mg, 0.442 mmol) was subjected to the general procedure for methylation. Once completed, the dried residue isolated from silica plug was dissolved in MeOH and $K_2CO_3$ (2 equiv) added. The reaction was stirred until complete by TLC. The title compound was purified via column chromatography ($SiO_2$, 1:1 ethyl acetate/hexanes) and isolated as an off-white solid (0.07 g, 46% 2 steps); $^1$H NMR (500 MHz, Chloroform-*d*) δ 8.72 (s, 2H), 7.69 (d, *J* = 5.2 Hz, 2H), 7.42 – 7.31 (m, 1H),

7.12 (d, *J* = 1.8 Hz, 1H), 6.08 (s, 2H), 2.42 (s, 1H), 1.64 (s, 6H). $^{13}$C NMR (126 MHz, $CDCl_3$) δ 150.3, 148.6, 144.2, 143.6, 141.4, 122.4, 119.0, 117.6, 107.3, 101.6, 90.8, 70.4, 70.4, 35.9, 31.9; IR (neat $cm^{-1}$) 3291, 3030, 2928, 1969, 1597, 1544, 1474, 1403, 1221, 1043, 943, 823, 651; HRMS (DART) calcd for $C_{17}H_{15}NO_2$ $[M+H]^+$: 266.1181, obs. 266.1208.

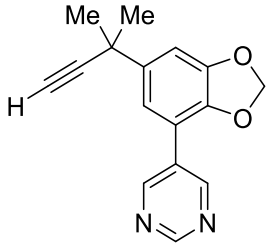


**5-[6-(1,1-Dimethyl-prop-2-ynyl)-benzo[1,3] dioxol-4-yl]-pyrimidine (13g)**

The tertiary alcohol (150 mg, 0.441 mmol) was subjected to the general procedure for methylation. Once completed, the dried residue isolated from silica plug was dissolved in MeOH and $K_2CO_3$ (2 equiv) added. The reaction was stirred until complete by TLC. The title compound was purified via column chromatography ($SiO_2$, 1:1 ethyl acetate/hexanes) and isolated as a yellow solid (0.08 g, 51% 2 steps); $^1$H NMR (500 MHz, Chloroform-*d*) δ 9.20 (s, 1H), 9.12 (s, 2H), 7.32 (d, *J* = 1.8 Hz, 1H), 7.13 (d, *J* = 1.8 Hz, 1H), 6.09 (s, 2H), 2.42 (s, 1H), 1.64 (s, 6H). $^{13}$C NMR (126 MHz, $CDCl_3$) δ 157.3, 155.4, 148.5, 143.9, 141.7, 130.0, 117.0, 114.9, 107.1, 101.6, 90.4, 70.4, 35.8, 31.7; IR (neat $cm^{-1}$) 3295, 2977, 2167, 1551, 1408, 1262, 1178, 1038, 940, 855, 724, 632; HRMS (DART) calcd for $C_{16}H_{14}N_2O_2$ $[M+H]^+$: 267.1133, obs. 267.1109.

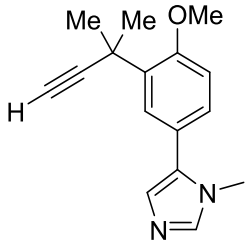


**5-[3-(1,1-Dimethyl-prop-2-ynyl)-4-methoxy-phenyl]-1-methyl-1H-imidazole (13h)**

The tertiary alcohol (150 mg, 0.457 mmol) was subjected to the general procedure for methylation. Once completed, the dried residue isolated from silica plug was dissolved in MeOH and $K_2CO_3$ (2 equiv) added. The reaction was stirred until complete by TLC. The title compound was purified via column chromatography ($SiO_2$, 1:1 ethyl acetate/hexanes) and isolated as a yellow solid (0.07 g, 48% 2 steps); $^1$H NMR (500 MHz, Chloroform-*d*) δ 7.77 (d, *J* = 2.2 Hz, 1H), 7.53 (s, 1H), 7.29 (dd, *J* = 8.3, 2.3 Hz, 2H), 7.08 (s, 1H), 6.98 (d, *J* = 8.4 Hz, 1H), 3.92 (s, 3H), 3.68 (s, 3H), 2.42 (s, 1H), 1.74 (s, 6H). $^{13}$C NMR (126 MHz, $CDCl_3$) δ 157.5, 138.7, 133.5, 133.3, 128.3, 128.3, 127.8, 127.5, 121.8, 112.0, 91.4, 70.1, 55.4, 35.9, 32.5, 28.8; IR (neat $cm^{-1}$) 3288, 2927, 2853, 1767, 1713, 1492, 1366, 1252, 1196, 1080, 1024, 817, 637; HRMS (DART) calcd for $C_{16}H_{18}N_2O$ $[M+H]^+$: 255.1497, obs. 255.1523.

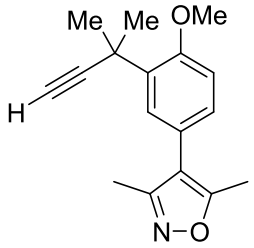


**4-[3-(1,1-Dimethyl-prop-2-ynyl)-4-methoxy-phenyl]-3,5-dimethyl-isoxazole (13i)**

The tertiary alcohol (150 mg, 0.437 mmol) was subjected to the general procedure for methylation. Once completed, the dried residue isolated from silica plug was dissolved in MeOH and $K_2CO_3$ (2 equiv) added. The reaction was stirred until complete by TLC. The title compound was purified via column chromatography ($SiO_2$, 1:1 ethyl acetate/hexanes) and isolated as a yellow solid (0.08 g, 54% 2 steps); $^1$H NMR (500 MHz, Chloroform-*d*) δ 7.66 (d, *J* = 2.2 Hz, 1H), 7.15 (dd, *J* = 8.3, 2.2 Hz, 1H), 6.98 (d, *J* = 8.3 Hz, 1H), 3.92 (s, 3H), 2.44 (s, 3H), 2.42 (s, 1H), 2.31 (s, 3H), 1.74 (s, 6H). $^{13}$C NMR (126 MHz, $CDCl_3$) δ 164.8, 158.9, 157.0, 133.4, 128.7, 128.4, 122.3, 116.4, 112.1, 91.4, 70.0, 55.3, 35.9, 28.9, 11.6, 10.9; IR (neat cm$^{-1}$) 3288, 2970, 2930, 1603, 1505, 1453, 1358, 1251, 1218, 1080, 1026, 819, 642; HRMS (DART) calcd for $C_{17}H_{19}NO_2$ $[M+H]^+$: 270.1494, obs. 270.1477.

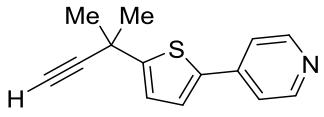


**4-[5-(1,1-Dimethyl-prop-2-ynyl)-thiophen-2-yl]-pyridine (13j)**

The tertiary alcohol (150 mg, 0.498 mmol) was subjected to the general procedure for methylation. Once completed, the dried residue isolated from silica plug was dissolved in MeOH and $K_2CO_3$ (2 equiv) added. The reaction was stirred until

complete by TLC. The title compound was purified via column chromatography ($SiO_2$, 1:1 ethyl acetate/hexanes) and isolated as a yellow solid (0.07 g, 46% 2 steps); $^{1}H$ NMR (500 MHz, Chloroform-*d*) δ 8.60 (s, 2H), 7.46 (d, *J* = 5.1 Hz, 2H), 7.35 (d, *J* = 3.8 Hz, 1H), 7.07 (d, *J* = 3.8 Hz, 1H), 2.41 (s, 1H), 1.73 (s, 6H). $^{13}C$ NMR (126 MHz, $CDCl_3$) δ 154.2, 150.3, 141.5, 139.1, 124.9, 124.3, 119.6, 89.5, 69.7, 34.0, 32.4; IR (neat $cm^{-1}$) 3284, 2987, 2967, 1594, 1495, 1412, 1221, 991, 808, 652; HRMS (DART) calcd for $C_{14}H_{13}NS$ $[M+H]^+$: 228.0847, obs. 228.0867.

## 4.8 References


(1) Srinivasan, R.; Tan, L. P.; Wu, H.; Yang, P.; Kalesh, K. A.; Yao, S. Q. *Org. Biomol. Chem.* **2009**, *7*, 1821.

(2) Liu, J.; Numa, M. M. D.; Liu, H.; Huang, S-J.; Sears, P.; Shikhman, A. R.; Wong, C-H. *J. Org. Chem.* **2004**, *69*, 6273.

(3) Isidro-L, A.; Murillo, T.; Bello, P.; Cilibrizzi, A.; Hodgkinson, J. T.; Galloway, W. R. J. D.; Bender, A.; Welch, M.; Spring, D. R. *Proc. Natl. Acad. Sci. USA.* **2011**, *108*, 6793.

(4) Tan, D. S.; Foley, M. A.; Stockwell, B. R.; Shair, M. D.; Schreiber, S. L. *J. Am. Chem. Soc.* **1999**, *121*, 9073.

(5) Kambe, T.; Correia, B. E.; Niphakis, M. J.; Cravatt, B. F. *J. Am. Chem. Soc.* **2014**, *136*, 10777.

(6) Grammel, M.; Hang, H. C. *Nat. Chem. Biol.* **2013**, *9*, 475.

(7) Yamaguchi, M.; Park, H. J.; Ishizuka, S.; Omata, K.; Hirama, M. *J. Med. Chem.* **1995**, *38*, 5015.

(8) Chandregowda, V.; Rao, G. V.; Reddy, G. C. *Org. Process Res. Dev.* **2007**, *11*, 813.

(9) Chinchilla, R.; Najera, C. *Chem. Soc. Rev.* **2011**, *40*, 5084.

(10) Schilz, M.; Plenio, H. *J. Org. Chem.* **2013**, *77*, 2798.

(11) Chinchilla, R.; Najera, C. *Chem. Rev.* **2007**, *107*, 874.

(12) Siemsen, P.; Livingston, R. C.; Diederich, F. *Angew. Chem., Int. Ed.* **2000**, *39*, 2632.

(13) Thirumurugan, P.; Matosiuk, D.; Jozwiak, K. *Chem. Rev.* **2013**, *113*, 4905.

(14) Nicholas, K. M.; Pettit, R. *J. Organometal. Chem.* **1972**; *44*, C21.

(15) Teobald, B. J. *Tetrahedron* **2002**, *58*, 4133.

(16) Wakabayashi, H.; Shishido, Y. WO 5789423, 1998.

(17) Lockwood, R. F.; Nicholas, K. M. *Tetrahedron Lett.* **1977**, *18*, 4163.

(18) Pelphrey, P. M.; Popov, V.; Joska, T. M.; Beierlein, J. M.; Bolstad, E.; Fillingham, Y.; Wright, D. L.; Anderson, A. C. *J. Med. Chem.* **2007**, *50*, 940.

(19) Viswanathan, K.; Frey, K.; Scocchera, E.; Martin, B.; Swain III, P.; Alverson, J.; Priestley, N. D.; Anderson, A. C.; Wright, D. L. *PLoS ONE* **2012**, *7*, e29434.

(20) G-Dayanandan, N.; Paulsen, J. L.; Viswanathan, K.; Keshipeddy, S.; Lombardo, M. N.; Zhou, W.; Lamb, K. M.; Sochia, A. E.; Alverson, J. B.; Priestley, N. D.; Wright, D. L.; Anderson, A. C. *J. Med. Chem.* **2014**, *57*, 2643.

(21) Paulsen, J. L.; Viswanathan, K.; Wright, D. L.; Anderson, A. C. *Bioorg. Med. Chem. Lett.* **2013**, *23*, 1279.

(22) Lamb, K. M.; G-Dayanandan, N.; Wright, D. L.; Anderson, A. C. *Biochemistry* **2013**, *52*, 7318.

(23) Zhou, W.; Viswanathan, K.; Hill, D.; Anderson, A. C.; Wright, D. L. *Drug. Metab. Dispos.* **2012**, *40*, 2002.

(24) Keshipeddy, S.; Reeve, S.; Anderson, A. C.; Wright, D. L. *J. Am. Chem. Soc.* **2015**, *137*, 8983.

(25) Bolstad D. B.; Bolstad, E. S. D.; Frey, K. M.; Wright, D. L.; Anderson, A. C. *J. Med. Chem.* **2008**, *51*, 6839.

(26) Ohira S. *Syn. Comm*. **1989**, *19*, 561.

(27) Saito, T.; Furukawa, N.; Otani, T. *Org. Biomol. Chem*. **2010**, *8*, 1126.

(28) Trost, B. M.; Rudd, M. T. *J. Am. Chem. Soc*. **2005**, *127*, 4763.

(29) Gaudilliere, B.; Jacobelli, H.; Wilson, M. W.; Picard, J. A. WO 2002331362, 2004.

(30) Kumar, G. G. K. S. N.; Laali, K. K. *Org. Biomol. Chem*. **2012**, *10*, 7347.

(31) Meyer, V. J.; Niggemann, M. *Chem. - A Eur. J*. **2012**, *18*, 4687.

(32) Sakai, N.; Hirasawa, M.; Konakahara, T. *Tetrahedron Lett*. **2005**, *46*, 6407.

(33) Georgy, M.; Boucard, V.; Debleds, O.; Zotto, C. D.; Campagne, J. M. *Tetrahedron* **2009**, *65*, 1758.

(34) Brinkmeyer, R. S.; Macdonald, T. L. *J. Chem. Soc. Chem. Commun*. **1978**, *20*, 876.

(35) Tang, X.; Woodward, S.; Krause, N. European *J. Org. Chem.* **2009**, *17*, 2836.

(36) Zhong, Y. W.; Matsuo, Y.; Nakamura, E. *Chem. - An Asian J*. **2007**, *2*, 358.

(37) Reetz, M. T.; Westermann, J.; Steinbach, R. *Angew. Chemie Int. Ed. English* **1980**, *19*, 901.

(38) Reetz, M. T.; Westermann, J. *J. Org. Chem.* **1983**, *48*, 254.

(39) Oblak, E. Z.; Vanheyst, M. D.; Li, J.; Wiemer, A. J.; Wright, D. L. *J. Am. Chem. Soc.* **2014**, *136*, 4309.

(40) Chung, M. E.; Hagenah, J. *J. Org. Chem*. **1987**, *52*, 1889.

(41) Imperio, D.; Pirali, T.; Galli, U.; Pagliai, F. *Bioorg. Med. Chem*. **2007**, *15*, 6748.

(42) Reetz, M.; Westermann, J.; Steinbach, R. *J. Chem. Soc., Chem. Commun.* **1981**, 237.

# 5 Unpublished NMR Data

# CHAPTER 3 NMR DATA

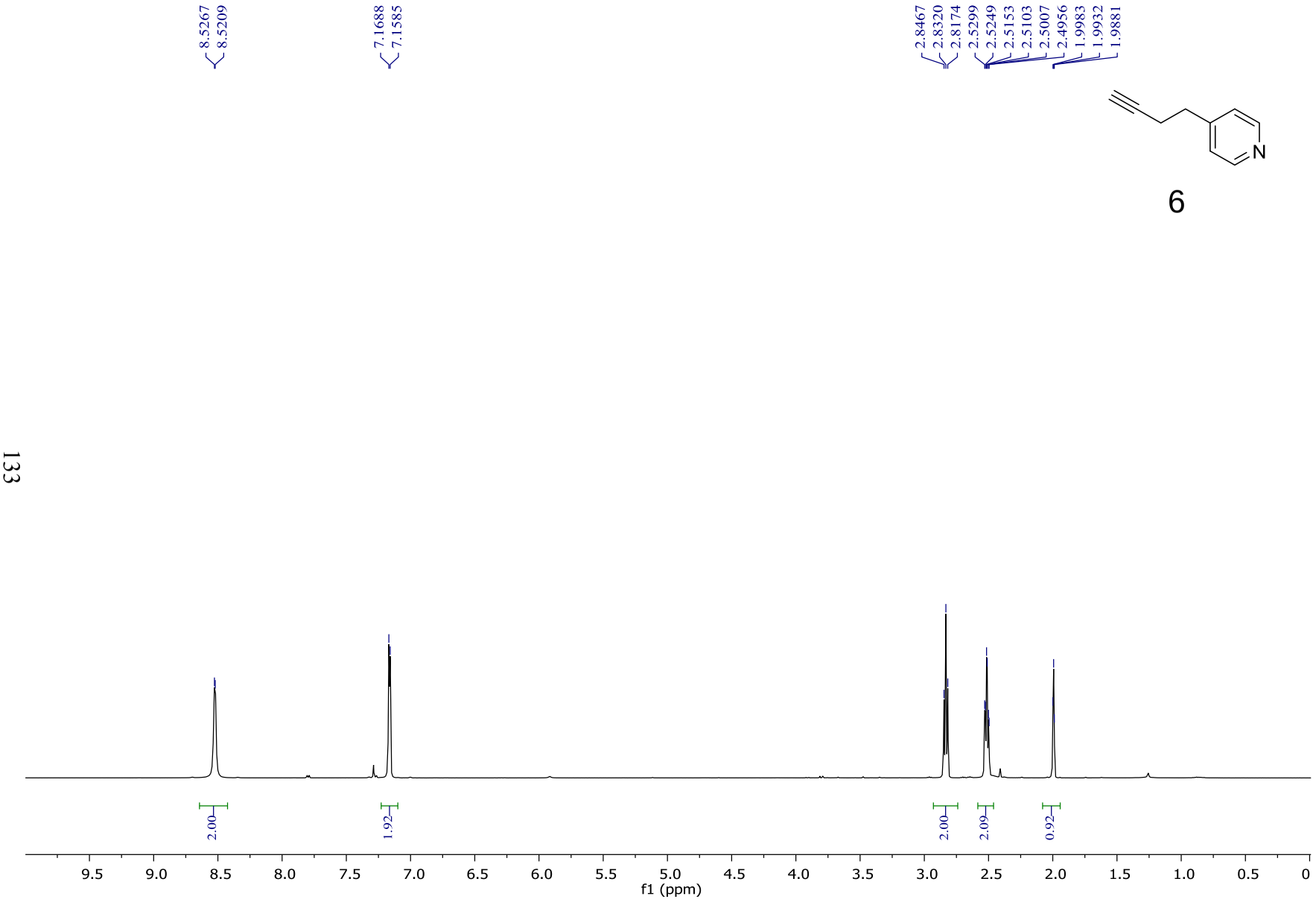
8.5267
8.5209
7.1688
7.1585
2.8467
2.8320
2.8174
2.5299
2.5249
2.5153
2.5103
2.5007
2.4956
1.9983
1.9932
1.9881
N
6
2.00
1.92
2.00
2.09
0.92
9.5
9.0
8.5
8.0
7.5
7.0
6.5
6.0
5.5
5.0
4.5
4.0
3.5
3.0
2.5
2.0
1.5
1.0
0.5
0
f1 (ppm)

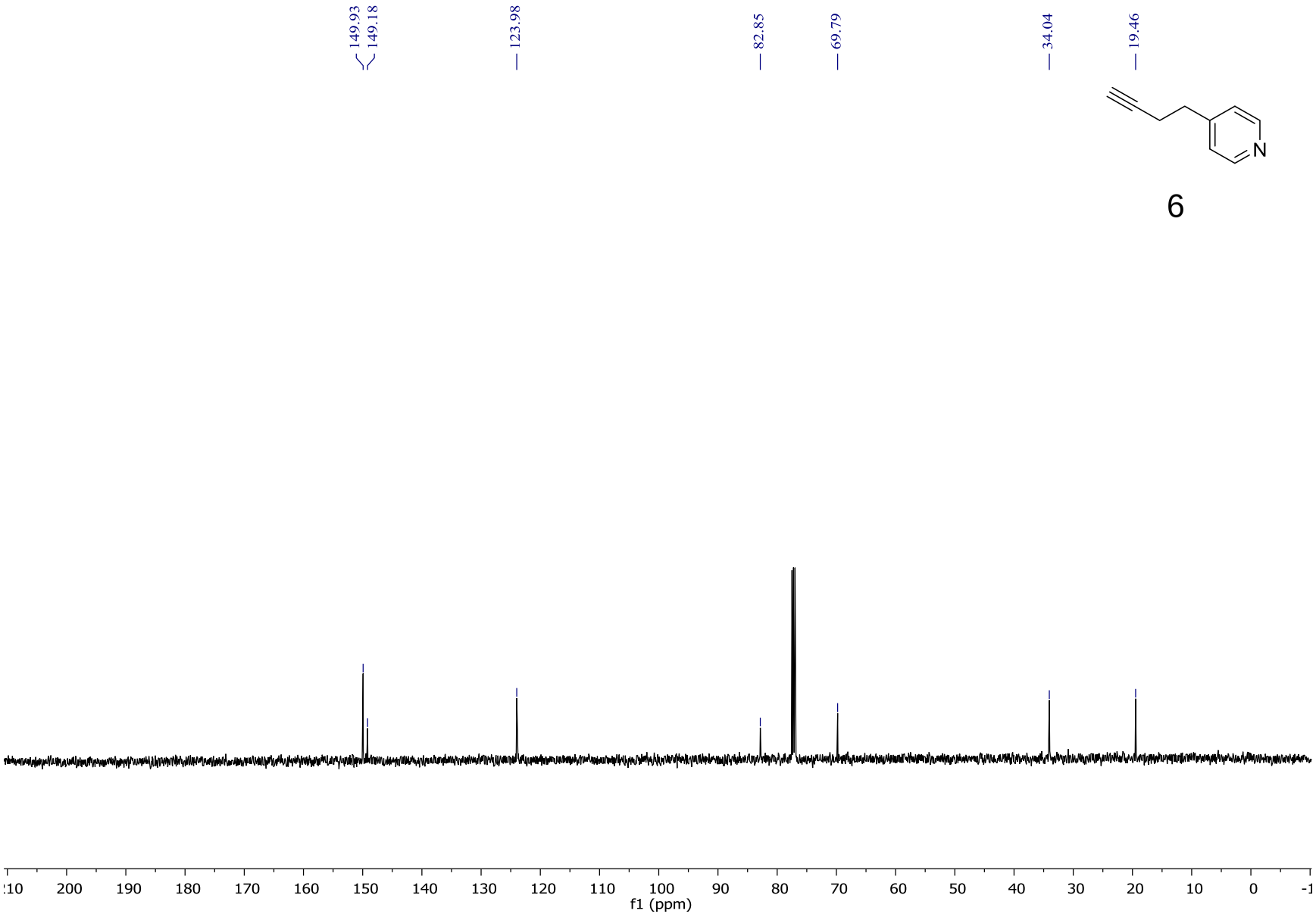


6

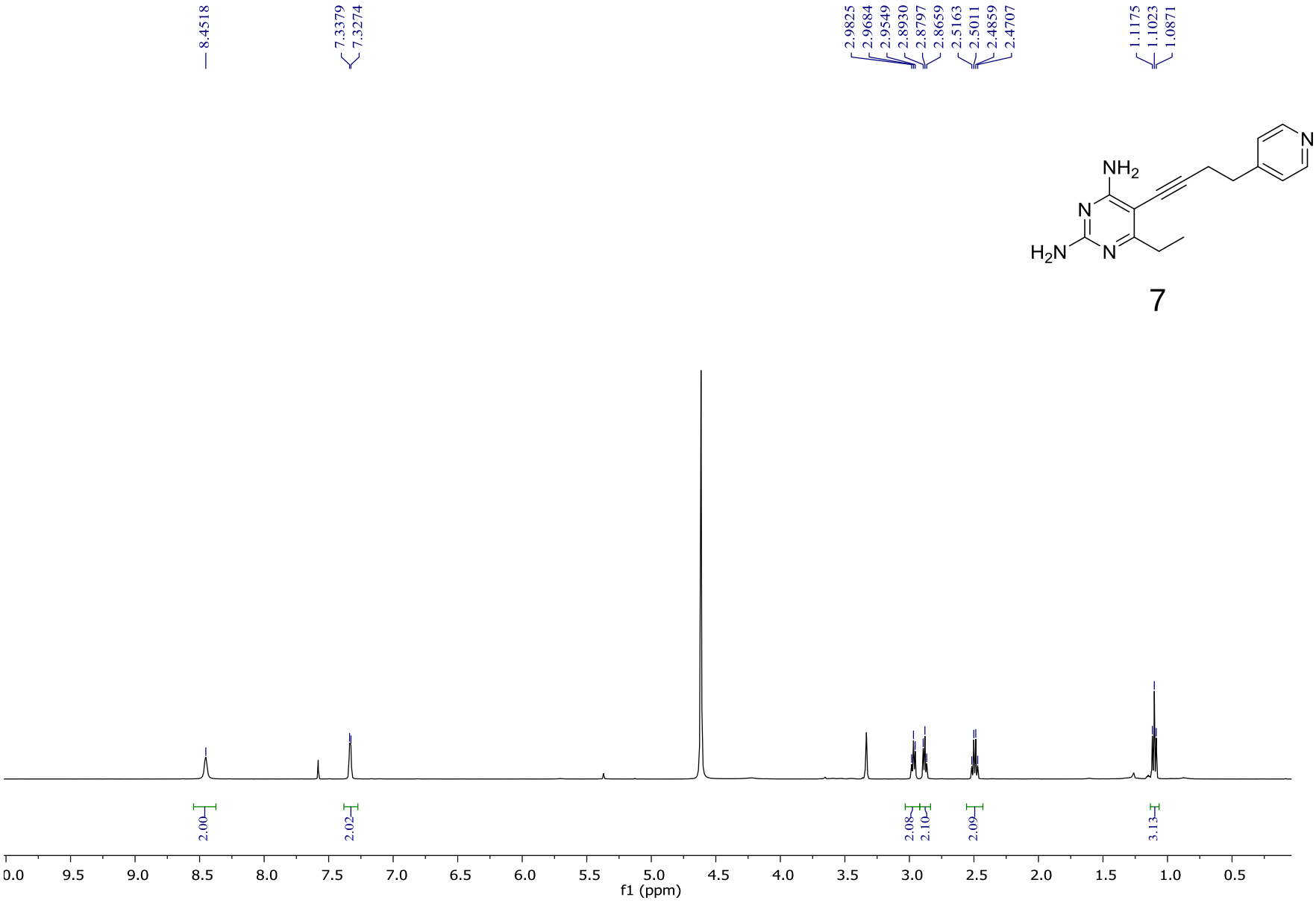
8.4518
7.3379
7.3274
2.9825
2.9684
2.9549
2.8930
2.8797
2.8659
2.5163
2.5011
2.4859
2.4707
1.1175
1.1023
1.0871
NH2
N
H2N
N
N
2.00
2.02
2.08
2.10
2.09
3.13
f1 (ppm)

7

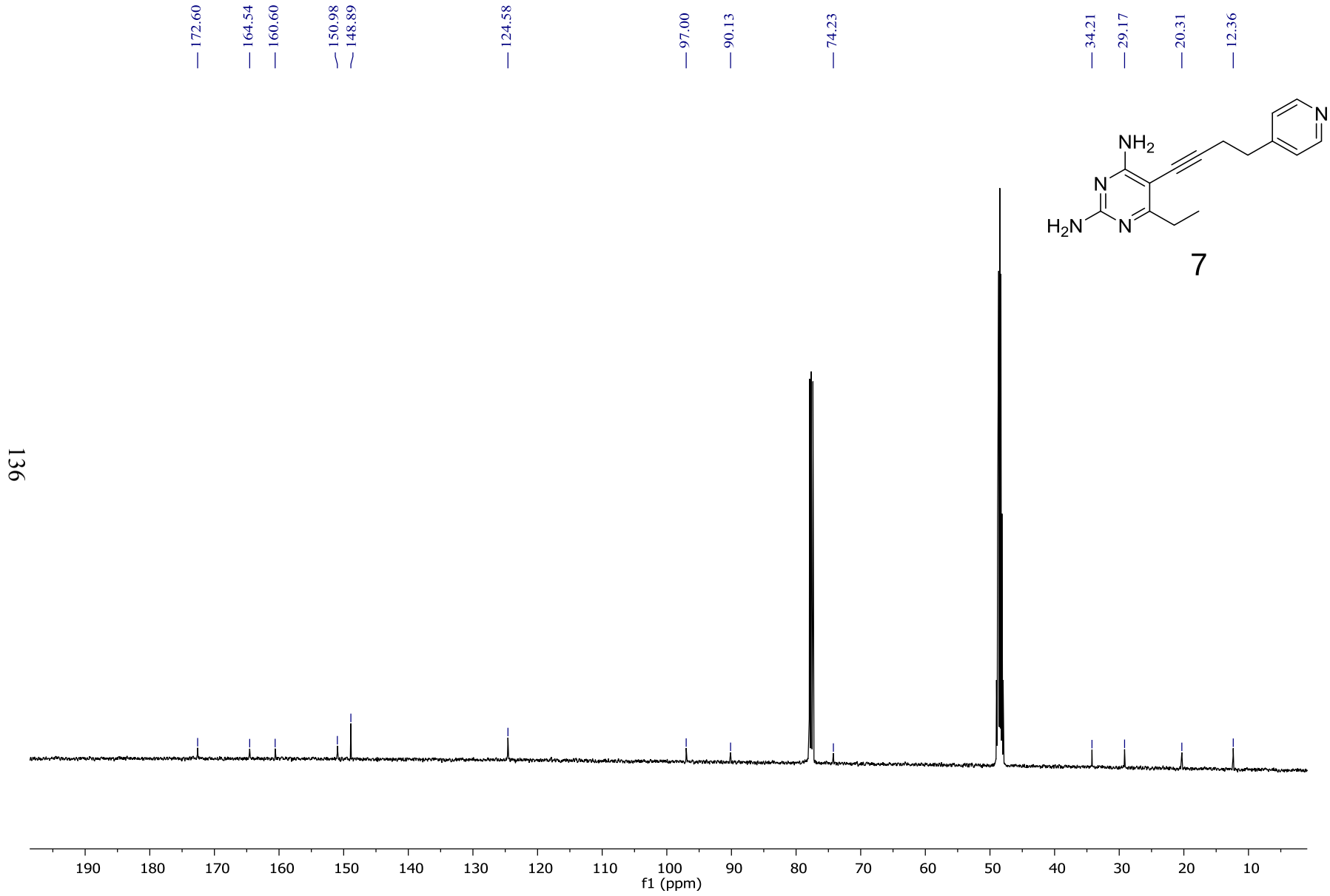
172.60
164.54
160.60
150.98
148.89
124.58
97.00
90.13
74.23
34.21
29.17
20.31
12.36
NH2
N
H2N
N
N
7
190
180
170
160
150
140
130
120
110
100
90
80
70
60
50
40
30
20
10
f1 (ppm)

3a
8.4401
8.4290
7.0766
7.0657
2.6972
2.6821
2.6666
2.1709
2.1657
2.1572
2.1520
2.1433
2.1381
1.9879
1.9827
1.9774
1.8236
1.8089
1.7935
1.7795
1.7654
2.00
1.98
2.03
0.90
2.04
2.06
f1 (ppm)

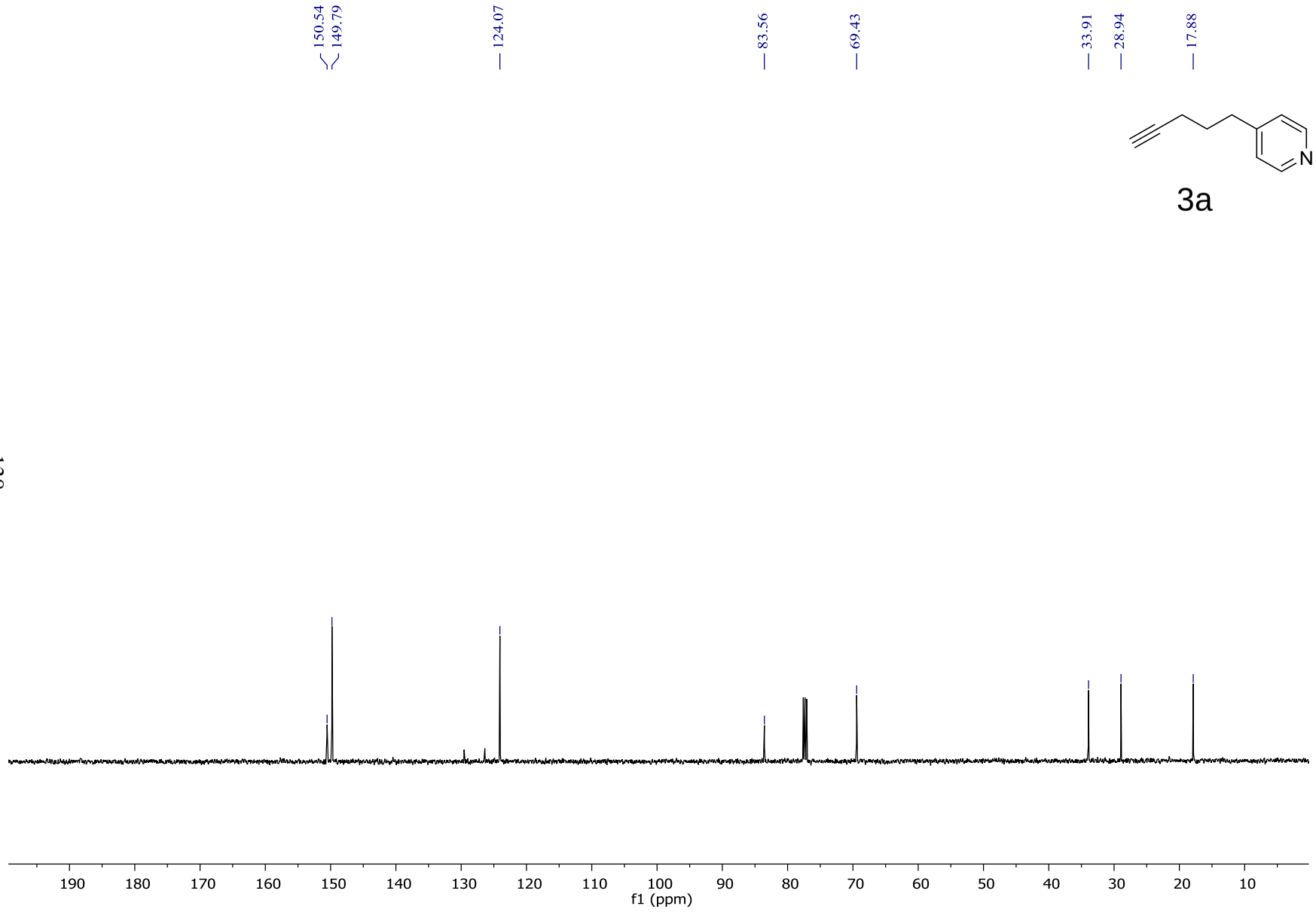
150.54
149.79
124.07
83.56
69.43
33.91
28.94
17.88
N
3a
190
180
170
160
150
140
130
120
110
100
90
80
70
60
50
40
30
20
10
f1 (ppm)

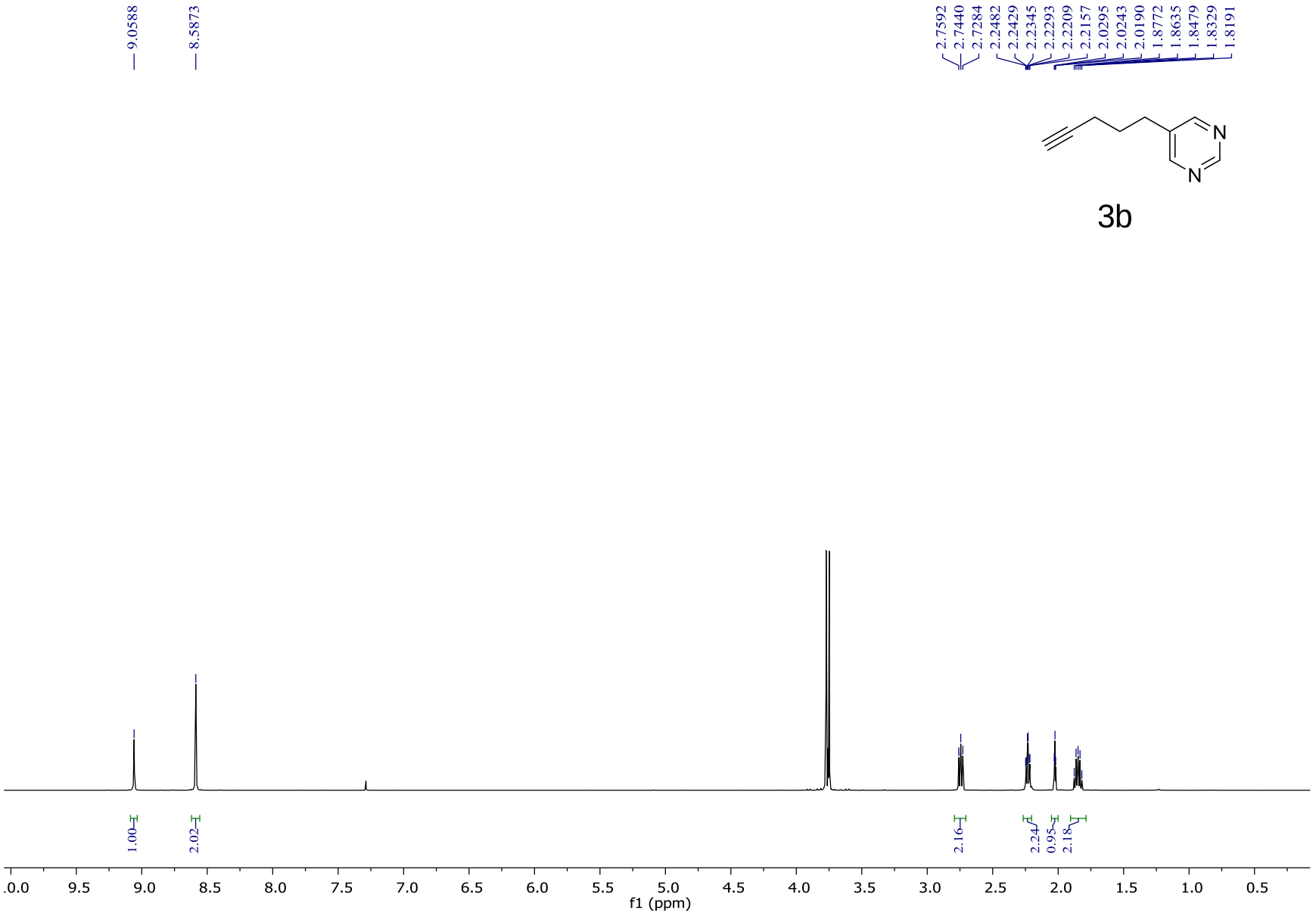
9.0588
8.5873
2.7592
2.7440
2.7284
2.2482
2.2429
2.2345
2.2293
2.2209
2.2157
2.0295
2.0243
2.0190
1.8772
1.8635
1.8479
1.8329
1.8191
N
N
3b
1.00
2.02
2.16
2.24
0.95
2.18
f1 (ppm)

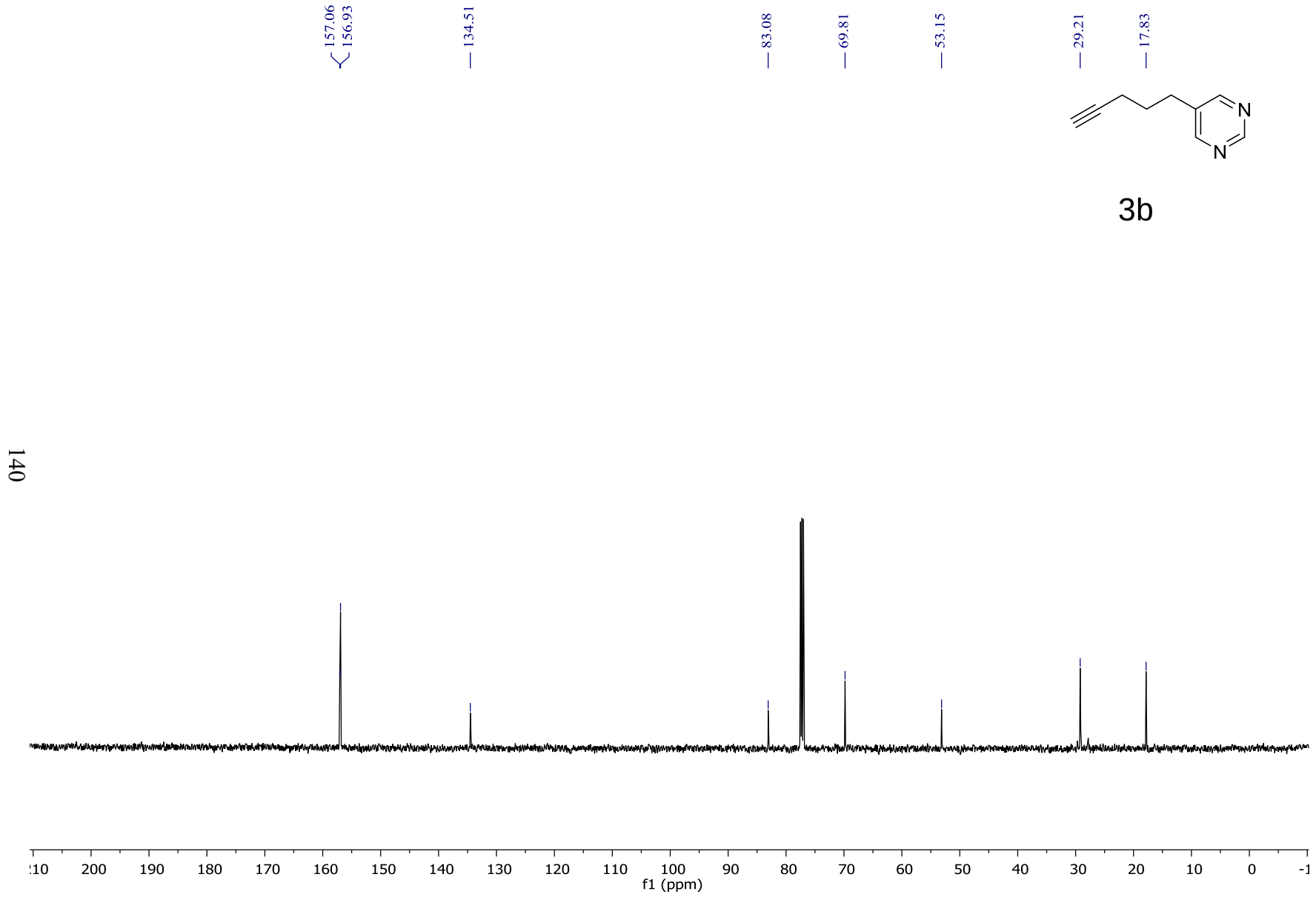
157.06
156.93
134.51
83.08
69.81
53.15
29.21
17.83
N
N
3b
140
f1 (ppm)

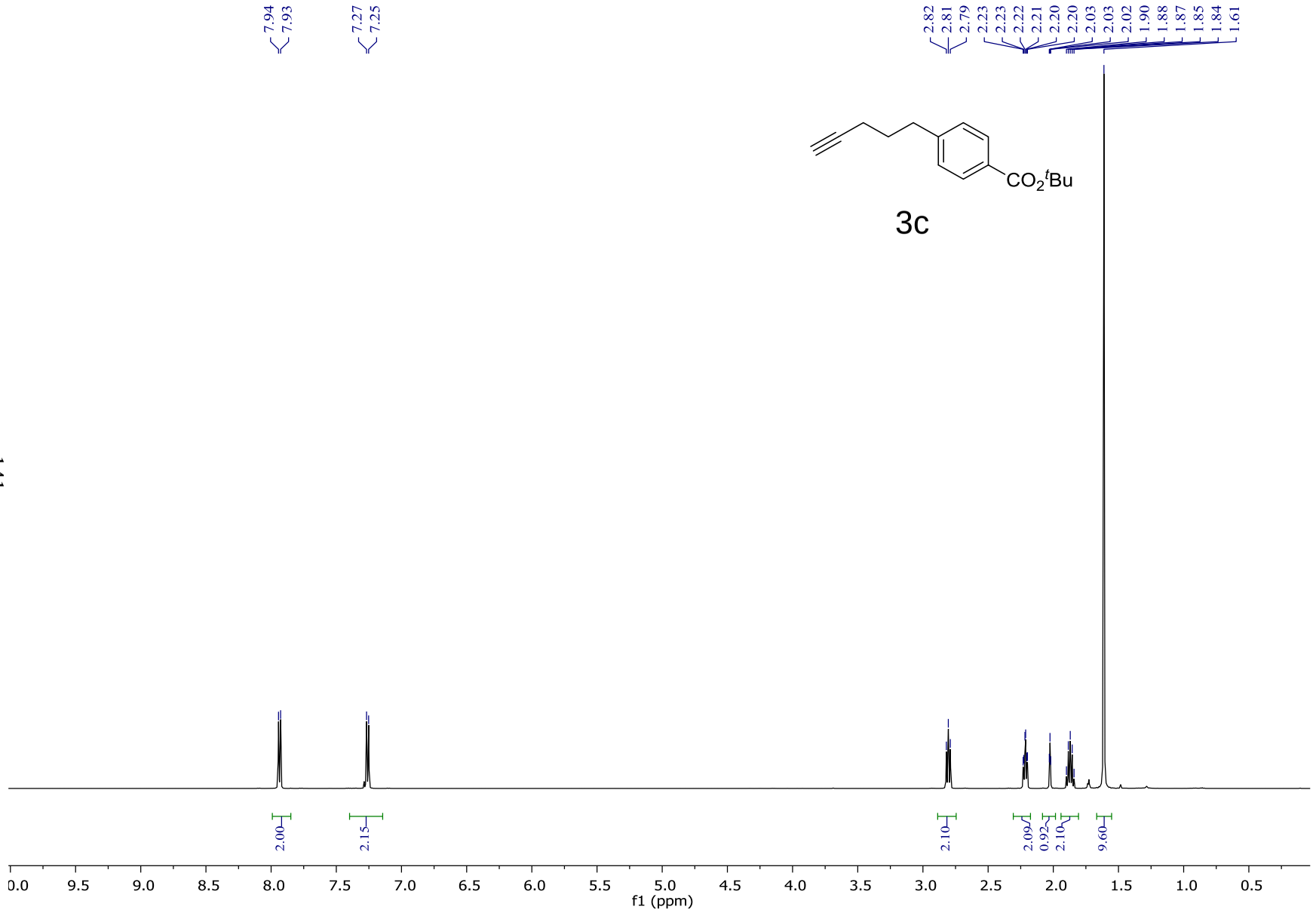
7.94
7.93
7.27
7.25
2.82
2.81
2.79
2.23
2.23
2.22
2.21
2.20
2.20
2.03
2.03
2.02
1.90
1.88
1.87
1.85
1.84
1.61
CO2tBu
3c
2.00
2.15
2.10
2.09
0.92
2.10
9.60
f1 (ppm)

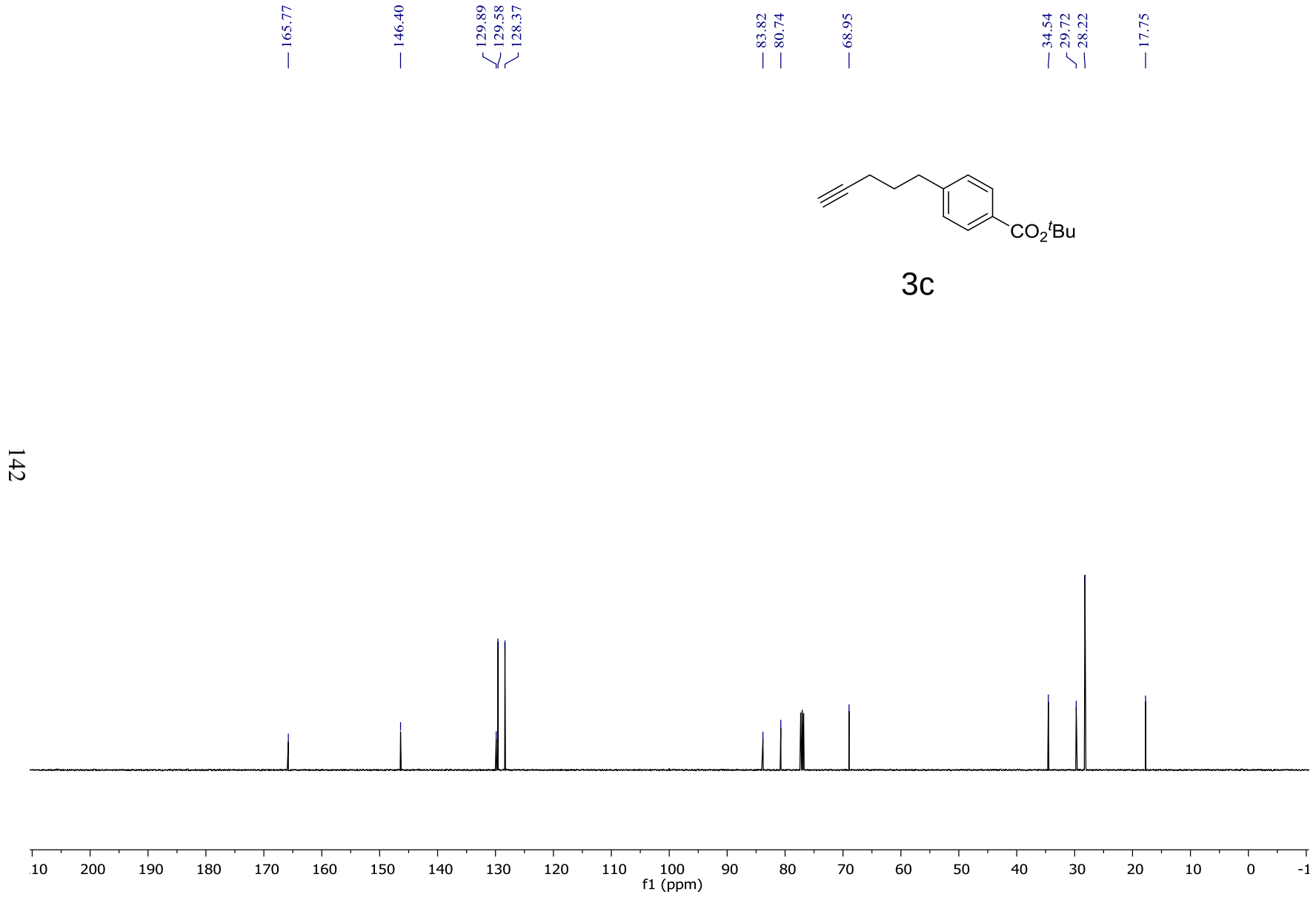
165.77
146.40
129.89
129.58
128.37
83.82
80.74
68.95
34.54
29.72
28.22
17.75
CO2tBu
f1 (ppm)

3c

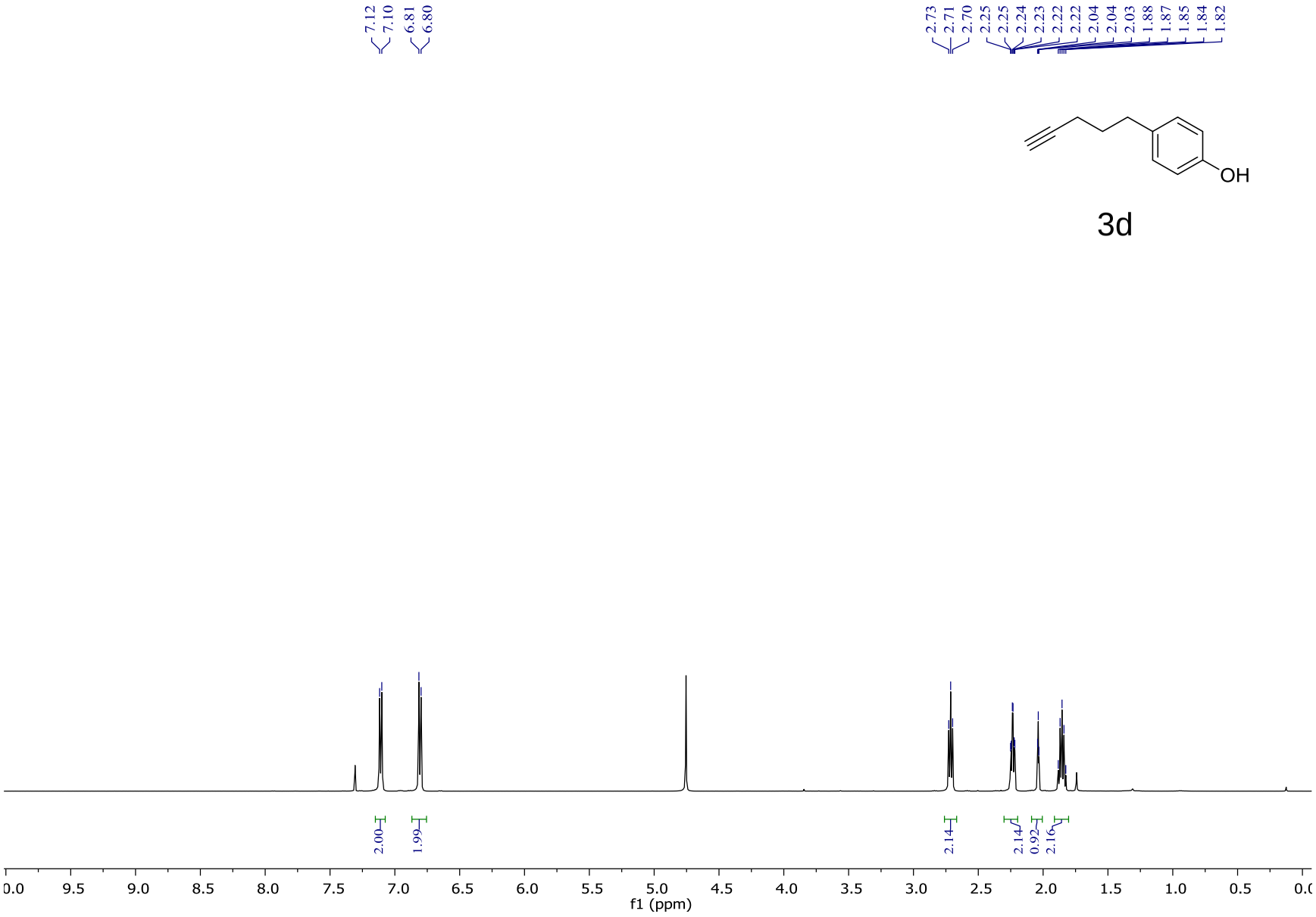
7.12
7.10
6.81
6.80
2.73
2.71
2.70
2.25
2.25
2.24
2.23
2.22
2.22
2.04
2.04
2.03
1.88
1.87
1.85
1.84
1.82
OH
3d
2.00
1.99
2.14
2.14
0.92
2.16
f1 (ppm)

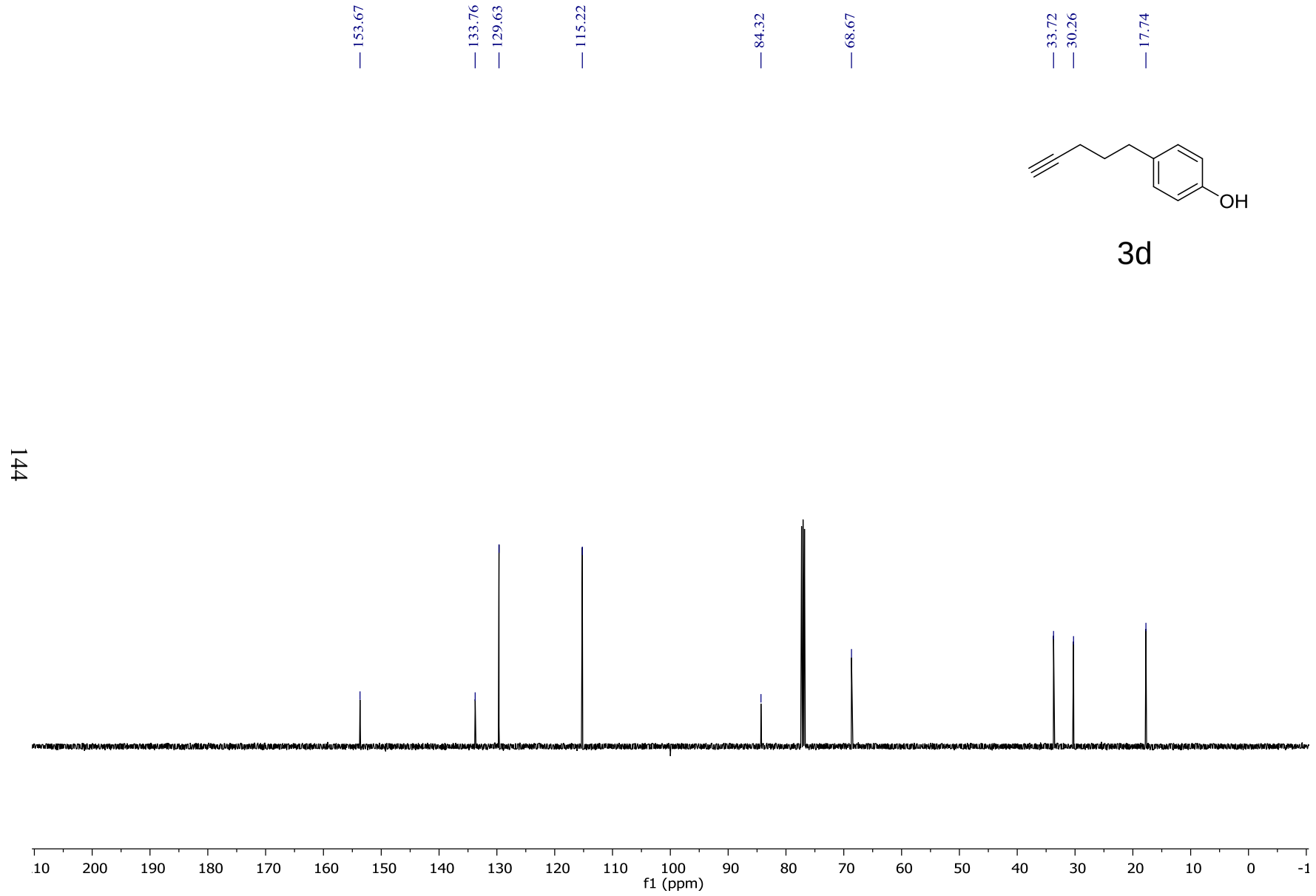
153.67
133.76
129.63
115.22
84.32
68.67
33.72
30.26
17.74
OH
3d
f1 (ppm)

8.5109
8.4990
7.1354
7.1236
2.6647
2.6495
2.6339
2.2646
2.2593
2.2506
2.2453
2.2366
2.2313
1.9833
1.9780
1.9727
1.8144
1.7994
1.7840
1.7682
1.7527
1.6179
1.6035
1.5888
1.5731
1.5591
8
2.00
1.99
1.93
2.04
1.06
1.96
2.07
f1 (ppm)

8
18.37
27.98
29.34
34.83
68.81
82.23
124.02
149.88
151.21
f1 (ppm)

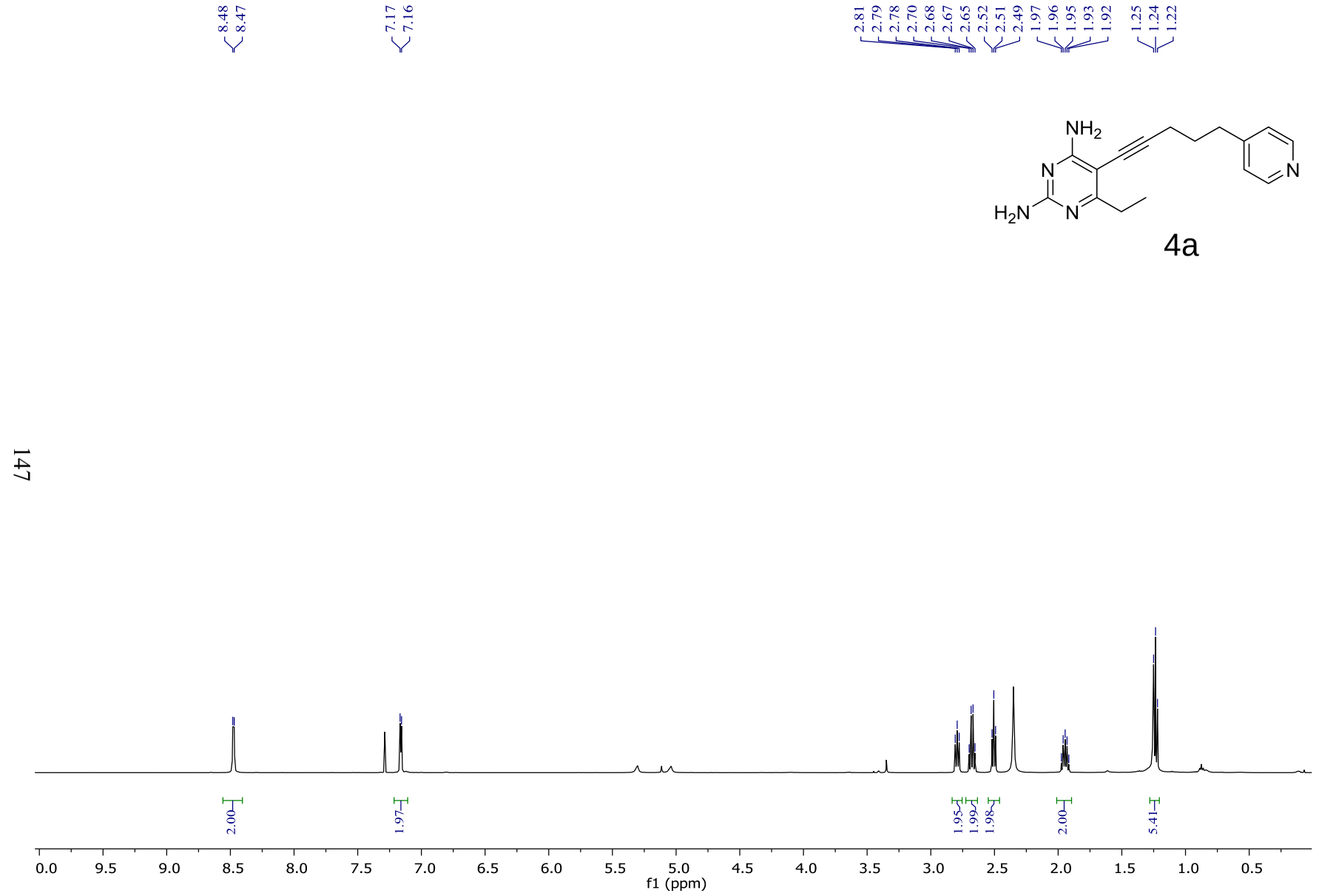
8.48
8.47
7.17
7.16
2.81
2.79
2.78
2.70
2.68
2.67
2.65
2.52
2.51
2.49
1.97
1.96
1.95
1.93
1.92
1.25
1.24
1.22
NH2
N
H2N
N
N
4a
2.00
1.97
1.95
1.99
1.98
2.00
5.41
0.0
9.5
9.0
8.5
8.0
7.5
7.0
6.5
6.0
5.5
5.0
4.5
4.0
3.5
3.0
2.5
2.0
1.5
1.0
0.5
f1 (ppm)

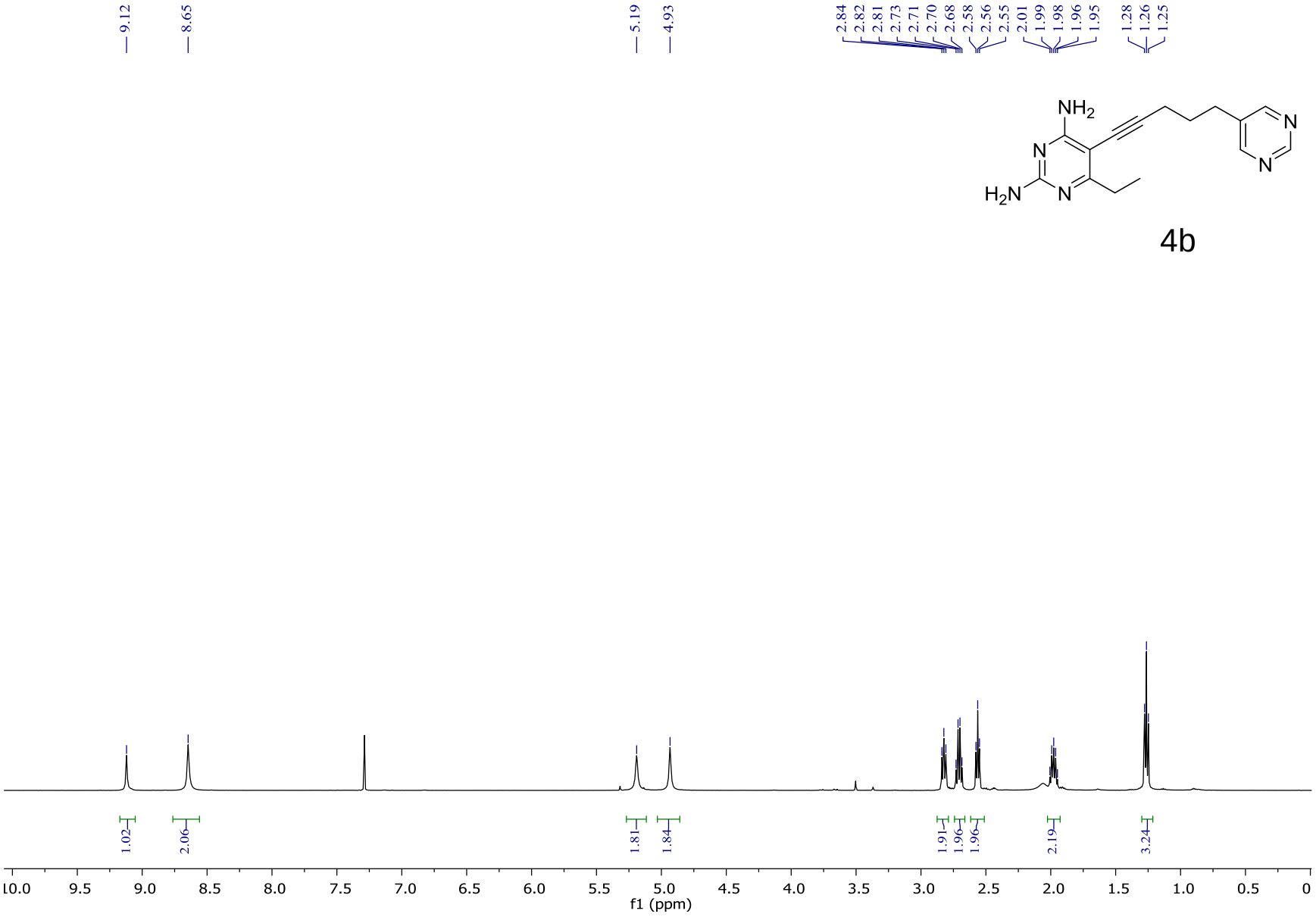
9.12
8.65
5.19
4.93
2.84
2.82
2.81
2.73
2.71
2.70
2.68
2.58
2.56
2.55
2.01
1.99
1.98
1.96
1.95
1.28
1.26
1.25
NH2
N
N
H2N
N
N
1.02
2.06
1.81
1.84
1.91
1.96
1.96
2.19
3.24
10.0
9.5
9.0
8.5
8.0
7.5
7.0
6.5
6.0
5.5
5.0
4.5
4.0
3.5
3.0
2.5
2.0
1.5
1.0
0.5
0
f1 (ppm)

4b

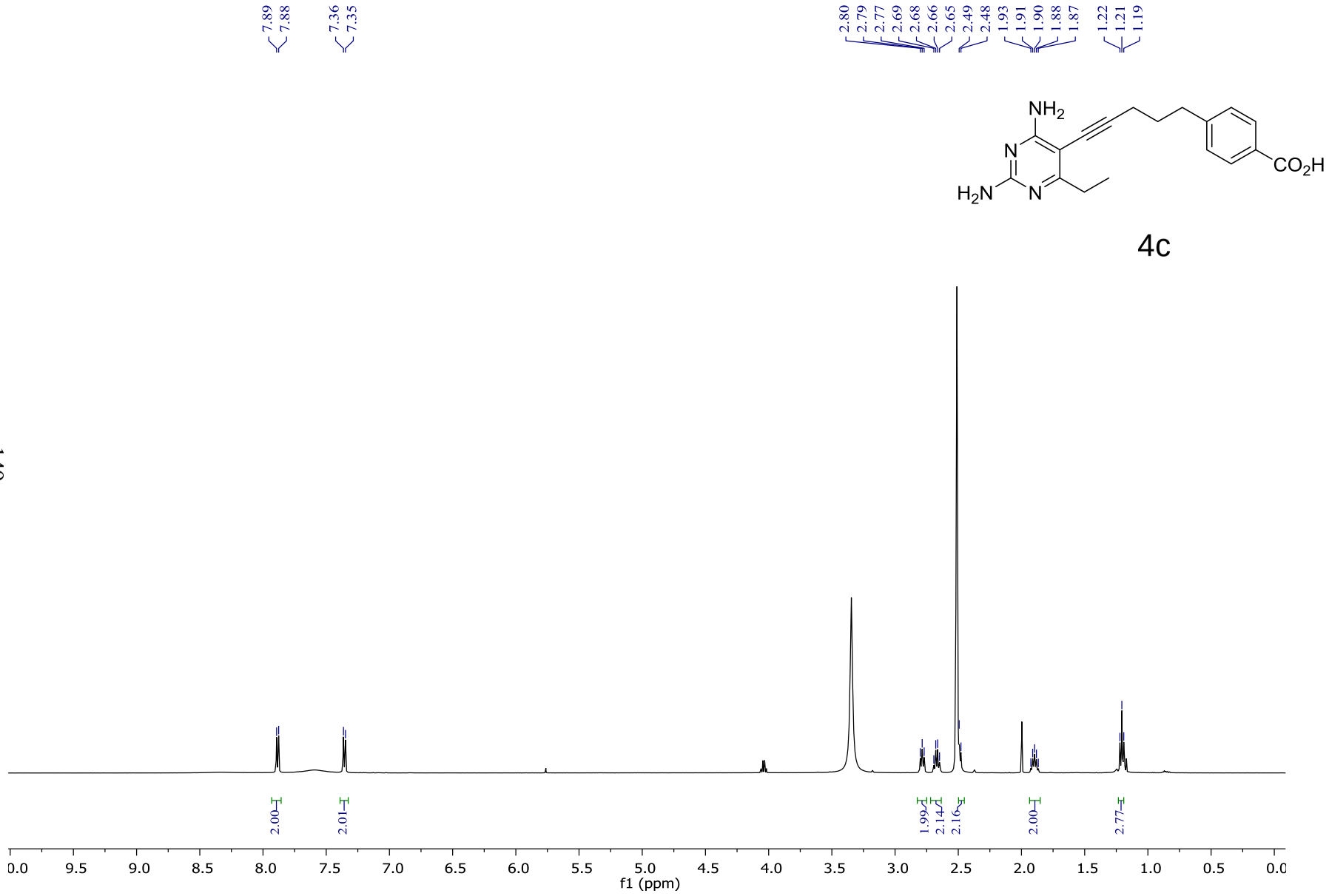
7.89
7.88
7.36
7.35
2.80
2.79
2.77
2.69
2.68
2.66
2.65
2.49
2.48
1.93
1.91
1.90
1.88
1.87
1.22
1.21
1.19
NH2
N
H2N
N
CO2H
4c
2.00
2.01
1.99
2.14
2.16
2.00
2.77
f1 (ppm)

7.07
7.05
6.79
6.77
2.72
2.71
2.70
2.70
2.69
2.67
2.49
2.48
2.47
1.93
1.91
1.90
1.88
1.87
1.26
1.25
1.23
4d
NH2
N
N
H2N
OH
3.07
2.19
2.00
3.91
1.78
1.81
0.0
0.5
1.0
1.5
2.0
2.5
3.0
3.5
4.0
4.5
5.0
5.5
6.0
6.5
7.0
7.5
8.0
8.5
9.0
9.5
f1 (ppm)

# CHAPTER 4 NMR DATA

8.5883
8.5792
7.4458
7.4424
7.4365
7.4332
7.3585
7.3510
7.0317
7.0297
7.0245
7.0224
4.0847
4.0827
4.0800
4.0780
4.0707
4.0686
4.0659
4.0638
4.0565
4.0543
4.0513
4.0493
4.0421
4.0398
4.0372
4.0353
2.3585
2.3534
1.6593
1.6452

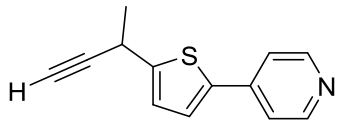


12i

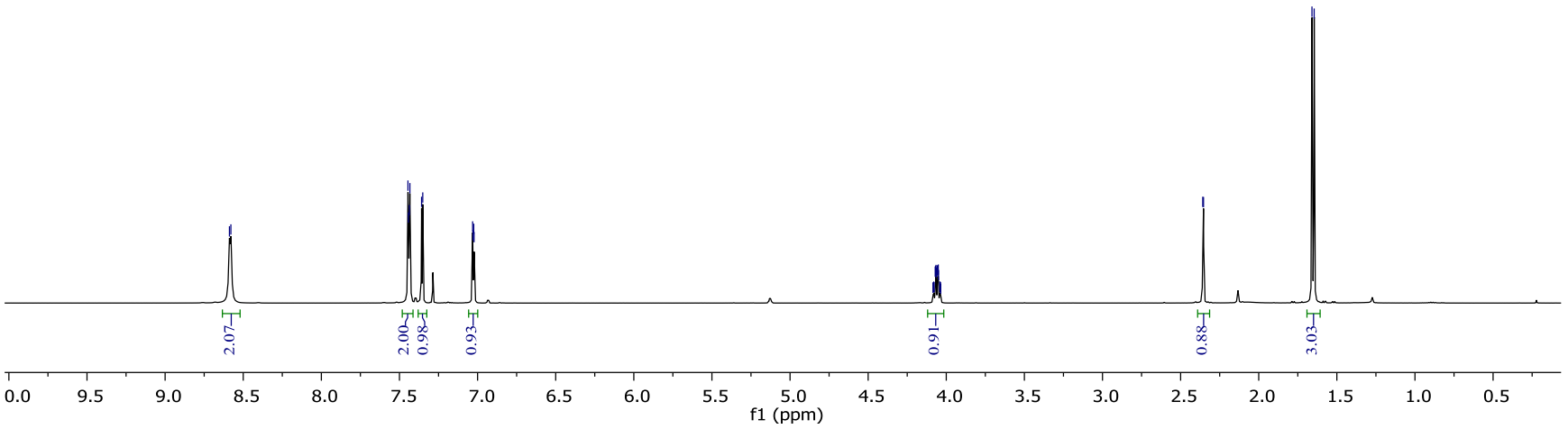

150.33
148.45
141.40
139.46
125.30
125.07
119.53
85.55
70.49
27.42
24.04

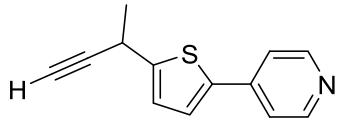


12i

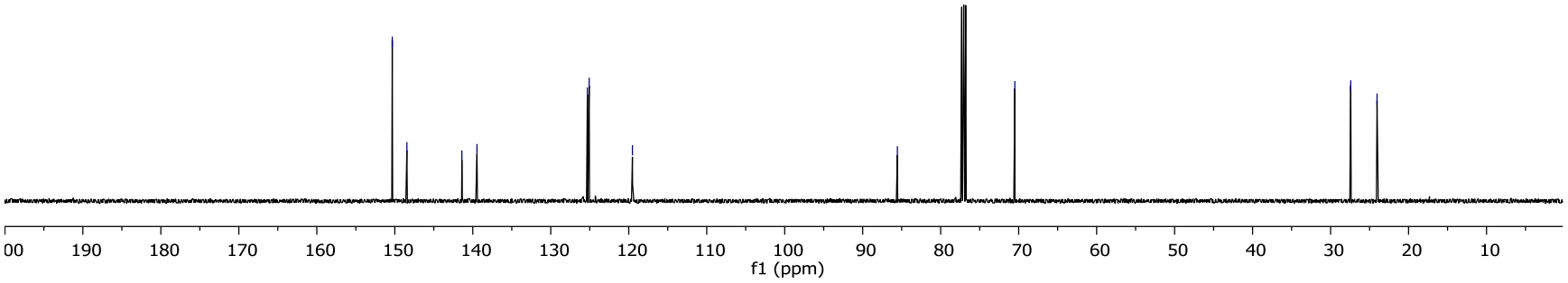

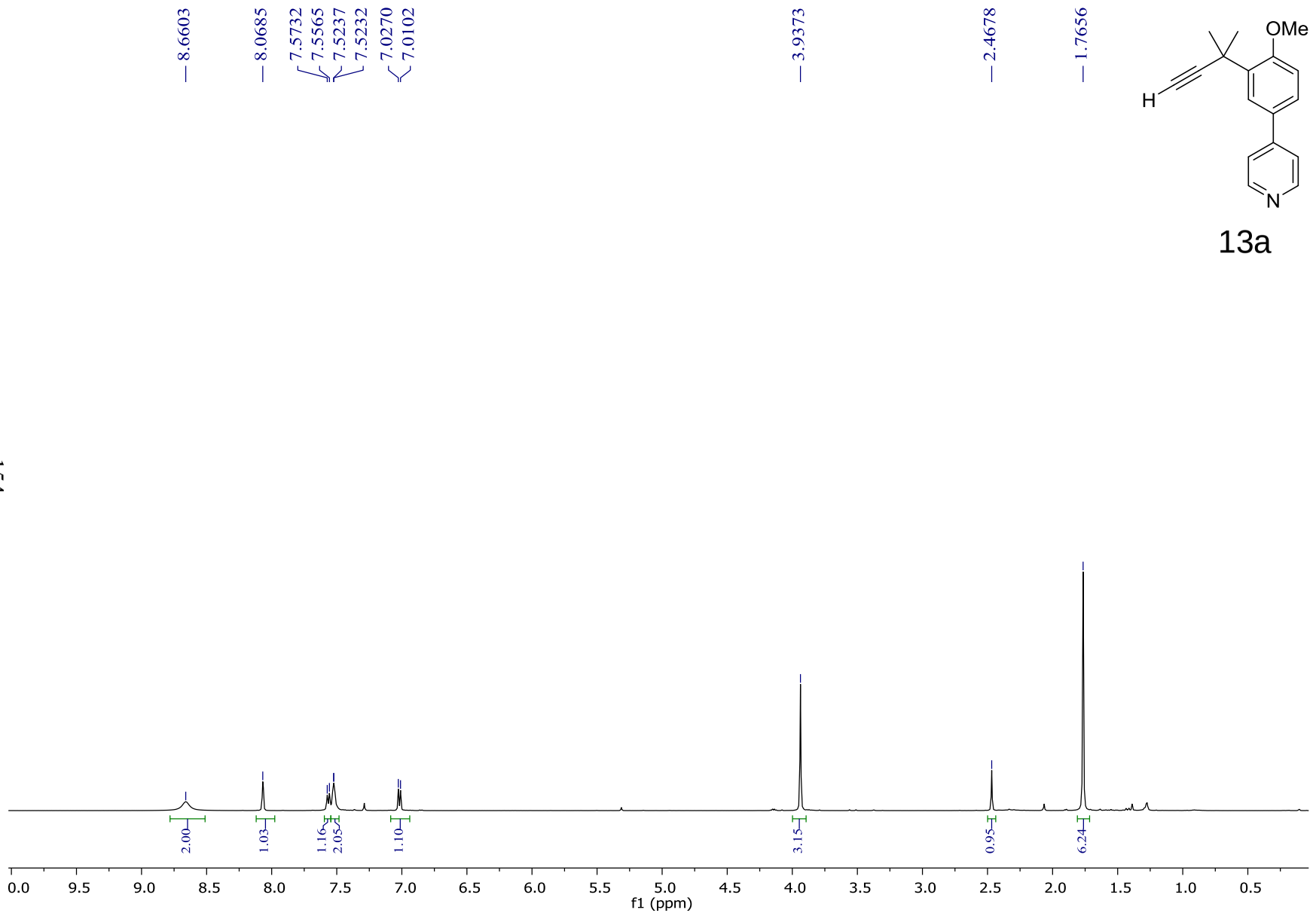
8.6603
8.0685
7.5732
7.5565
7.5237
7.5232
7.0270
7.0102
3.9373
2.4678
1.7656
OMe
H
N
2.00
1.03
1.16
2.05
1.10
3.15
0.95
6.24
f1 (ppm)

13a

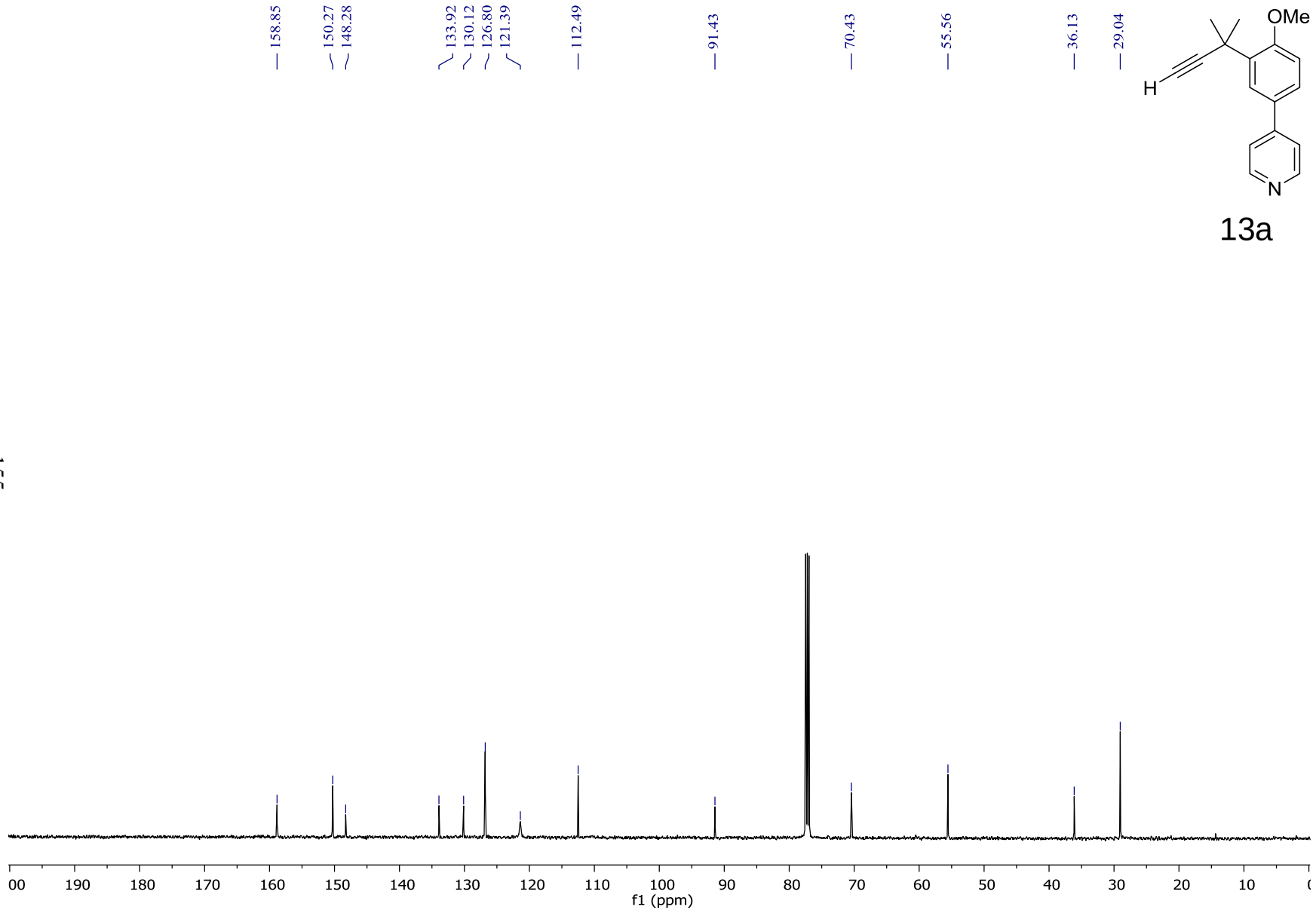
158.85
150.27
148.28
133.92
130.12
126.80
121.39
112.49
91.43
70.43
55.56
36.13
29.04
OMe
H
N
13a
155
f1 (ppm)

OMe
N
H
13b
1.6689
2.4181
3.9067
8.6863
8.6834
8.6740
7.5289
7.5199
7.5165
7.4394
7.4362
7.4335
7.2273
7.2233
7.0368
7.0329
7.0296
2.00
2.02
0.93
0.96
1.01
3.07
0.92
5.69
f1 (ppm)

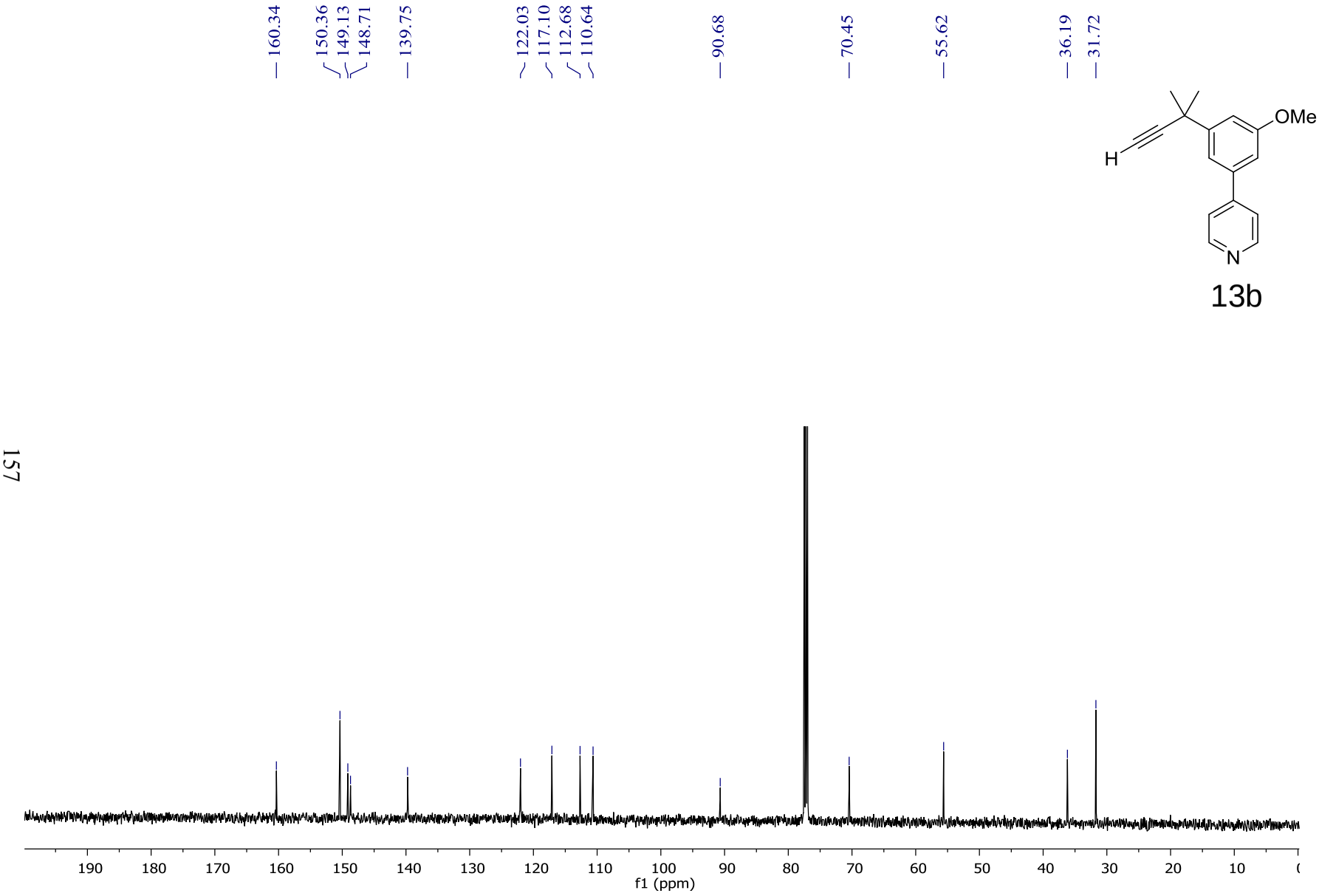
160.34
150.36
149.13
148.71
139.75
122.03
117.10
112.68
110.64
90.68
70.45
55.62
36.19
31.72
OMe
H
N
13b
157
190
180
170
160
150
140
130
120
110
100
90
80
70
60
50
40
30
20
10
f1 (ppm)

OMe
OMe
N
H

13c


8.6785
7.5210
7.5127
7.2462
7.2429
7.1176
7.1140
3.9630
3.6357
2.3994
1.6534
2.00
2.10
1.09
0.96
3.22
2.89
0.88
5.92
f1 (ppm)

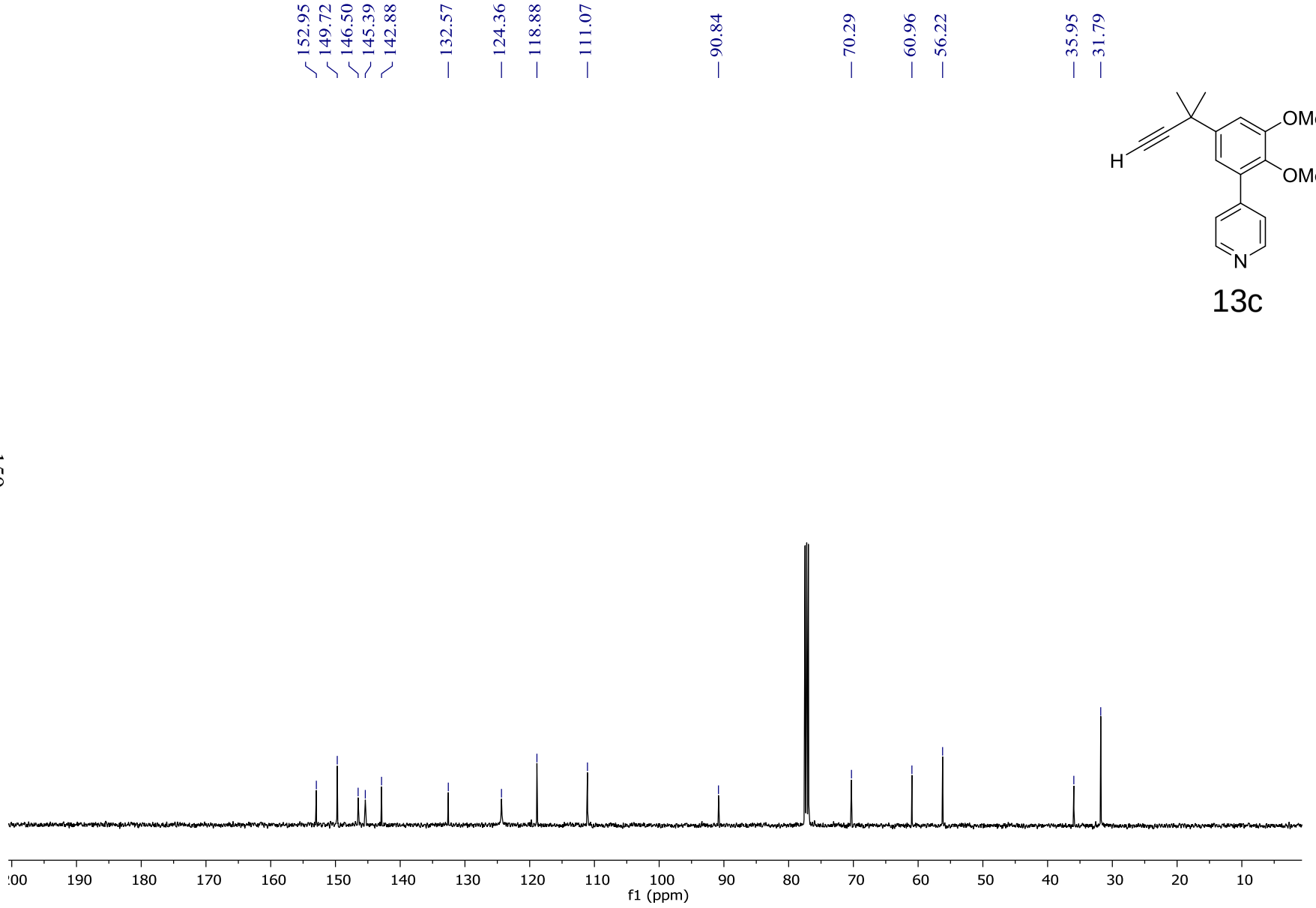
152.95
149.72
146.50
145.39
142.88
132.57
124.36
118.88
111.07
90.84
70.29
60.96
56.22
35.95
31.79
H
OMe
OMe
N
13c
f1 (ppm)

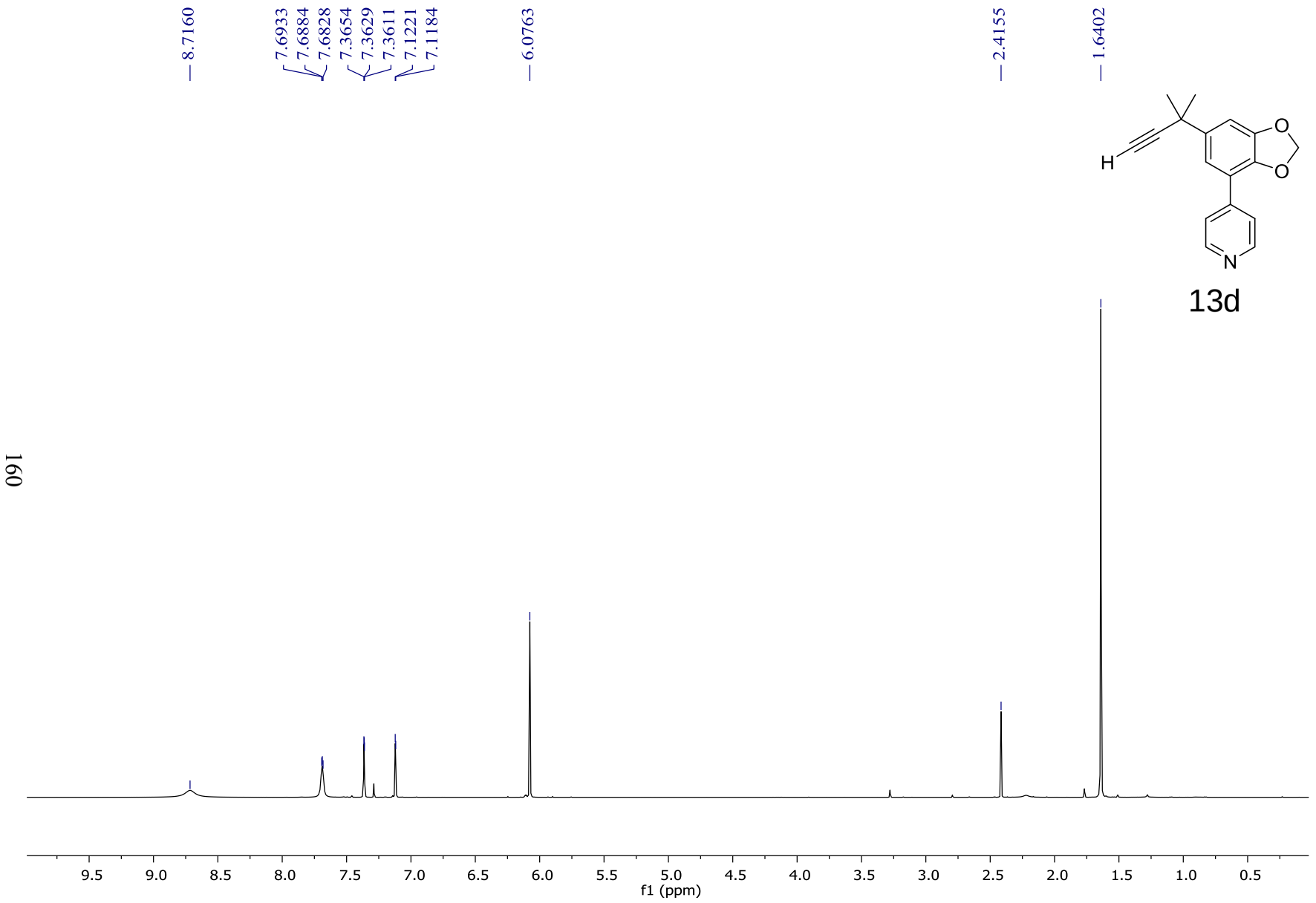
8.7160
7.6933
7.6884
7.6828
7.3654
7.3629
7.3611
7.1221
7.1184
6.0763
2.4155
1.6402
H
O
O
N
13d
160
9.5
9.0
8.5
8.0
7.5
7.0
6.5
6.0
5.5
5.0
4.5
4.0
3.5
3.0
2.5
2.0
1.5
1.0
0.5
f1 (ppm)

13d
O
O
N
H
31.86
35.94
70.39
70.36
90.79
101.60
107.27
117.56
119.02
122.44
141.41
143.63
144.23
148.60
150.25
f1 (ppm)

13e
OMe
N
N
H
9.0342
8.6198
8.4700
8.4172
8.4131
7.9613
7.9572
7.9443
7.9402
7.0600
7.0430
3.9581
2.4579
1.7751
1.00
1.10
0.94
1.04
1.04
1.06
3.24
0.94
6.18
f1 (ppm)

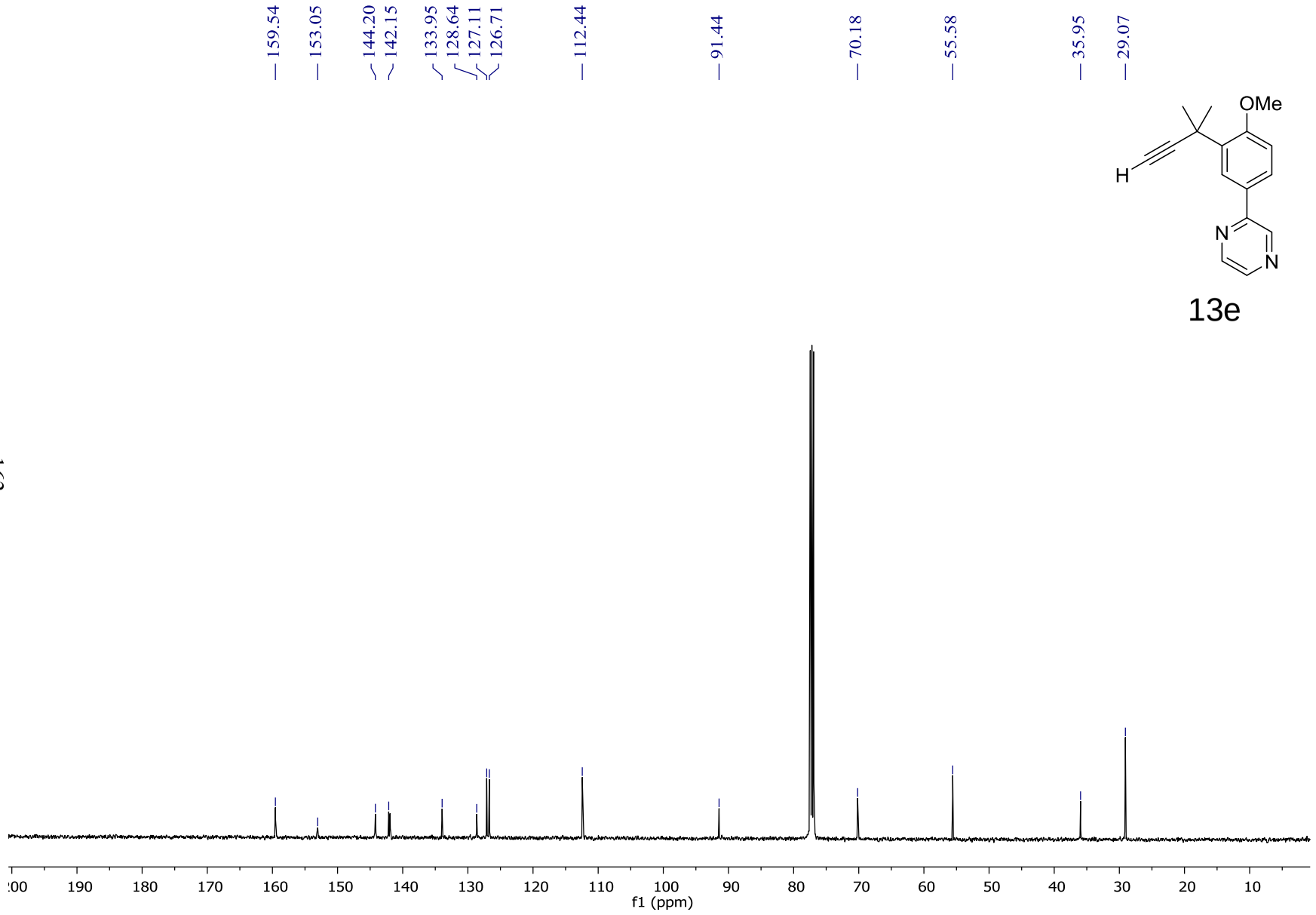
159.54
153.05
144.20
142.15
133.95
128.64
127.11
126.71
112.44
91.44
70.18
55.58
35.95
29.07
OMe
H
N
N
13e
f1 (ppm)

13f
9.1972
9.1181
7.3225
7.3189
7.1300
7.1263
6.0943
2.4196
1.6443
2.01
1.00
1.03
1.00
2.24
0.97
6.21
f1 (ppm)

13f
31.69
35.81
70.37
90.44
101.58
107.14
114.87
117.04
129.97
141.74
143.90
148.50
155.40
157.33
f1 (ppm)

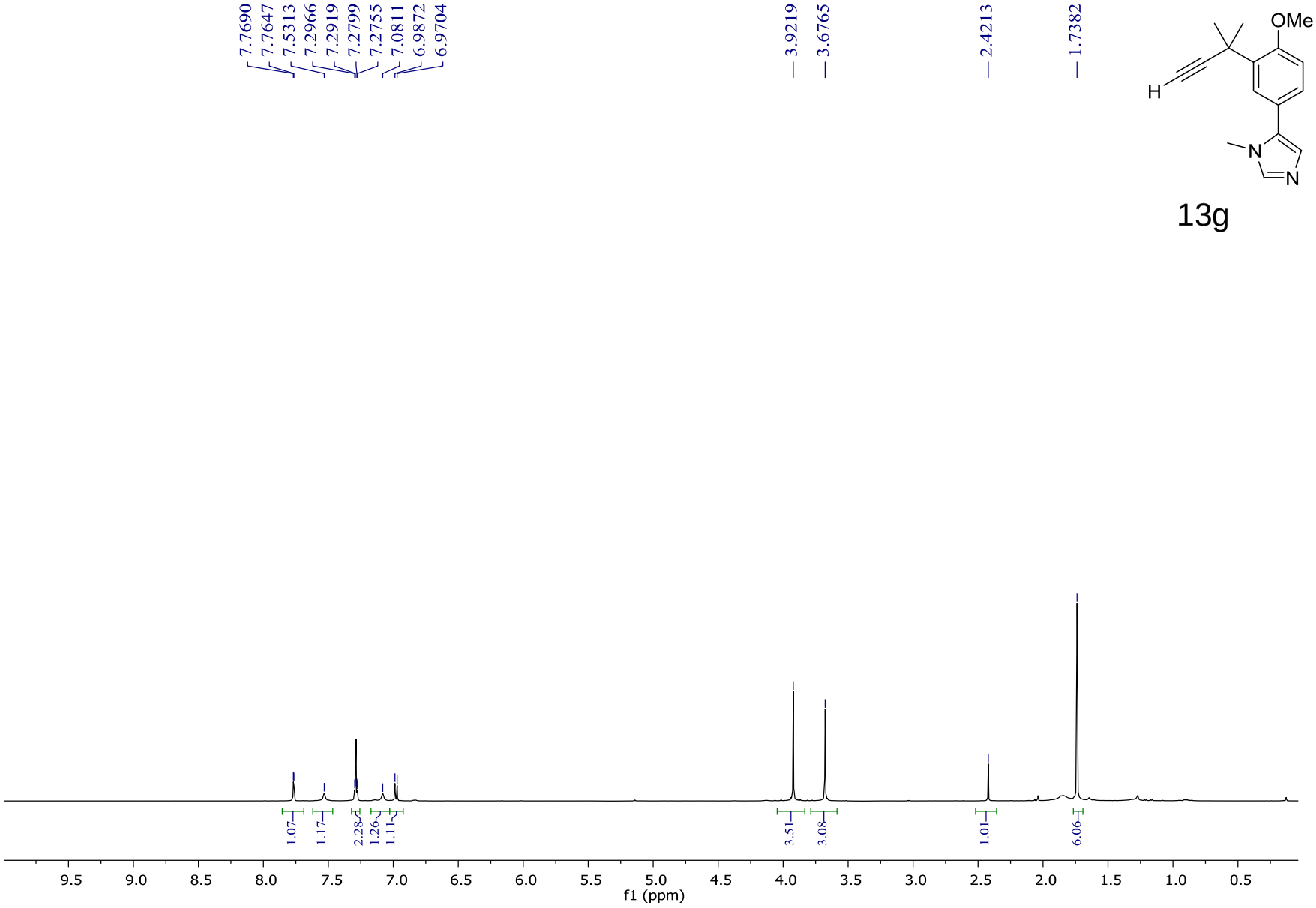
7.7690
7.7647
7.5313
7.2966
7.2919
7.2799
7.2755
7.0811
6.9872
6.9704
3.9219
3.6765
2.4213
1.7382
OMe
H
N
N
1.07
1.17
2.28
1.26
1.11
3.51
3.08
1.01
6.06
9.5
9.0
8.5
8.0
7.5
7.0
6.5
6.0
5.5
5.0
4.5
4.0
3.5
3.0
2.5
2.0
1.5
1.0
0.5
f1 (ppm)

13g

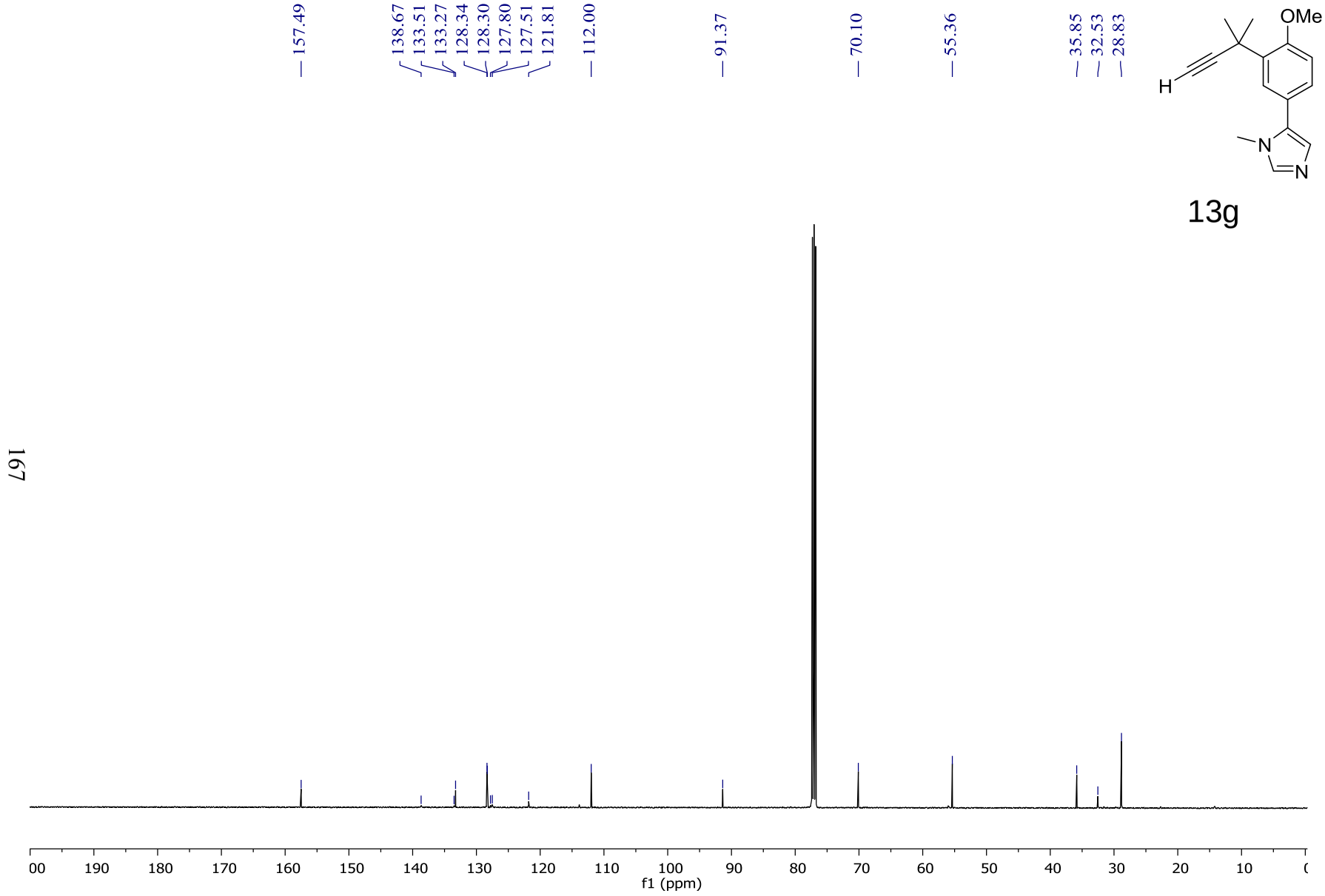
157.49
138.67
133.51
133.27
128.34
128.30
127.80
127.51
121.81
112.00
91.37
70.10
55.36
35.85
32.53
28.83
OMe
H
N
N
13g
167
f1 (ppm)

OMe
N
N
H

13h


9.2136
9.2127
9.0094
8.0045
7.9998
7.5058
7.5011
7.4889
7.4842
7.0501
7.0669
3.9494
2.4675
1.7669
1.02
1.94
0.94
1.04
0.99
2.96
0.88
5.63
9.5
9.0
8.5
8.0
7.5
7.0
6.5
6.0
5.5
5.0
4.5
4.0
3.5
3.0
2.5
2.0
1.5
1.0
0.5
f1 (ppm)

158.74
156.88
154.63
134.41
126.90
126.77
126.34
112.81
91.25
70.71
70.69
55.59
36.24
28.96

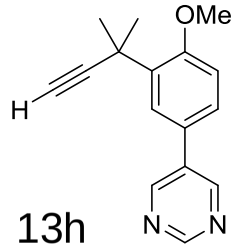


13h

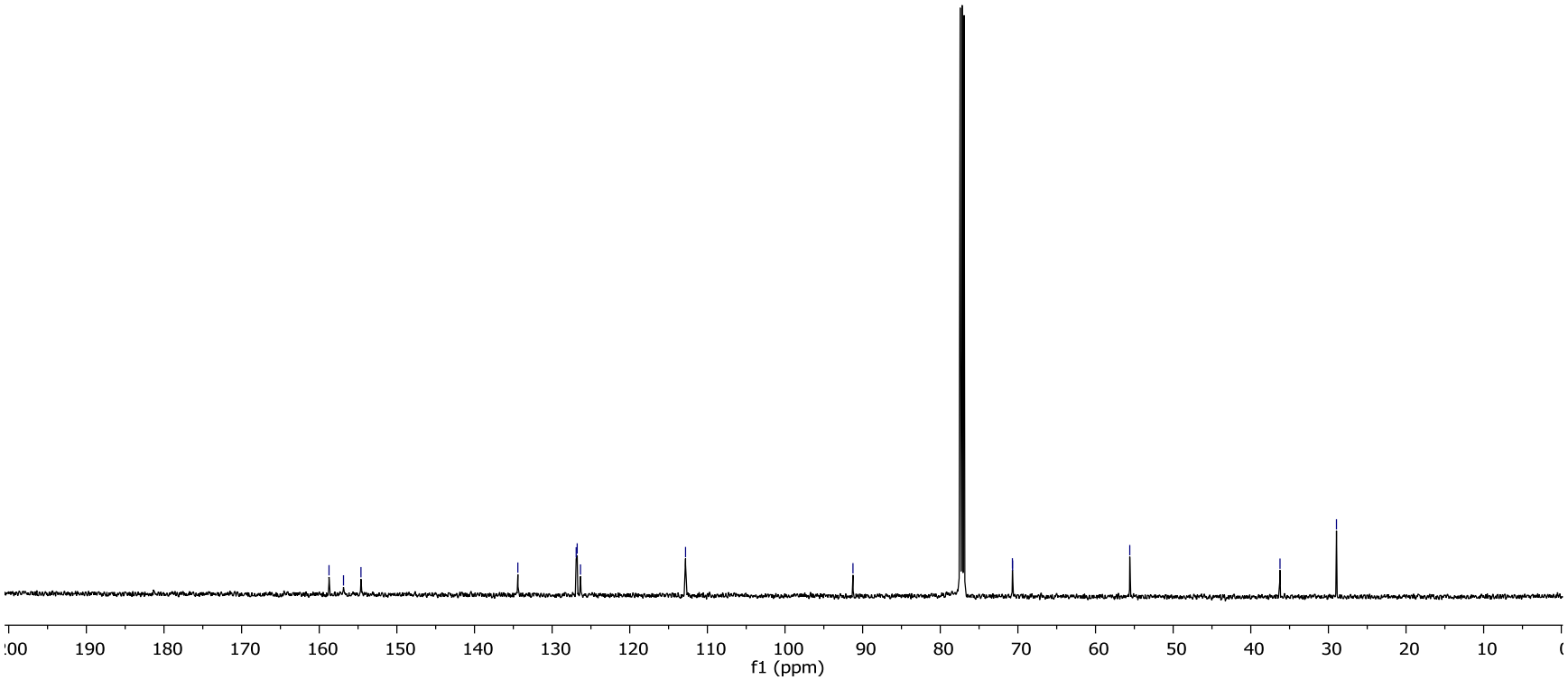

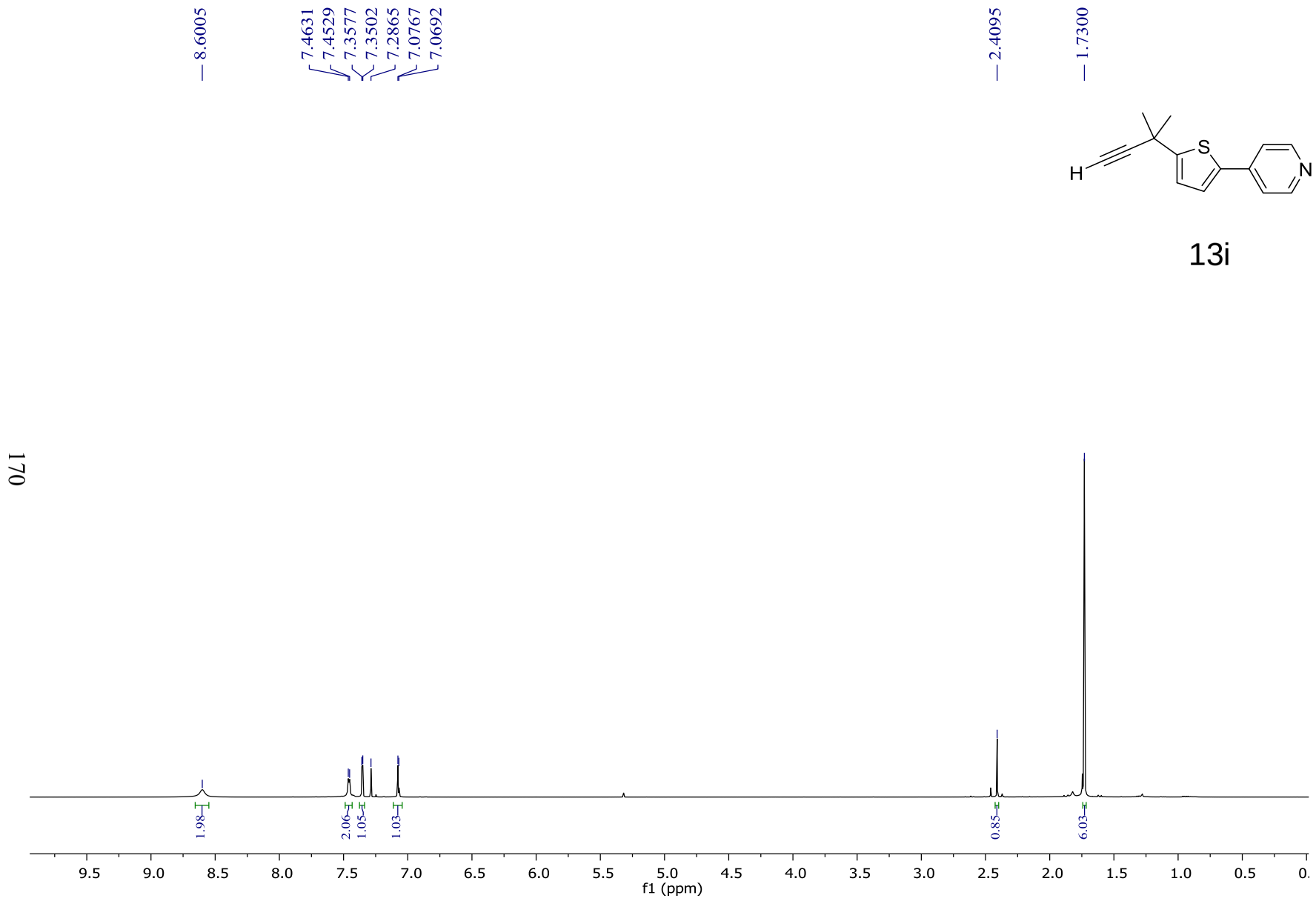
8.6005
7.4631
7.4529
7.3577
7.3502
7.2865
7.0767
7.0692
2.4095
1.7300
S
N
H
1.98
2.06
1.05
1.03
0.85
6.03
f1 (ppm)

13i

13i
N
S
H
32.44
33.97
69.66
89.54
119.57
124.26
124.93
139.06
141.48
150.29
154.20
f1 (ppm)

13j
OMe
O
N
H
1.7436
2.3084
2.4190
2.4357
3.9197
6.9725
6.9892
7.1433
7.1478
7.1600
7.1645
7.6622
7.6666
1.00
1.04
1.05
3.12
2.96
0.95
3.12
6.27
f1 (ppm)

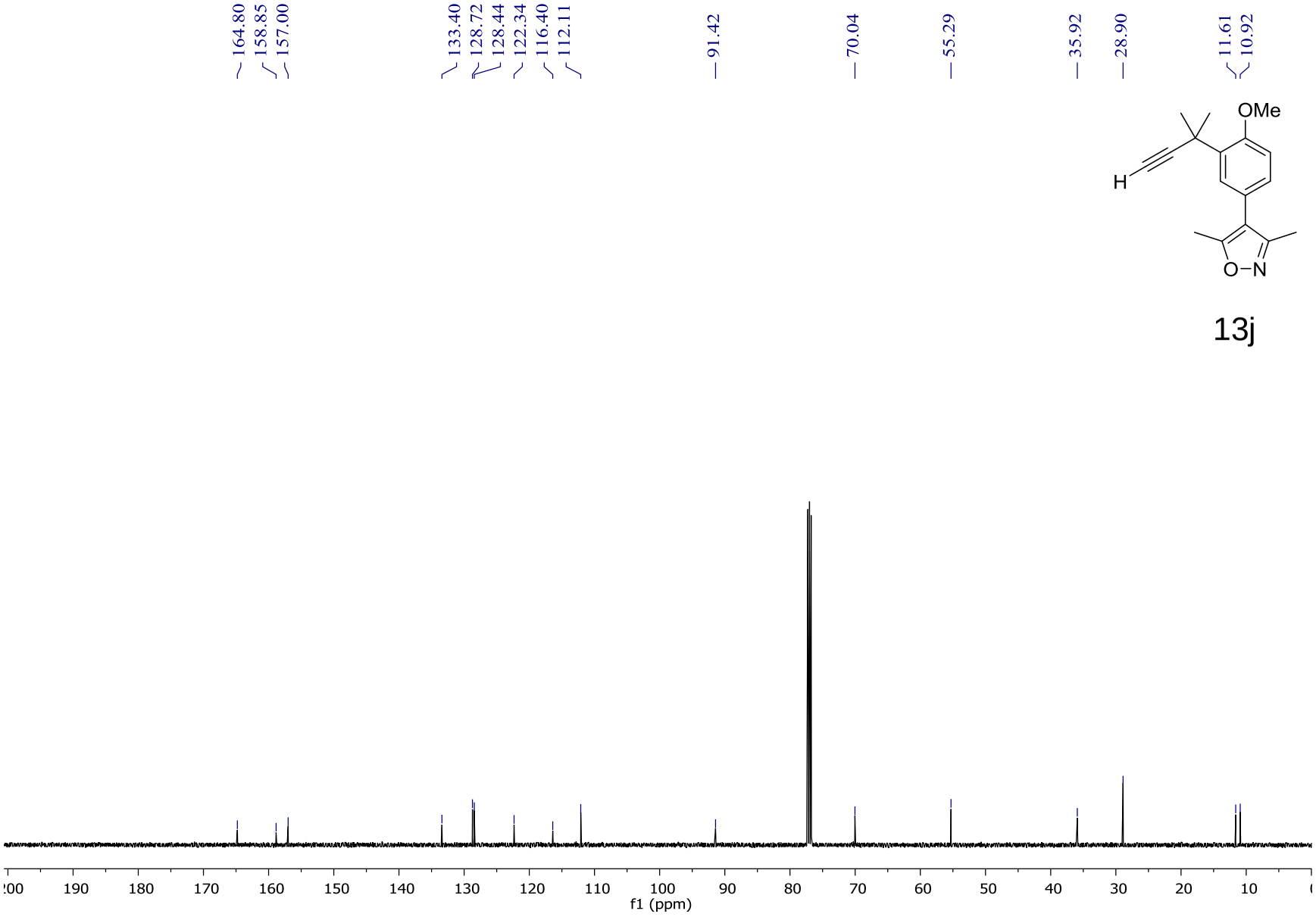
164.80
158.85
157.00
133.40
128.72
128.44
122.34
116.40
112.11
91.42
70.04
55.29
35.92
28.90
11.61
10.92
OMe
H
O–N
f1 (ppm)

13j